

## ELECTRONIC REPRINT ORDER FORM

After publication of your journal article, electronic (PDF) reprints may be purchased by arrangement with Springer and Aries Systems Corporation.

The PDF file you will receive will be protected with a copyright system called DocuRights®. Purchasing 50 reprints will enable you to redistribute the PDF file to up to 50 computers. You may distribute your allotted number of PDFs as you wish; for example, you may send it out via e-mail or post it to your website. You will be able to print five (5) copies of your article from each one of the PDF reprints.

**Please type or print carefully. Fill out each item completely.**

1. Your name: \_\_\_\_\_  
Your e-mail address: \_\_\_\_\_  
Your phone number: \_\_\_\_\_  
Your fax number: \_\_\_\_\_
2. Journal title (vol, iss, pp): \_\_\_\_\_
3. Article title: \_\_\_\_\_
4. Article author(s): \_\_\_\_\_
5. How many PDF reprints do you want? \_\_\_\_\_
6. Please refer to the pricing chart below to calculate the cost of your order.

Number of PDF reprints	Cost (in U.S. dollars)
50	\$200
100	\$275
150	\$325
200	\$350

NOTE: Prices shown apply only to orders submitted by individual article authors or editors. Commercial orders must be directed to the Publisher.

All orders must be prepaid. Payments must be made in one of the following forms:

- a check drawn on a U.S. bank
- an international money order
- Visa, MasterCard, or American Express (no other credit cards can be accepted)

PAYMENT (type or print carefully):

Amount of check enclosed: \_\_\_\_\_ (payable to Aries Systems Corporation)

VISA \_\_\_\_\_

MasterCard \_\_\_\_\_

American Express \_\_\_\_\_

Expiration date: \_\_\_\_\_ Signature: \_\_\_\_\_

Print and send this form with payment information to:

Aries Systems Corporation  
200 Sutton Street  
North Andover, Massachusetts 01845  
Attn.: Electronic Reprints  
— OR —  
Fax this to Aries at: 978-975-3811

Your PDF reprint file will be sent to the above e-mail address. If you have any questions about your order, or if you need technical support, please contact: [support@docurights.com](mailto:support@docurights.com)

For subscriptions and to see all of our other products and services, visit the Springer website at:

<http://www.springeronline.com>

## COLOUR CONSENT FORM

Dear **Alain Destexhe**

Springer offers two options for reproducing colour illustrations in our publications. Check the author instructions for the submission of electronic figures.

Please select the option you prefer:

**Option 1**  **Free Online Colour**

Colour figures will only appear in colour on [www.springerlink.com](http://www.springerlink.com) **and not** in the printed version of the journal

**Option 2**  **Online and Printed Colour**

Colour figures will appear in colour on [www.springerlink.com](http://www.springerlink.com) **and** in the printed version of the journal

**Charges** Springer charges authors for the reproduction of colour figures in print.

The charges are **€ 950** or **\$ 1.150** per article. If you agree to the colour charges then please complete the form below:

Journal Title (abbreviated title):

**Journal of Computational Neuroscience**

Manuscript number:

Author's name:

**Alain Destexhe**

Invoice Address:

**Unite de Neurosciences Integratives, et Computationnelles (UNIC), CNRS (Bat 33), 1 Avenue de la Terrasse, 91190, Gif-sur-Yvette, France**

I enclose payment to the amount of **€ 950 / \$ 1150**

Please charge my credit card account (incl. check digits):

Expiry date:

Access

Visa

Eurocard

American Express

Bank Americard

Diners Club

Master Card

Date

Signature

**Regardless whether you have chosen option 1 or 2, please sign and return this form.**

# Copyright Transfer Statement

The copyright to this article is transferred to Springer (respective to owner if other than Springer and for U.S. government employees: to the extent transferable) effective if and when the article is accepted for publication. The author warrants that his/her contribution is original and that he/she has full power to make this grant. The author signs for and accepts responsibility for releasing this material on behalf of any and all co-authors. The copyright transfer covers the exclusive right to reproduce and distribute the article, including reprints, translations, photographic reproductions, microform, electronic form (offline, online) or any other reproductions of similar nature.

An author may self-archive an author-created version of his/her article on his/her own website and his/her institution's repository, including his/her final version; however he/she may not use the publisher's PDF version which is posted on [www.springerlink.com](http://www.springerlink.com). Furthermore, the author may only post his/her version provided acknowledgement is given to the original source of publication and a link is inserted to the published article on Springer's website. The link must be accompanied by the following text: "The original publication is available at [www.springerlink.com](http://www.springerlink.com)".

Please use the appropriate DOI for the article (go to the Linking Options in the article, then to OpenURL and use the link with the DOI). Articles disseminated via [www.springerlink.com](http://www.springerlink.com) are indexed, abstracted, and referenced by many abstracting and information services, bibliographic networks, subscription agencies, library networks, and consortia.

After submission of this agreement signed by the corresponding author, changes of authorship or in the order of the authors listed will not be accepted by Springer.

Journal

**Journal of Computational Neuroscience**

Title of article

**Simulation of networks of spiking neurons: A review of tools and strategies**

Author(s)

**Brette · Rudolph · Carnevale · Hines · Beeman · Bower · Diesmann · Morrison · Goodman · Harris · Zirpe · Natschlag · Pecevski · Ermentrout · Djurfeldt · Lansner · Rochel · Vieville · Muller · Davison · El Boustani · Destexhe**

Author's signature

Date

## Metadata of the article that will be visualized in OnlineFirst

1	Article Title	<b>Simulation of networks of spiking neurons: A review of tools and strategies</b>
2	Journal Name	Journal of Computational Neuroscience
3		Family Name <b>Destexhe</b>
4		Particle
5		Given Name <b>Alain</b>
6		Suffix
7		Organization CNRS (Bat 33)
8	Corresponding Author	Division Unité de Neurosciences Intégratives, et Computationnelles (UNIC)
9		Address 1 Avenue de la Terrasse, Gif-sur-Yvette 91190, France
10		Organization CNRS
11		Division
12		Address Gif-sur-Yvette , France
13		e-mail destexhe@iaf.cnrs-gif.fr
14		Family Name <b>Brette</b>
15		Particle
16		Given Name <b>Romain</b>
17		Suffix
18	Author	Organization Ecole Normale Supérieure
19		Division
20		Address Paris , France
21		e-mail
22		Family Name <b>Rudolph</b>
23		Particle
24		Given Name <b>Michelle</b>
25		Suffix
26	Author	Organization CNRS
27		Division
28		Address Gif-sur-Yvette , France
29		e-mail
30		Family Name <b>Carnevale</b>
31		Particle
32		Given Name <b>Ted</b>
33	Author	Suffix
34		Organization Yale University
35		Division

36		Address	New Haven , CT, USA
37		e-mail	
38		Family Name	<b>Hines</b>
39		Particle	
40		Given Name	<b>Michael</b>
41		Suffix	
42	Author	Organization	Yale University
43		Division	
44		Address	New Haven , CT, USA
45		e-mail	
46		Family Name	<b>Beeman</b>
47		Particle	
48		Given Name	<b>David</b>
49		Suffix	
50	Author	Organization	University of Colorado
51		Division	
52		Address	Boulder , CO, USA
53		e-mail	
54		Family Name	<b>Bower</b>
55		Particle	
56		Given Name	<b>James M.</b>
57		Suffix	
58	Author	Organization	University of Texas
59		Division	
60		Address	San Antonio , TX, USA
61		e-mail	
62		Family Name	<b>Diesmann</b>
63		Particle	
64		Given Name	<b>Markus</b>
65		Suffix	
66		Organization	University of Freiburg
67	Author	Division	
68		Address	Freiburg , Germany
69		Organization	RIKEN Brain Science Institute
70		Division	
71		Address	Wako City , Japan
72		e-mail	
73		Family Name	<b>Morrison</b>
74		Particle	
75		Given Name	

		<b>Abigail</b>
76	Suffix	
77	Organization	RIKEN Brain Science Institute
78	Author Division	
79	Address	Wako City , Japan
80	e-mail	
81	Family Name	<b>Goodman</b>
82	Particle	
83	Given Name	<b>Philip H.</b>
84	Suffix	
85	Author Organization	University of Nevada
86	Division	
87	Address	Reno , NV, USA
88	e-mail	
89	Family Name	<b>Harris</b>
90	Particle	
91	Given Name	<b>Frederick C.</b>
92	Author Suffix	<b>Jr.</b>
93	Organization	University of Nevada
94	Division	
95	Address	Reno , NV, USA
96	e-mail	
97	Family Name	<b>Zirpe</b>
98	Particle	
99	Given Name	<b>Milind</b>
100	Suffix	
101	Author Organization	University of Nevada
102	Division	
103	Address	Reno , NV, USA
104	e-mail	
105	Family Name	<b>Natschläger</b>
106	Particle	
107	Given Name	<b>Thomas</b>
108	Suffix	
109	Author Organization	Software Competence Center Hagenberg
110	Division	
111	Address	Hagenberg , Austria
112	e-mail	
113	Family Name	<b>Pecevski</b>
114	Particle	

115		Given Name	<b>Dejan</b>
116		Suffix	
117	Author	Organization	Technical University of Graz
118		Division	
119		Address	Graz , Austria
120		e-mail	
<hr/>			
121		Family Name	<b>Ermentrout</b>
122		Particle	
123		Given Name	<b>Bard</b>
124	Author	Suffix	
125		Organization	University of Pittsburgh
126		Division	
127		Address	Pittsburgh , PA, USA
128		e-mail	
<hr/>			
129		Family Name	<b>Djurfeldt</b>
130		Particle	
131		Given Name	<b>Mikael</b>
132	Author	Suffix	
133		Organization	KTH
134		Division	
135		Address	Stockholm , Sweden
136		e-mail	
<hr/>			
137		Family Name	<b>Lansner</b>
138		Particle	
139		Given Name	<b>Anders</b>
140	Author	Suffix	
141		Organization	KTH
142		Division	
143		Address	Stockholm , Sweden
144		e-mail	
<hr/>			
145		Family Name	<b>Rochel</b>
146		Particle	
147		Given Name	<b>Olivier</b>
148	Author	Suffix	
149		Organization	University of Leeds
150		Division	
151		Address	Leeds , UK
152		e-mail	
<hr/>			
153		Family Name	<b>Vieville</b>

154		Particle	
155		Given Name	<b>Thierry</b>
156		Suffix	
157	Author	Organization	INRIA
158		Division	
159		Address	Nice , France
160		e-mail	
161		Family Name	<b>Muller</b>
162		Particle	
163		Given Name	<b>Eilif</b>
164		Suffix	
165	Author	Organization	University of Heidelberg
166		Division	
167		Address	Heidelberg , Germany
168		e-mail	
169		Family Name	<b>Davison</b>
170		Particle	
171		Given Name	<b>Andrew P.</b>
172		Suffix	
173	Author	Organization	CNRS
174		Division	
175		Address	Gif-sur-Yvette , France
176		e-mail	
177		Family Name	<b>El Boustani</b>
178		Particle	
179		Given Name	<b>Sami</b>
180		Suffix	
181	Author	Organization	CNRS
182		Division	
183		Address	Gif-sur-Yvette , France
184		e-mail	
185		Received	29 November 2006
186	Schedule	Revised	2 April 2007
187		Accepted	12 April 2007
188	Abstract	We review different aspects of the simulation of spiking neural networks. We start by reviewing the different types of simulation strategies and algorithms that are currently implemented. We next review the precision of those simulation strategies, in particular in cases where plasticity depends on the exact timing of the spikes. We overview different simulators and simulation environments presently available (restricted to those freely available, open source and documented). For each simulation tool, its advantages and pitfalls are reviewed, with an aim to allow the reader to identify which simulator is appropriate for a given task. Finally, we provide a series of benchmark	



simulations of different types of networks of spiking neurons, including Hodgkin–Huxley type, integrate-and-fire models, interacting with current-based or conductance-based synapses, using clock-driven or event-driven integration strategies. The same set of models are implemented on the different simulators, and the codes are made available. The ultimate goal of this review is to provide a resource to facilitate identifying the appropriate integration strategy and simulation tool to use for a given modeling problem related to spiking neural networks.

---

189	Keywords separated by ' - '	Spiking neural networks - Simulation tools - Integration strategies
190	Foot note information	<b>Action Editor: Barry J. Richmond</b>

---

# Simulation of networks of spiking neurons: A review of tools and strategies

**Romain Brette · Michelle Rudolph · Ted Carnevale ·  
Michael Hines · David Beeman · James M. Bower ·  
Markus Diesmann · Abigail Morrison ·  
Philip H. Goodman · Frederick C. Harris, Jr. ·  
Milind Zirpe · Thomas Natschläger · Dejan Pecevski ·  
Bard Ermentrout · Mikael Djurfeldt ·  
Anders Lansner · Olivier Rochel · Thierry Vieville ·  
Eilif Muller · Andrew P. Davison ·  
Sami El Boustani · Alain Destexhe**

Received: 29 November 2006 / Revised: 2 April 2007 / Accepted: 12 April 2007  
© Springer Science + Business Media, LLC 2007

**1 Abstract** We review different aspects of the simulation  
2 of spiking neural networks. We start by reviewing the  
3 different types of simulation strategies and algorithms  
4 that are currently implemented. We next review the  
5 precision of those simulation strategies, in particular in  
6 cases where plasticity depends on the exact timing of

the spikes. We overview different simulators and sim- 7  
8 ulation environments presently available (restricted to 8  
9 those freely available, open source and documented). 9  
10 For each simulation tool, its advantages and pitfalls are 10  
11 reviewed, with an aim to allow the reader to identify 11  
12 which simulator is appropriate for a given task. Finally, 12

---

## Action Editor: Barry J. Richmond

---

R. Brette  
Ecole Normale Supérieure, Paris, France

M. Rudolph · A. P. Davison · S. El Boustani · A. Destexhe  
CNRS, Gif-sur-Yvette, France

T. Carnevale · M. Hines  
Yale University, New Haven, CT, USA

D. Beeman  
University of Colorado, Boulder, CO, USA

J. M. Bower  
University of Texas, San Antonio, TX, USA

M. Diesmann  
University of Freiburg, Freiburg, Germany

M. Diesmann · A. Morrison  
RIKEN Brain Science Institute, Wako City, Japan

P. H. Goodman · F. C. Harris, Jr. · M. Zirpe  
University of Nevada, Reno NV, USA

T. Natschläger  
Software Competence Center Hagenberg,  
Hagenberg, Austria

D. Pecevski  
Technical University of Graz,  
Graz, Austria

B. Ermentrout  
University of Pittsburgh,  
Pittsburgh, PA, USA

M. Djurfeldt · A. Lansner  
KTH, Stockholm, Sweden

O. Rochel  
University of Leeds, Leeds, UK

T. Vieville  
INRIA, Nice, France

E. Muller  
University of Heidelberg, Heidelberg, Germany

A. Destexhe (✉)  
Unité de Neurosciences Intégratives  
et Computationnelles (UNIC),  
CNRS (Bat 33),  
1 Avenue de la Terrasse,  
91190 Gif-sur-Yvette, France  
e-mail: destexhe@iaf.cnrs-gif.fr

13 we provide a series of benchmark simulations of dif-  
14 ferent types of networks of spiking neurons, including  
15 Hodgkin–Huxley type, integrate-and-fire models, in-  
16 teracting with current-based or conductance-based  
17 synapses, using clock-driven or event-driven integra-  
18 tion strategies. The same set of models are imple-  
19 mented on the different simulators, and the codes are  
20 made available. The ultimate goal of this review is to  
21 provide a resource to facilitate identifying the appro-  
22 priate integration strategy and simulation tool to use  
23 for a given modeling problem related to spiking neural  
24 networks.

Q1 25 **Keywords** Spiking neural networks ·  
26 Simulation tools · Integration strategies

## 27 1 Introduction

28 The growing experimental evidence that spike timing  
29 may be important to explain neural computations has  
30 motivated the use of spiking neuron models, rather  
31 than the traditional rate-based models. At the same  
32 time, a growing number of tools have appeared, al-  
33 lowing the simulation of spiking neural networks. Such  
34 tools offer the user to obtain precise simulations of a  
35 given computational paradigm, as well as publishable  
36 figures in a relatively short amount of time. However,  
37 the range of computational problems related to spiking  
38 neurons is very large. It requires in some cases to use  
39 detailed biophysical representations of the neurons, for  
40 example when intracellular electrophysiological mea-  
41 surements are to be reproduced (e.g., see Destexhe and  
42 Sejnowski 2001). In this case, one uses conductance-  
43 based (COBA) models, such as the Hodgkin and  
44 Huxley (1952) type of models. In other cases, one does  
45 not need to realistically capture the spike generating  
46 mechanisms, and simpler models, such as the integrate-  
47 and-fire (IF) model are sufficient. IF type models are  
48 also very fast to simulate, and are particularly attractive  
49 for large-scale network simulations.

50 There are two families of algorithms for the simula-  
51 tion of neural networks: synchronous or “clock-driven”  
52 algorithms, in which all neurons are updated simulta-  
53 neously at every tick of a clock, and asynchronous or  
54 “event-driven” algorithms, in which neurons are upda-  
55 ted only when they receive or emit a spike (hybrid strat-  
56 egies also exist). Synchronous algorithms can be easily  
57 coded and apply to any model. Because spike times  
58 are typically bound to a discrete time grid, the preci-  
59 sion of the simulation can be an issue. Asynchronous

algorithms have been developed mostly for exact sim- 60  
ulation, which is possible for simple models. For very 61  
large networks, the simulation time for both methods 62  
scale as the total number of spike transmissions, but 63  
each strategy has its own assets and disadvantages. 64

In this paper, we start by providing an overview of 65  
different simulation strategies, and outline to which 66  
extent the temporal precision of spiking events impacts 67  
on neuronal dynamics of single as well as small net- 68  
works of IF neurons with plastic synapses. Next, we 69  
review the currently available simulators or simulation 70  
environments, with an aim to focus only on publically- 71  
available and non-commercial tools to simulate net- 72  
works of spiking neurons. For each type of simulator, 73  
we describe the simulation strategy used, outline the 74  
type of models which are most optimal, as well as 75  
provide concrete examples. The ultimate goal of this 76  
paper is to provide a resource to enable the researcher 77  
to identify which strategy or simulator to use for a given 78  
modeling problem related to spiking neural networks. 79

## 2 Simulation strategies 80

This discussion is restricted to serial algorithms for 81  
brevity. The specific sections of NEST and SPLIT con- 82  
tain additional information on concepts for parallel 83  
computing. 84

There are two families of algorithms for the simu- 85  
lation of neural networks: synchronous or clock-driven 86  
algorithms, in which all neurons are updated simulta- 87  
neously at every tick of a clock, and asynchronous or 88  
event-driven algorithms, in which neurons are updated 89  
only when they receive or emit a spike. These two 90  
approaches have some common features that we will 91  
first describe by expressing the problem of simulating 92  
neural networks in the formalism of hybrid systems, i.e., 93  
differential equations with discrete events (spikes). In 94  
this framework some common strategies for efficient 95  
representation and simulation appear. 96

Since we are going to compare algorithms in terms 97  
of computational efficiency, let us first ask ourselves 98  
the following question: how much time can it possibly 99  
take for a good algorithm to simulate a large network? 100  
Suppose there are  $N$  neurons whose average firing 101  
rate is  $F$  and average number of synapses is  $p$ . If all 102  
spike transmissions are taken into account, then a simu- 103  
lation lasting 1 s (biological time) must process  $N \times p \times$  104  
 $F$  spike transmissions. The goal of efficient algorithm 105  
design is to reach this minimal number of operations 106  
(of course, up to a constant multiplicative factor). If 107

108 the simulation is not restricted to spike-mediated in-  
 109 teractions, e.g. if the model includes gap junctions or  
 110 dendro-dendritic interactions, then the optimal num-  
 111 ber of operations can be much larger, but in this re-  
 112 view we chose not to address the problem of graded  
 113 interactions.

114 2.1 A hybrid system formalism

115 Mathematically, neurons can be described as *hybrid*  
 116 *systems*: the state of a neuron evolves continuously  
 117 according to some biophysical equations, which are typ-  
 118 ically differential equations (deterministic or stochastic,  
 119 ordinary or partial differential equations), and spikes  
 120 received through the synapses trigger changes in some  
 121 of the variables. Thus the dynamics of a neuron can be  
 122 described as follows:

$$\frac{d\mathbf{X}}{dt} = f(\mathbf{X})$$

$$\mathbf{X} \leftarrow g_i(\mathbf{X}) \quad \text{upon spike from synapse } i$$

123 where  $\mathbf{X}$  is a vector describing the state of the neuron.  
 124 In theory, taking into account the morphology of the  
 125 neuron would lead to partial differential equations;  
 126 however, in practice, one usually approximates the  
 127 dendritic tree by coupled isopotential compartments,  
 128 which also leads to a differential system with discrete  
 129 events. Spikes are emitted when some threshold con-  
 130 dition is satisfied, for instance  $V_m \geq \theta$  for IF models  
 131 (where  $V_m$  is the membrane potential and would be  
 132 the first component of vector  $\mathbf{X}$ ), and/or  $dV_m/dt \geq \theta$   
 133 for Hodgkin-Huxley (HH) type models. This can be  
 134 summarized by saying that a spike is emitted whenever  
 135 some condition  $\mathbf{X} \in \mathbf{A}$  is satisfied. For IF models, the  
 136 membrane potential, which would be the first compo-  
 137 nent of  $\mathbf{X}$ , is reset when a spike is produced. The reset  
 138 can be integrated into the hybrid system formalism by  
 139 considering for example that outgoing spikes act on  $\mathbf{X}$   
 140 through an additional (virtual) synapse:  $\mathbf{X} \leftarrow g_0(\mathbf{X})$ .

141 With this formalism, it appears clearly that *spike*  
 142 *times need not be stored* (except of course if transmis-  
 143 sion delays are included), even though it would seem  
 144 so from more phenomenological formulations. For ex-  
 145 ample, consider the following IF model (described for  
 146 example in Gütig and Sompolinsky (2006)):

$$V(t) = \sum_i \omega_i \sum_{t_i} K(t - t_i) + V_{\text{rest}}$$

147 where  $V(t)$  is the membrane potential,  $V_{\text{rest}}$  is the  
 148 rest potential,  $\omega_i$  is the synaptic weight of synapse  $i$ ,

$t_i$  are the timings of the spikes coming from synapse 149  
 $i$ , and  $K(t - t_i) = \exp(-(t - t_i)/\tau) - \exp(-(t - t_i)/\tau_s)$  is 150  
 the post-synaptic potential (PSP) contributed by each 151  
 incoming spike. The model can be restated as a two- 152  
 variables differential system with discrete events as 153  
 follows: 154

$$\tau \frac{dV}{dt} = V_{\text{rest}} - V + J$$

$$\tau_s \frac{dJ}{dt} = -J$$

$$J \leftarrow J + \frac{\tau - \tau_s}{\tau} w_i \quad \text{upon spike from synapse } i$$

Virtually all PSPs or currents described in the litera- 155  
 ture (e.g.  $\alpha$ -functions, bi-exponential functions) can be 156  
 expressed this way. Several authors have described the 157  
 transformation from phenomenological expressions to 158  
 the hybrid system formalism for synaptic conductances 159  
 and currents (Destexhe et al. 1994a,b; Rotter and 160  
 Diesmann 1999; Giugliano 2000), short-term synaptic 161  
 depression (Giugliano et al. 1999), and spike-timing- 162  
 dependent plasticity (Song et al. 2000). In many cases, 163  
 the spike response model (Gerstner and Kistler 2002) 164  
 is also the integral expression of a hybrid system. To 165  
 derive the differential formulation of a given post- 166  
 synaptic current or conductance, one way is to see 167  
 the latter as the impulse response of a linear time- 168  
 invariant system [which can be seen as a filter (Jahnke 169  
 et al. 1998)] and use transformation tools from signal 170  
 processing theory such as the Z-transform (Kohn and 171  
 Wörgötter 1998) (see also Sanchez-Montanez 2001) or 172  
 the Laplace transform (the Z-transform is the equiva- 173  
 lent of the Laplace transform in the digital time domain, 174  
 i.e., for synchronous algorithms). 175

2.2 Using linearities for fast synaptic simulation 176

In general, the number of state variables of a neuron 177  
 (length of vector  $\mathbf{X}$ ) scales with the number of synapses, 178  
 since each synapse has its own dynamics. This fact 179  
 constitutes a major problem for efficient simulation of 180  
 neural networks, both in terms of memory consumption 181  
 and computation time. However, several authors have 182  
 observed that all synaptic variables sharing the same 183  
 linear dynamics can be reduced to a single one (Wilson 184  
 and Bower 1989; Bernard et al. 1994; Lytton 1996; 185  
 Song et al. 2000). For example, the following set of 186

187 differential equations, describing an IF model with  $n$   
 188 synapses with exponential conductances:

$$C \frac{dV}{dt} = V_0 - V + \sum_i g_i(t)(V - E_s)$$

$$\tau_s \frac{dg_1}{dt} = -g_1$$

...

$$\tau_s \frac{dg_n}{dt} = -g_n$$

$g_i \leftarrow g_i + w_i$  upon spike arriving at synapse  $i$

189 is mathematically equivalent to the following set of two  
 190 differential equations:

$$C \frac{dV}{dt} = V_0 - V + g(t)(V - E_s)$$

$$\tau_s \frac{dg}{dt} = -g$$

$g \leftarrow g + w_i$  upon spike arriving at synapse  $i$

191 where  $g$  is the total synaptic conductance. The same  
 192 reduction applies to synapses with higher dimensional  
 193 dynamics, as long as it is linear and the spike-triggered  
 194 changes ( $g_i \leftarrow g_i + w_i$ ) are additive and do not depend  
 195 on the state of the synapse (e.g. the rule  $g_i \leftarrow g_i + w_i * f(g_i)$  would cause a problem). Some models of spike-  
 196 timing dependent plasticity (with linear interactions  
 197 between pairs of spikes) can also be simulated in this  
 198 way (see e.g. Abbott and Nelson 2000). However,  
 199 some important biophysical models are not linear and  
 200 thus cannot benefit from this optimization, in particular  
 201 NMDA-mediated interactions and saturating synapses.

203 2.3 Synchronous or clock-driven algorithms

204 In a synchronous or clock-driven algorithm (see  
 205 pseudo-code in Fig. 1), the state variables of all neurons  
 206 (and possibly synapses) are updated at every tick of  
 207 a clock:  $\mathbf{X}(t) \rightarrow \mathbf{X}(t + dt)$ . With non-linear differential  
 208 equations, one would use an integration method such  
 209 as Euler or Runge–Kutta (Press et al. 1993) or, for HH  
 210 models, implicit methods (Hines 1984). Neurons with  
 211 complex morphologies are usually spatially discretized  
 212 and modelled as interacting compartments: they are  
 213 also described mathematically by coupled differential  
 214 equations, for which dedicated integration methods  
 215 have been developed (for details see e.g. the specific  
 216 section of Neuron in this review). If the differential  
 217 equations are linear, then the update operation  $\mathbf{X}(t) \rightarrow$   
 218  $\mathbf{X}(t + dt)$  is also linear, which means updating the state

```

t=0
while t<duration
  for every neuron
    process incoming spikes
    advance neuron dynamics by dt
  end

  for every neuron
    if vm>threshold
      reset neuron
      for every connection
        send spike
      end
    end
  end

  t=t+dt
end
    
```

*State updates*

*Propagation of spikes*

**Fig. 1** A basic clock-driven algorithm

variables amounts simply to multiplying  $\mathbf{X}$  by a matrix:  $\mathbf{X}(t + dt) = \mathbf{A}\mathbf{X}(t)$  (Hirsch and Smale 1974) (see also Rotter and Diesmann 1999, for an application to neural networks), which is very convenient in vector-based scientific softwares such as Matlab or Scilab. Then, after updating all variables, the threshold condition is checked for every neuron. Each neuron that satisfies this condition produces a spike which is transmitted to its target neurons, updating the corresponding variables ( $\mathbf{X} \leftarrow g_i(\mathbf{X})$ ). For IF models, the membrane potential of every spiking neuron is reset.

2.3.1 Computational complexity

The simulation time of such an algorithm consists of two parts: (1) state updates and (2) propagation of spikes. Assuming the number of state variables for the whole network scales with the number of neurons  $N$  in the network (which is the case when the reduction described in Section 2.2 applies), the cost of the update phase is of order  $N$  for each step, so it is  $O(N/dt)$  per second of biological time ( $dt$  is the duration of the time bin). This component grows with the complexity of the neuron models and the precision of the simulation. Every second (biological time), an average of  $F \times N$  spikes are produced by the neurons ( $F$  is the average firing rate), and each of these needs to be propagated to  $p$  target neurons. Thus, the propagation phase consists in  $F \times N \times p$  spike propagations per second. These are essentially additions of weights  $w_i$  to state variables, and thus are simple operations whose cost does not

248 grow with the complexity of the models. Summing up,  
 249 the total computational cost per second of biological  
 250 time is of order

*Update + Propagation*

$$c_U \times \frac{N}{dt} + c_P \times F \times N \times p \quad (*)$$

251 where  $c_U$  is the cost of one update and  $c_P$  is the cost  
 252 of one spike propagation; typically,  $c_U$  is much higher  
 253 than  $c_P$  but this is implementation-dependent. There-  
 254 fore, for very dense networks, the total is dominated  
 255 by the propagation phase and is linear in the number  
 256 of synapses, which is optimal. However, in practice  
 257 the first phase is negligible only when the following  
 258 condition is met:

$$\frac{c_P}{c_U} \times F \times p \times dt \gg 1$$

259 For example, the average firing rate in the cortex might  
 260 be as low as  $F = 1$  Hz (Olshausen and Field 2005),  
 261 and assuming  $p = 10,000$  synapses per neuron and  $dt =$   
 262  $0.1$  ms, we get  $F \times p \times dt = 1$ . In this case, considering  
 263 that each operation in the update phase is heavier  
 264 than in the propagation phase (especially for complex  
 265 models), i.e.,  $c_P < c_U$ , the former is likely to dominate  
 266 the total computational cost. Thus, it appears that even  
 267 in networks with realistic connectivity, increases in pre-  
 268 cision (smaller  $dt$ , see Section 3) can be detrimental to  
 269 the efficiency of the simulation.

270 *2.3.2 Delays*

271 For the sake of simplicity, we ignored transmission  
 272 delays in the description above. However it is not very  
 273 complicated to include them in a synchronous clock-  
 274 driven algorithm. The straightforward way is to store  
 275 the future synaptic events in a circular array. Each  
 276 element of the array corresponds to a time bin and  
 277 contains a list of synaptic events that are scheduled for  
 278 that time (see e.g. Morrison et al. 2005). For example, if  
 279 neuron  $i$  sends a spike to neuron  $j$  with delay  $d$  (in units  
 280 of the time bin  $dt$ ), then the synaptic event " $i \rightarrow j$ " is  
 281 placed in the circular array at position  $p + d$ , where  $p$  is  
 282 the present position. Circularity of the array means the  
 283 addition  $p + d$  is modular ( $(p + d) \bmod n$ , where  $n$  is  
 284 the size of the array—which corresponds to the largest  
 285 delay in the system).

286 What is the additional computational cost of man-  
 287 aging delays? In fact, it is not very high and does not  
 288 depend on the duration of the time bin. Since every  
 289 synaptic event ( $i \rightarrow j$ ) is stored and retrieved exactly

once, the computational cost of managing delays for 1 s 290  
 of biological time is 291

$$c_D \times F \times N \times p$$

where  $c_D$  is the cost of one store and one retrieve opera- 292  
 tion in the circular array (which is low). In other words, 293  
 managing delays increases the cost of the propagation 294  
 phase in equation (\*) by a small multiplicative factor. 295

296 *2.3.3 Exact clock-driven simulation*

297 The obvious drawback of clock-driven algorithms as  
 298 described above is that spike timings are aligned to  
 299 a grid (ticks of the clock), thus the simulation is ap-  
 300 proximate even when the differential equations are  
 301 computed exactly. Other specific errors come from the  
 302 fact that threshold conditions are checked only at the  
 303 ticks of the clock, implying that some spikes might  
 304 be missed (see Section 3). However, in principle, it is  
 305 possible to simulate a network exactly in a clock-driven  
 306 fashion when the minimum transmission delay is larger  
 307 than the time step. It implies that the precise timing  
 308 of synaptic events is stored in the circular array (as  
 309 described in Morrison et al. 2006). Then within each  
 310 time bin, synaptic events for each neuron are sorted  
 311 and processed in the right order, and when the neuron  
 312 spikes, the exact spike timing is calculated. Neurons can  
 313 be processed independently in this way only because  
 314 the time bin is smaller than the smallest transmission  
 315 delay (neurons have no influence on each other within  
 316 one time bin).

317 Some sort of clock signals can also be used in general  
 318 event-driven algorithms without the assumption of a  
 319 minimum positive delay. For example, one efficient  
 320 data structure used in discrete event systems to store  
 321 events is a priority queue known as "calendar queue"  
 322 (Brown 1988), which is a dynamic circular array of  
 323 sorted lists. Each "day" corresponds to a time bin, as  
 324 in a classical circular array, and each event is placed  
 325 in the calendar at the corresponding day; all events on  
 326 a given day are sorted according to their scheduling  
 327 time. If the duration of the day is correctly set, then  
 328 insertions and extractions of events take constant time  
 329 on average. Note that, in contrast with standard clock-  
 330 driven simulations, the state variables are not updated  
 331 at ticks of the clock and the duration of the days de-  
 332 pends neither on the precision of the simulation or on  
 333 the transmission delays (it is rather linked to the rate of  
 334 events)—in fact, the management of the priority queue  
 335 is separated from the simulation itself.

336 Note however that in all these cases, state variables  
 337 need to be updated at the time of every incoming  
 338 spike rather than at every tick of the clock in order

339 to simulate the network exactly (e.g. simple vector-  
 340 based updates  $\mathbf{X} \leftarrow \mathbf{A}\mathbf{X}$  are not possible), so that the  
 341 term *event-driven* may be a better description of these  
 342 algorithms (the precise terminology may vary between  
 343 authors).

344 *2.3.4 Noise in synchronous algorithms*

345 Noise can be introduced in synchronous simulations by  
 346 essentially two means:

- 347 1. Adding random external spikes
- 348 2. Simulating a stochastic process

349 Suppose a given neuron receives  $F$  random spikes  
 350 per second, according to a Poisson process. Then the  
 351 number of spikes in one time bin follows a Poisson  
 352 distribution with mean  $F \times dt$ . Thus one can simulate  
 353 random external spike trains by letting each tick of the  
 354 clock trigger a random number of synaptic updates.  
 355 If  $F \times dt$  is low, the Poisson distribution is almost a  
 356 Bernoulli distribution (i.e., there is one spike with  
 357 probability  $F \times dt$ ). It is straightforward to extend the  
 358 procedure to inhomogeneous Poisson processes by al-  
 359 lowing  $F$  to vary in time. The additional computational  
 360 cost is proportional to  $F_{\text{ext}} \times N$ , where  $F_{\text{ext}}$  is the av-  
 361 erage rate of external synaptic events for each neuron  
 362 and  $N$  is the number of neurons. Note that  $F_{\text{ext}}$  can be  
 363 quite large since it represents the sum of firing rates of  
 364 all external neurons (for example it would be 10,000  
 365 Hz for 10,000 external synapses per neuron with rate  
 366 1 Hz).

367 To simulate a large number of external random  
 368 spikes, it can be advantageous to simulate directly the  
 369 total external synaptic input as a stochastic process, e.g.  
 370 white or colored noise (Ornstein–Uhlenbeck). Linear  
 371 stochastic differential equations are analytically solv-  
 372 able, therefore the update  $\mathbf{X}(t) \rightarrow \mathbf{X}(t + dt)$  can be  
 373 calculated exactly with matrix computations (Arnold  
 374 1974) ( $\mathbf{X}(t + dt)$  is, conditionally to  $\mathbf{X}(t)$ , a normally dis-  
 375 tributed random variable whose mean and covariance  
 376 matrix can be calculated as a function of  $\mathbf{X}(t)$ ). Nonlin-  
 377 ear stochastic differential equations can be simulated  
 378 using approximation schemes, e.g. stochastic Runge–  
 379 Kutta (Honeycutt 1992).

380 *2.4 Asynchronous or event-driven algorithms*

381 Asynchronous or event-driven algorithms are not as  
 382 widely used as clock-driven ones because they are  
 383 significantly more complex to implement (see pseudo-  
 384 code in Fig. 3) and less universal. Their key advantages  
 385 are a potential gain in speed due to not calculating  
 386 many small update steps for a neuron in which no

event arrives and that spike timings are computed 387  
 exactly (but see below for approximate event-driven 388  
 algorithms); in particular, spike timings are not aligned 389  
 to a time grid anymore (which is a source of potential 390  
 errors, see Section 3). 391

The problem of simulating dynamical systems with 392  
 discrete events is a well established research topic 393  
 in computer science (Ferscha 1996; Sloot et al. 1999; 394  
 Fujimoto 2000; Zeigler et al. 2000) (see also Rochel and 395  
 Martinez 2003; Mayrhofer et al. 2002), with appropriate 396  
 data structures and algorithms already available to the 397  
 computational neuroscience community. We start by 398  
 describing the simple case when synaptic interactions 399  
 are instantaneous, i.e., when spikes can be produced 400  
 only at times of incoming spikes (no latency); then we 401  
 will turn to the most general case. 402

2.4.1 *Instantaneous synaptic interactions* 403

In an asynchronous or event-driven algorithm, the sim- 404  
 ulation advances from one event to the next event. 405  
 Events can be spikes coming from neurons in the 406  
 network or external spikes (typically random spikes 407  
 described by a Poisson process). For models in which 408  
 spikes can be produced by a neuron only at times of 409  
 incoming spikes, event-driven simulation is relatively 410  
 easy (see pseudo-code in Fig. 2). Timed events are 411  
 stored in a queue (which is some sort of sorted list). One 412  
 iteration consists in 413

1. Extracting the next event 414
2. Updating the state of the corresponding neuron 415  
 (i.e., calculating the state according to the differ- 416  
 ential equation and adding the synaptic weight) 417
3. Checking if the neuron satisfies the threshold con- 418  
 dition, in which case events are inserted in the 419  
 queue for each downstream neuron 420

```

while queue not empty and t<duration
  extract event with lowest timing      Process event
  (= timing t, target i, weight w)
  compute state of neuron i at time t
  update state of neuron i (+w)
  if vm>threshold
    for each connection i->j          Propagate spike
      insert event in the queue
    end
  reset neuron i
end
end
    
```

**Fig. 2** A basic event-driven algorithm with instantaneous synap-  
 tic interactions

421 In the simple case of identical transmission de-  
 422 lays, the data structure for the queue can be just  
 423 a FIFO queue (first in, first out), which has fast  
 424 implementations (Cormen et al. 2001). When the delays  
 425 take values in a small discrete set, the easiest way is to  
 426 use one FIFO queue for each delay value, as described  
 427 in Mattia and Del Giudice (2000). It is also more  
 428 efficient to use a separate FIFO queue for handling  
 429 random external events (see paragraph about noise  
 430 below).

431 In the case of arbitrary delays, one needs a more  
 432 complex data structure. In computer science, efficient  
 433 data structures to maintain an ordered list of time-  
 434 stamped events are grouped under the name *priority*  
 435 *queues* (Cormen et al. 2001). The topic of priority  
 436 queues is dense and well documented; examples are  
 437 binary heaps, Fibonacci heaps (Cormen et al. 2001),  
 438 calendar queues (Brown 1988; Claverol et al. 2002) or  
 439 van Emde Boas trees (van Emde Boas et al. 1976) (see  
 440 also Connolly et al. 2003, in which various priority  
 441 queues are compared). Using an efficient priority queue  
 442 is a crucial element of a good event-driven algorithm. It  
 443 is even more crucial when synaptic interactions are not  
 444 instantaneous.

445 *2.4.2 Non-instantaneous synaptic interactions*

446 For models in which spike times do not necessarily oc-  
 447 cur at times of incoming spikes, event-driven simulation  
 448 is more complex. We first describe the basic algorithm  
 449 with no delays and no external events (see pseudo-code  
 450 in Fig. 3). One iteration consists in

451 1. Finding which neuron is the next one to spike

```

for every neuron i
    compute timing of next spike           Initialization
    insert event in priority queue
end

while queue not empty and t < duration
    extract event with lowest timing       Process spike
    (event = timing t, neuron i)
    compute state of neuron i at time t
    reset membrane potential
    compute timing of next spike
    insert event in queue

    for every connection i->j           Communicate spike
        compute state of neuron j at time t
        change state with weight w(i,j)
        compute timing of next spike
        insert/change/suppress event in queue
    end
end
    
```

**Fig. 3** A basic event-driven algorithm with non-instantaneous synaptic interactions

2. Updating this neuron 452
3. Propagating the spike, i.e., updating its target 453  
neurons 454

The general way to do that is to maintain a sorted list 455  
 of the future spike timings of all neurons. These spike 456  
 timings are only provisory since any spike in the net- 457  
 work can modify all future spike timings. However, the 458  
 spike with lowest timing in the list is certified. There- 459  
 fore, the following algorithm for one iteration guaran- 460  
 tees the correctness of the simulation (see Fig. 3): 461

1. Extract the spike with lowest timing in the list 462
2. Update the state of the corresponding neuron and 463  
recalculate its future spike timing 464
3. Update the state of its target neurons 465
4. Recalculate the future spike timings of the target 466  
neurons 467

For the sake of simplicity, we ignored transmission 468  
 delays in the description above. Including them in an 469  
 event-driven algorithm is not as straightforward as in a 470  
 clock-driven algorithm, but it is a minor complication. 471  
 When a spike is produced by a neuron, the future 472  
 synaptic events are stored in another priority queue 473  
 in which the timings of events are non-modifiable. 474  
 The first phase of the algorithm (extracting the spike 475  
 with lowest timing) is replaced by extracting the next 476  
 event, which can be either a synaptic event or a spike 477  
 emission. One can use two separate queues or a single 478  
 one. External events can be handled in the same way. 479  
 Although delays introduce complications in coding 480  
 event-driven algorithms, they can in fact simplify the 481  
 management of the priority queue for outgoing spikes. 482  
 Indeed, the main difficulty in simulating networks with 483  
 non-instantaneous synaptic interactions is that sched- 484  
 uled outgoing spikes can be canceled, postponed or 485  
 advanced by future incoming spikes. If transmission 486  
 delays are greater than some positive value  $\tau_{min}$ , then 487  
 all outgoing spikes scheduled in  $[t, t + \tau_{min}]$  ( $t$  being the 488  
 present time) are certified. Thus, algorithms can exploit 489  
 the structure of delays to speed up the simulation (Lee 490  
 and Farhat 2001). 491

492 *2.4.3 Computational complexity*

Putting aside the cost of handling external events 493  
 (which is minor), we can subdivide the computational 494  
 cost of handling one outgoing spike as follows (assum- 495  
 ing  $p$  is the average number of synapses per neuron): 496

- Extracting the event (in case of non-instantaneous 497  
synaptic interactions) 498
- Updating the neuron and its targets:  $p + 1$  updates 499



- 500 • Inserting  $p$  synaptic events in the queue (in case of  
501 delays)
- 502 • Updating the spike times of  $p + 1$  neurons (in case  
503 of non-instantaneous synaptic interactions)
- 504 • Inserting or rescheduling  $p + 1$  events in the queue  
505 (future spikes for non-instantaneous synaptic  
506 interactions)

507 Since there are  $F \times N$  spikes per second of biological  
508 time, the number of operations is approximately pro-  
509 portional to  $F \times N \times p$ . The total computational cost  
510 per second of biological time can be written concisely  
511 as follows:

$$\text{Update} + \text{Spike} + \text{Queue} \\ (c_U + c_S + c_Q) \times F \times N \times p$$

512 where  $c_U$  is the cost of one update of the state variables,  
513  $c_S$  is the cost of calculating the time of the next spike  
514 (non-instantaneous synaptic interactions) and  $c_Q$  is the  
515 average cost of insertions and extractions in the priority  
516 queue(s). Thus, the simulation time is linear in the  
517 number of synapses, which is optimal. Nevertheless, we  
518 note that the operations involved are heavier than in  
519 the propagation phase of clock-driven algorithms (see  
520 previous section), therefore the multiplicative factor is  
521 likely to be larger. We have also assumed that  $c_Q$  is  
522  $O(1)$ , i.e., that the dequeue and enqueue operations can  
523 be done in constant average time with the data struc-  
524 ture chosen for the priority queue. In the simple case of  
525 instantaneous synaptic interactions and homogeneous  
526 delays, one can use a simple FIFO queue (First In,  
527 First Out), in which insertions and extractions are very  
528 fast and take constant time. For the general case, data  
529 structures for which dequeue and enqueue operations  
530 take constant average time ( $O(1)$ ) exist, e.g. calendar  
531 queues (Brown 1988; Claverol et al. 2002), however  
532 they are quite complex, i.e.,  $c_Q$  is a large constant.  
533 In simpler implementations of priority queues such  
534 as binary heaps, the dequeue and enqueue operations  
535 take  $O(\log m)$  operations, where  $m$  is the number of  
536 events in the queue. Overall, it appears that the crucial  
537 component in general event-driven algorithms is the  
538 queue management.

#### 539 2.4.4 What models can be simulated in an event-driven 540 fashion?

541 Event-driven algorithms implicitly assume that we can  
542 calculate the state of a neuron at any given time, i.e., we  
543 have an explicit solution of the differential equations  
544 (but see below for approximate event-driven simula-  
545 tion). This would not be the case with e.g. HH models.  
546 Besides, when synaptic interactions are not instanta-

neous, we also need a function that maps the current 547  
state of the neuron to the timing of the next spike 548  
(possibly  $+\infty$  if there is none). 549

So far, algorithms have been developed for simple 550  
pulse-coupled IF models (Watts 1994; Claverol et al. 551  
2002; Delorme and Thorpe 2003) and more complex 552  
ones such as some instances of the Spike Response 553  
Model (Makino 2003; Marian et al. 2002; Gerstner 554  
and Kistler 2002) (note that the SRM model can 555  
usually be restated in the differential formalism of 556  
Section 2.1). Recently, Djurfeldt et al. (2005) intro- 557  
duced several IF models with synaptic conductances 558  
which are suitable for event-driven simulation. Al- 559  
gorithms were also recently developed by Brette to 560  
simulate exactly IF models with exponential synaptic 561  
currents (Brette 2007) and conductances (Brette 2006), 562  
and (Tonnelier et al., submitted for publication) ex- 563  
tended this work to the quadratic model (Ermentrout 564  
and Kopell 1986). However, there are still efforts to be 565  
made to design suitable algorithms for more complex 566  
models [for example the two-variable IF models of 567  
Izhikevich (2003) and Brette and Gerstner (2005)], or 568  
to develop more realistic models that are suitable for 569  
event-driven simulation. 570

#### 2.4.5 Noise in event-driven algorithms 571

As for synchronous algorithms, there are two ways to 572  
introduce noise in a simulation: (1) adding random 573  
external spikes; (2) simulating a stochastic process. 574

The former case is by far easier in asynchronous 575  
algorithms. It simply amounts to adding a queue with 576  
external events, which is usually easy to implement. For 577  
example, if external spikes are generated according to a 578  
Poisson process with rate  $F$ , the timing of the next event 579  
if random variable with exponential distribution with 580  
 $1/F$ . If  $n$  neurons receive external spike trains given 581  
by independent Poisson processes with rate  $F$ , then the 582  
time of the next event is exponentially distributed with 583  
mean  $1/(nF)$  and the label of the neuron receiving this 584  
event is picked at random in  $\{1, 2, \dots, n\}$ . Inhomoge- 585  
neous Poisson processes can be simulated exactly in 586  
a similar way (Daley and Vere-Jones 1988). If  $r(t)$  is 587  
the instantaneous rate of the Poisson process and is 588  
bounded by  $M$  ( $r(t) \leq M$ ), then one way to generate 589  
a spike train according to this Poisson process in the in- 590  
terval  $[0, T]$  is as follows: generate a spike train in  $[0, T]$  591  
according to a homogeneous Poisson process with rate 592  
 $T * M$ ; for each spike at time  $t_i$ , draw a random number 593  
 $x_i$  from a uniform distribution in  $[0, M]$ ; select all spikes 594  
such that  $x_i \leq r(t_i)$ . 595

Simulating directly a stochastic process in asynchro- 596  
nous algorithms is much harder because even for the 597

598 simplest stochastic neuron models, there is no closed  
 599 analytical formula for the distribution of the time to  
 600 the next spike (see e.g. Tuckwell 1988). It is however  
 601 possible to use precalculated tables when the dynamical  
 602 systems are low dimensional (Reutimann et al. 2003)  
 603 (i.e., not more than 2 dimensions). Note that simu-  
 604 lating noise in this way introduces provisory events  
 605 in the same way as for non-instantaneous synaptic  
 606 interactions.

607 *2.4.6 Approximate event-driven algorithms*

608 We have described asynchronous algorithms for sim-  
 609 ulating neural networks exactly. For complex neuron  
 610 models of the HH type, Lytton and Hines (2005) have  
 611 developed an asynchronous simulation algorithm which  
 612 consists in using for each neuron an independent time  
 613 step whose width is reduced when the membrane po-  
 614 tential approaches the action potential threshold.

615 **3 Precision of different simulation strategies**

616 As shown in this paper, a steadily growing number of  
 617 neural simulation environments does endow computa-  
 618 tional neuroscience with tools which, together with the  
 619 steady improvement of computational hardware, allow  
 620 to simulate neural systems with increasing complexity,  
 621 ranging from detailed biophysical models of single cells  
 622 up to large-scale neural networks. Each of these simula-  
 623 tion tools pursues the quest for a compromise between  
 624 efficiency in speed and memory consumption, flexibility  
 625 in the type of questions addressable, and precision or  
 626 exactness in the numerical treatment of the latter. In  
 627 all cases, this quest leads to the implementation of  
 628 a specific strategy for numerical simulations which is  
 629 found to be optimal given the set of constraints set  
 630 by the particular simulation tool. However, as shown  
 631 recently (Hansel et al. 1998; Lee and Farhat 2001;  
 632 Morrison et al. 2006), quantitative results and their  
 633 qualitative interpretation strongly depend on the sim-  
 634 ulation strategy utilized, and may vary across available  
 635 simulation tools or for different settings within the same  
 636 simulator. The specificity of neuronal simulations is that  
 637 spikes induce either a discontinuity in the dynamics (IF  
 638 models) or have very fast dynamics (HH type models).  
 639 When using approximation methods, this problem can  
 640 be tackled by spike timing interpolation in the former  
 641 case (Hansel et al. 1998; Shelley and Tao 2001) or  
 642 integration with adaptive time step in the latter case  
 643 (Lytton and Hines 2005). Specifically in networks of  
 644 IF neurons, which to date remain almost exclusively  
 645 the basis for accessing dynamics of large-scale neural

populations (but see Section 4.7), crucial differences in  
 the appearance of synchronous activity patterns were  
 observed, depending on the temporal resolution of the  
 neural simulator or the integration method used.

In this section we address this question using one  
 of the most simple analytically solvable leaky IF (LIF)  
 neuron model, namely the classic LIF neuron, de-  
 scribed by the state equation

$$\tau_m \frac{dm(t)}{dt} + m(t) = 0, \tag{1}$$

where  $\tau_m = 20$  ms denotes the membrane time constant  
 and  $0 \leq m(t) \leq 1$ . Upon arrival of a synaptic event at  
 time  $t_0$ ,  $m(t)$  is updated by a constant  $\Delta m = 0.1$  ( $\Delta m =$   
 $0.0085$  in network simulations) after which it decays  
 according to

$$m(t) = m(t_0) \exp \left[ -\frac{t - t_0}{\tau_m} \right]. \tag{2}$$

If  $m$  exceeds a threshold  $m_{thres} = 1$ , the neuron fires and  
 is afterwards reset to a resting state  $m_{rest} = 0$  in which it  
 stays for an absolute refractory period  $t_{ref} = 1$  ms. The  
 neurons were subject to non-plastic or plastic synaptic  
 interactions. In the latter case, spike-timing-dependent  
 synaptic plasticity (STDP) was used according to a  
 model by Song and Abbott (2001). In this case, upon  
 arrival of a synaptic input at time  $t_{pre}$ , synaptic weights  
 are changed according to

$$g \leftarrow g + F(\Delta t) g_{max}, \tag{3}$$

where

$$F(\Delta t) = \pm A_{\pm} \exp\{\pm \Delta t / \tau_{\pm}\} \tag{4}$$

for  $\Delta t = t_{pre} - t_{post} < 0$  and  $\Delta t \geq 0$ , respectively. Here,  
 $t_{post}$  denotes the time of the nearest postsynaptic  
 spike,  $A_{\pm}$  quantify the maximal change of synaptic  
 efficacy, and  $\tau_{\pm}$  determine the range of pre- to postsy-  
 naptic spike intervals in which synaptic weight changes  
 occur. Comparing simulation strategies at the both  
 ends of a wide spectrum, namely a clock-driven algo-  
 rithm (see Section 2.3) and event-driven algorithm (see  
 Section 2.4), we evaluate to which extent the temporal  
 precision of spiking events impacts on neuronal dynam-  
 ics of single as well as small networks. These results  
 support the argument that the speed of neuronal sim-  
 ulations should not be the sole criteria for evaluation of  
 simulation tools, but must complement an evaluation of  
 their exactness.

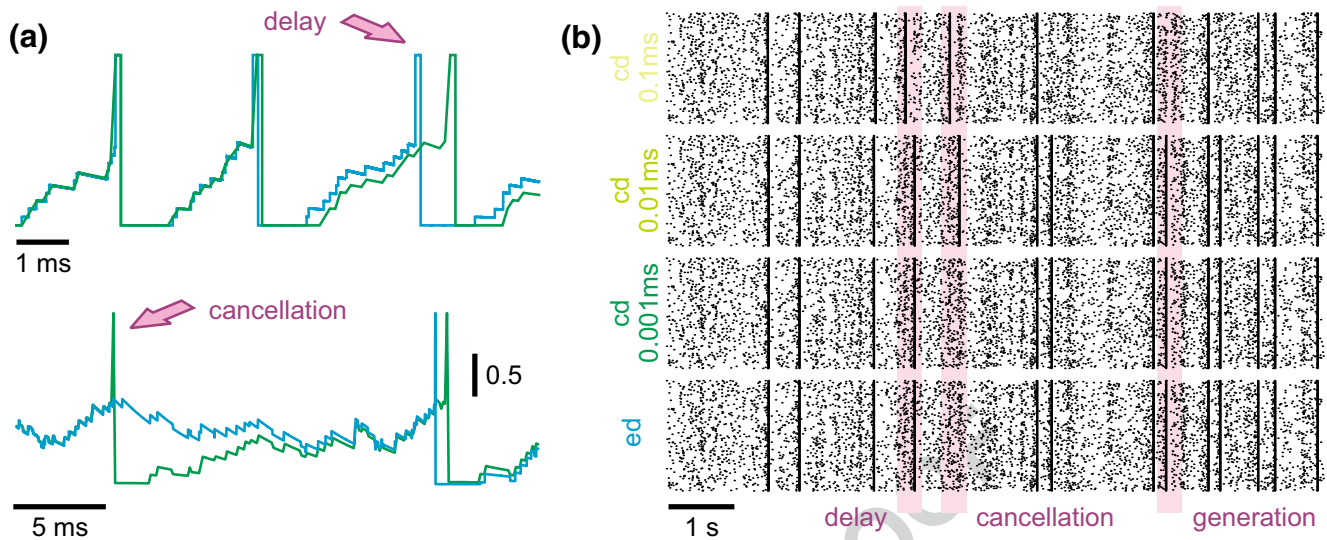


**Fig. 4** Modelling strategies and dynamics in neuronal systems without STDP. **(a)** Small differences in spike times can accumulate and lead to severe delays or even cancellation (see *arrows*) of spikes, depending on the simulation strategy utilized or the temporal resolution within clock-driven strategies used. **(b)** Raster-plots of spike events in a small neuronal network of LIF neurons

simulated with event-driven and clock-driven approaches with different temporal resolutions. Observed differences in neural network dynamics include delays, cancellation or generation of synchronous network events [figure modified from Rudolph and Destexhe (2007)]

B/W IN PRINT

684 3.1 Neuronal systems without STDP

685 In the case of a single LIF neuron with non-plastic  
 686 synapses subject to a frozen synaptic input pattern  
 687 drawn from a Poisson distribution with rate  $v_{inp} =$   
 688 250 Hz, differences in the discharge behavior seen  
 689 in clock-driven simulations at different resolutions  
 690 (0.1 ms, 0.01 ms, 0.001 ms) and event-driven simulations  
 691 occurred already after short periods of simulated neural  
 692 activity (Fig. 4(a)). These deviations were caused by  
 693 subtle differences in the subthreshold integration of  
 694 synaptic input events due to temporal binning, and “de-  
 695 cayed” with a constant which depended on the mem-  
 696 brane time constant. However, for a strong synaptic  
 697 drive, subthreshold deviations could accumulate and  
 698 lead to marked delays in spike times, cancellation of  
 699 spikes or occurrence of additional spikes. Although  
 700 differences at the single cell level remained widely  
 701 constrained and did not lead to changes in the sta-  
 702 tistical characterization of the discharge activity when  
 703 long periods of neural activity were considered, already  
 704 small differences in spike times of individual neurons  
 705 can lead to crucial differences in the population activity,  
 706 such as synchronization (see Hansel et al. 1998; Lee  
 707 and Farhat 2001), if neural networks are concerned.  
 708 We investigated this possibility using a small network  
 709 of 15×15 LIF neurons with all-to-all excitatory con-  
 710 nectivity with fixed weights and not distance-dependent

synaptic transmission delay (0.2 ms), driven by a fixed 711  
 pattern of superthreshold random synaptic inputs to 712  
 each neuron (average rate 250 Hz; weight  $\Delta m = 0.1$ ). In 713  
 such a small network, the activity remained primarily 714  
 driven by the external inputs, i.e. the influence of in- 715  
 trinsic connectivity is small. However, due to small dif- 716  
 ferences in spike times due to temporal binning could 717  
 had severe effects on the occurrence of synchronous 718  
 network events where all (or most) cells discharge at 719  
 the same time. Such events could be delayed, canceled 720  
 or generated depending on the simulation strategy or 721  
 temporal resolution utilized (Fig. 4(b)). 722

3.2 Neuronal systems with STDP 723

The above described differences in the behavior of 724  
 neural systems simulated by using different simulation 725  
 strategies remain constrained to the observed neuronal 726  
 dynamics and are minor if some statistical measures, 727  
 such as average firing rates, are considered. More severe 728  
 effects can be expected if biophysical mechanism 729  
 which depend on the exact times of spikes are incorpo- 730  
 rated into the neural model. One of these mechanism 731  
 is short-term synaptic plasticity, in particular STDP. In 732  
 this case, the self-organizing capability of the neural 733  
 system considered will yield different paths along which 734  
 the systems will develop, and, thus, possibly lead to a 735

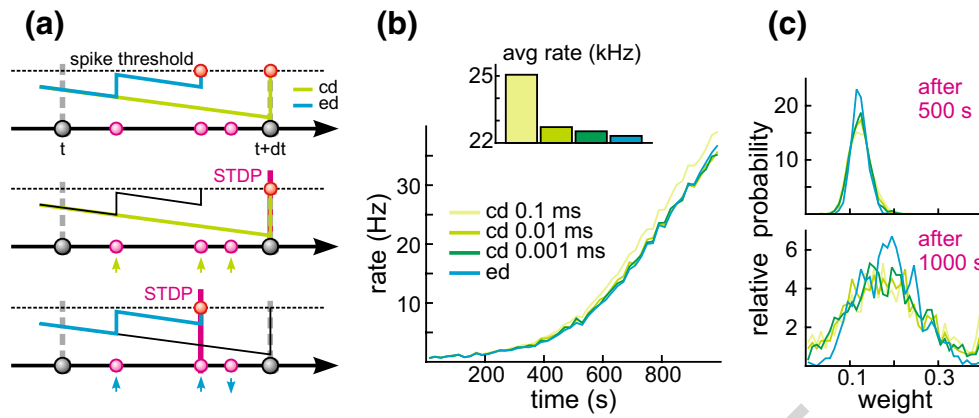


**Fig. 5** Dynamics in neuronal systems with STDP. **(a)** Impact of the simulation strategy (clock-driven: *cd*; event-driven: *ed*) on the facilitation and depression of synapses. **(b)** Time course and average rate (inset) in a LIF model with multiple synaptic

input channels for different simulation strategies and temporal resolution. **(c)** Synaptic weight distribution after 500 and 1,000 s [figure modified from Rudolph and Destexhe (2007)]

B/W IN PRINT

736 neural behavior which not only quantitatively but also  
737 qualitatively may differ across various tools utilized for  
738 the numerical simulation.

739 To explain why such small differences in the ex-  
740 act timing of events are crucial if models with STDP  
741 are considered, consider a situation in which multiple  
742 synaptic input events arrive in between two state up-  
743 dates at  $t$  and  $t + dt$  in a clock-driven simulation. In the  
744 latter case, the times of these events are assigned to the  
745 end of the interval (Fig. 5(a)). In the case these inputs  
746 drive the cell over firing threshold, the synaptic weights  
747 of all three synaptic input channels will be facilitated by  
748 the same amount according to the used STDP model.  
749 In contrast, if exact times are considered, the same  
750 input pattern could cause a discharge already after only  
751 two synaptic inputs. In this case the synaptic weights  
752 linked to these inputs will be facilitated, whereas the  
753 weight of the input arriving after the discharge will be  
754 depressed.

755 Although the chance for the occurrence of situa-  
756 tions such as those described above may appear small,  
757 already one instance will push the considered neural  
758 system onto a different path in its self-organization. The  
759 latter may lead to systems whose qualitative behavior  
760 may, after some time, markedly vary from a system with  
761 the same initial state but simulated by another, tempo-  
762 rally more or less precise simulation strategy. Such a  
763 scenario was investigated by using a single LIF neuron  
764 ( $\tau_m = 4.424$  ms) with 1,000 plastic synapses ( $A_+ = 0.005$ ,  
765  $A_-/A_+ = 1.05$ ,  $\tau_+ = 20$  ms,  $\tau_- = 20$  ms,  $g_{max} = 0.4$ )  
766 driven by the same pattern of Poisson-distributed ran-  
767 dom inputs (average rate 5 Hz,  $\Delta m = 0.1$ ). Simulating  
768 only 1,000 s neural activity led to marked differences  
769 in the temporal development of the average rate be-

tween clock-driven simulations with a temporal resolution of 0.1 ms and event-driven simulations (Fig. 5(b)). Considering the average firing rate over the whole simulated window, clock-driven simulations led to an about 10 % higher value compared to the event-driven approach, and approached the value observed in event-driven simulations only when the temporal resolution was increased by two orders of magnitude. Moreover, different simulation strategies and temporal resolutions led also to a significant difference in the synaptic weight distribution at different times (Fig. 5(c)).

Both findings show that the small differences in the precision of synaptic events can have a severe impact even on statistically very robust measures, such as average rate or weight distribution. Considering the temporal development of individual synaptic weights, both depression and facilitation were observed depending on the temporal precision of the numerical simulation. Indeed, the latter could have severe impact on the qualitative interpretation of the temporal dynamics of structured networks, as this result suggests that synaptic connections in otherwise identical models can be strengthened or weakened due to the influence of the utilized simulation strategy or simulation parameters.

In conclusion, the results presented in this section suggest that the strategy and temporal precision used for neural simulations can severely alter simulated neural dynamics. Although dependent on the neural system modeled, observed differences may turn out to be crucial for the qualitative interpretation of the result of numerical simulations, in particular in simulations involving biophysical processes depending on the exact order or time of spike events (e.g. as in STDP). Thus, the search for an optimal neural simulation tool or

804 strategy for the numerical solution of a given problem  
805 should be guided not only by its absolute speed and  
806 memory consumption, but also its numerical exactness.

## 807 4 Overview of simulation environments

### 808 4.1 NEURON

#### 809 4.1.1 NEURON's domain of utility

810 NEURON is a simulation environment for creating  
811 and using empirically-based models of biological neu-  
812 rons and neural circuits. Initially it earned a reputation  
813 for being well-suited for COBA models of cells with  
814 complex branched anatomy, including extracellular po-  
815 tential near the membrane, and biophysical properties  
816 such as multiple channel types, inhomogeneous chan-  
817 nel distribution, ionic accumulation and diffusion, and  
818 second messengers. In the early 1990s, NEURON was  
819 already being used in some laboratories for network  
820 models with many of thousands of cells, and over the  
821 past decade it has undergone many enhancements that  
822 make the construction and simulation of large-scale  
823 network models easier and more efficient.

824 To date, more than 600 papers and books have de-  
825 scribed NEURON models that range from a membrane  
826 patch to large scale networks with tens of thousands  
827 of COBA or artificial spiking cells.<sup>1</sup> In 2005, over 50  
828 papers were published on topics such as mechanisms  
829 underlying synaptic transmission and plasticity (Banitt  
830 et al. 2005), modulation of synaptic integration by sub-  
831 threshold active currents (Prescott and De Koninck  
832 2005), dendritic excitability (Day et al. 2005), the role  
833 of gap junctions in networks (Migliore et al. 2005),  
834 effects of synaptic plasticity on the development and  
835 operation of biological networks (Saghatelian et al.  
836 2005), neuronal gain (Azouz 2005), the consequences of  
837 synaptic and channel noise for information processing  
838 in neurons and networks (Badoual et al. 2005), cellu-  
839 lar and network mechanisms of temporal coding and  
840 recognition (Kanold and Manis 2005), network states  
841 and oscillations (Wolf et al. 2005), effects of aging  
842 on neuronal function (Markaki et al. 2005), cortical  
843 recording (Moffitt and McIntyre 2005), deep brain stim-  
844 ulation (Grill et al. 2005), and epilepsy resulting from  
845 channel mutations (Vitko et al. 2005) and brain trauma  
846 (Houweling et al. 2005).

4.1.2 How NEURON differs from other 847  
neurosimulators 848

The chief rationale for domain-specific simulators over 849  
general purpose tools lies in the promise of improved 850  
conceptual control, and the possibility of exploiting 851  
the structure of model equations for the sake of com- 852  
putational robustness, accuracy, and efficiency. Some 853  
of the key differences between NEURON and other 854  
neurosimulators are embodied in the way that they 855  
approach these goals. 856

4.1.2.1 Conceptual control The cycle of hypothesis 857  
formulation, testing, and revision, which lies at the 858  
core of all scientific research, presupposes that one can 859  
infer the consequences of a hypothesis. The principal 860  
motivation for computational modeling is its utility for 861  
dealing with hypotheses whose consequences cannot 862  
be determined by unaided intuition or analytical ap- 863  
proaches. The value of any model as a means for eval- 864  
uating a particular hypothesis depends critically on the 865  
existence of a close match between model and hypoth- 866  
esis. Without such a match, simulation results cannot 867  
be a fair test of the hypothesis. From the user's view- 868  
point, the first barrier to computational modeling is the 869  
difficulty of achieving conceptual control, i.e. making 870  
sure that a computational model faithfully reflects one's 871  
hypothesis. 872

NEURON has several features that facilitate con- 873  
ceptual control, and it is acquiring more of them as 874  
it evolves to meet the changing needs of computa- 875  
tional neuroscientists. Many of these features fall into 876  
the general category of "native syntax" specification 877  
of model properties: that is, key attributes of biolog- 878  
ical neurons and networks have direct counterparts 879  
in NEURON. For instance, NEURON users specify 880  
the gating properties of voltage- and ligand-gated ion 881  
channels with kinetic schemes or families of HH style 882  
differential equations. Another example is that models 883  
may include electronic circuits constructed with the 884  
LinearCircuitBuilder, a GUI tool whose palette in- 885  
cludes resistors, capacitors, voltage and current sources, 886  
and operational amplifiers. NEURON's most striking 887  
application of native syntax may lie in how it handles 888  
the cable properties of neurons, which is very differ- 889  
ent from any other neurosimulator. NEURON users 890  
never have to deal directly with compartments. Instead, 891  
cells are represented by unbranched neurites, called 892  
sections, which can be assembled into branched archi- 893  
tectures (the topology of a model cell). Each section has 894  
its own anatomical and biophysical properties, plus a 895

<sup>1</sup><http://www.neuron.yale.edu/neuron/bib/usednrn.html>

896 discretization parameter that specifies the local resolu-  
 897 tion of the spatial grid. The properties of a section can  
 898 vary continuously along its length, and spatially inho-  
 899 mogeneous variables are accessed in terms of normal-  
 900 ized distance along each section (Hines and Carnevale  
 901 1997) (Chapter 5 in Carnevale and Hines 2006). Once  
 902 the user has specified cell topology, and the geometry,  
 903 biophysical properties, and discretization parameter for  
 904 each section, NEURON automatically sets up the inter-  
 905 nal data structures that correspond to a family of ODEs  
 906 for the model's discretized cable equation.

907 **4.1.2.2 Computational robustness, accuracy, and**  
 908 **efficiency** NEURON's spatial discretization of COBA  
 909 model neurons uses a central difference approximation  
 910 that is second order correct in space. The discretization  
 911 parameter for each section can be specified by the user,  
 912 or assigned automatically according to the `d_lambda`  
 913 rule (see Hines and Carnevale 1997) (Chapters 4 and  
 914 5 in Carnevale and Hines 2006).

915 For efficiency, NEURON's computational engine  
 916 uses algorithms that are tailored to the model sys-  
 917 tem equations (Hines 1984, 1989; Hines and Carnevale  
 918 1997). To advance simulations in time, users have a  
 919 choice of built-in clock driven (fixed step backward  
 920 Euler and Crank-Nicholson) and event driven meth-  
 921 ods (global variable step and local variable step with  
 922 second order threshold detection); the latter are based  
 923 on CVODES and IDA from SUNDIALS (Hindmarsh  
 924 et al. 2005). Networks of artificial spiking cells are  
 925 solved analytically by a discrete event method that  
 926 is several orders of magnitude faster than continu-  
 927 ous system simulation (Hines and Carnevale 1997).  
 928 NEURON fully supports hybrid simulations, and mod-  
 929 els can contain any combination of COBA neurons and  
 930 analytically computable artificial spiking cells. Simu-  
 931 lations of networks that contain COBA neurons are  
 932 second order correct if adaptive integration is used  
 933 (Lytton and Hines 2005).

934 Synapse and artificial cell models accept discrete  
 935 events with input stream specific state information. It is  
 936 often extremely useful for artificial cell models to send  
 937 events to themselves in order to implement refractory  
 938 periods and intrinsic firing properties; the delivery time  
 939 of these "self events" can also be adjusted in response  
 940 to intervening events. Thus instantaneous and non-  
 941 instantaneous interactions of Section 2.4 are supported.

942 Built-in synapses exploit the methods described in  
 943 Section 2.2. Arbitrary delay between generation of an  
 944 event at its source, and delivery to the target (including  
 945 0 delay events), is supported by a splay-tree queue

(Sleator and Tarjan 1983) which can be replaced at 946  
 configuration time by a calendar queue. If the minimum 947  
 delay between cells is greater than 0, self events do 948  
 not use the queue and parallel network simulations 949  
 are supported. For the fixed step method, when queue 950  
 handling is the rate limiting step, a bin queue can 951  
 be selected. For the fixed step method with parallel 952  
 simulations, when spike exchange is the rate limiting 953  
 step, six-fold spike compression can be selected. 954

#### 4.1.3 Creating and using models with NEURON 955

Models can be created by writing programs in an in- 956  
 terpreted language based on hoc (Kernighan and Pike 957  
 1984), which has been enhanced to simplify the task of 958  
 representing the properties of biological neurons and 959  
 networks. Users can extend NEURON by writing new 960  
 function and biophysical mechanism specifications in 961  
 the NMODL language, which is then compiled and dy- 962  
 namically linked (Hines and Carnevale 1997) (chapter 9 963  
 in Carnevale and Hines 2006). There is also a powerful 964  
 GUI for conveniently building and using models; this 965  
 can be combined with hoc programming to exploit the 966  
 strengths of both (Fig. 6). 967

The past decade has seen many enhancements to 968  
 NEURON's capabilities for network modeling. First 969  
 and most important was the addition of an event deliv- 970  
 ery system that substantially reduces the computational 971  
 burden of simulating spike-triggered synaptic transmis- 972  
 sion, and enabled the creation of analytic IF cell models 973  
 which can be used in any combination with COBA 974  
 cells. Just in the past year the event delivery system was 975  
 extended so that NEURON can now simulate models 976  
 of networks and cells that are distributed over parallel 977  
 hardware (see NEURON in a parallel environment 978  
 below). 979

**4.1.3.1 The GUI** The GUI contains a large num- 980  
 ber of tools that can be used to construct models, 981  
 exercise simulations, and analyze results, so that no 982  
 knowledge of programming is necessary for the pro- 983  
 ductive use of NEURON. In addition, many GUI tools 984  
 provide functionality that would be quite difficult for 985  
 users to replicate by writing their own code. Some 986  
 examples are: 987

- Model specification tools 988
  - Channel builder—specifies voltage- and ligand- 989
 gated ion channels in terms of ODEs (HH-style, 990

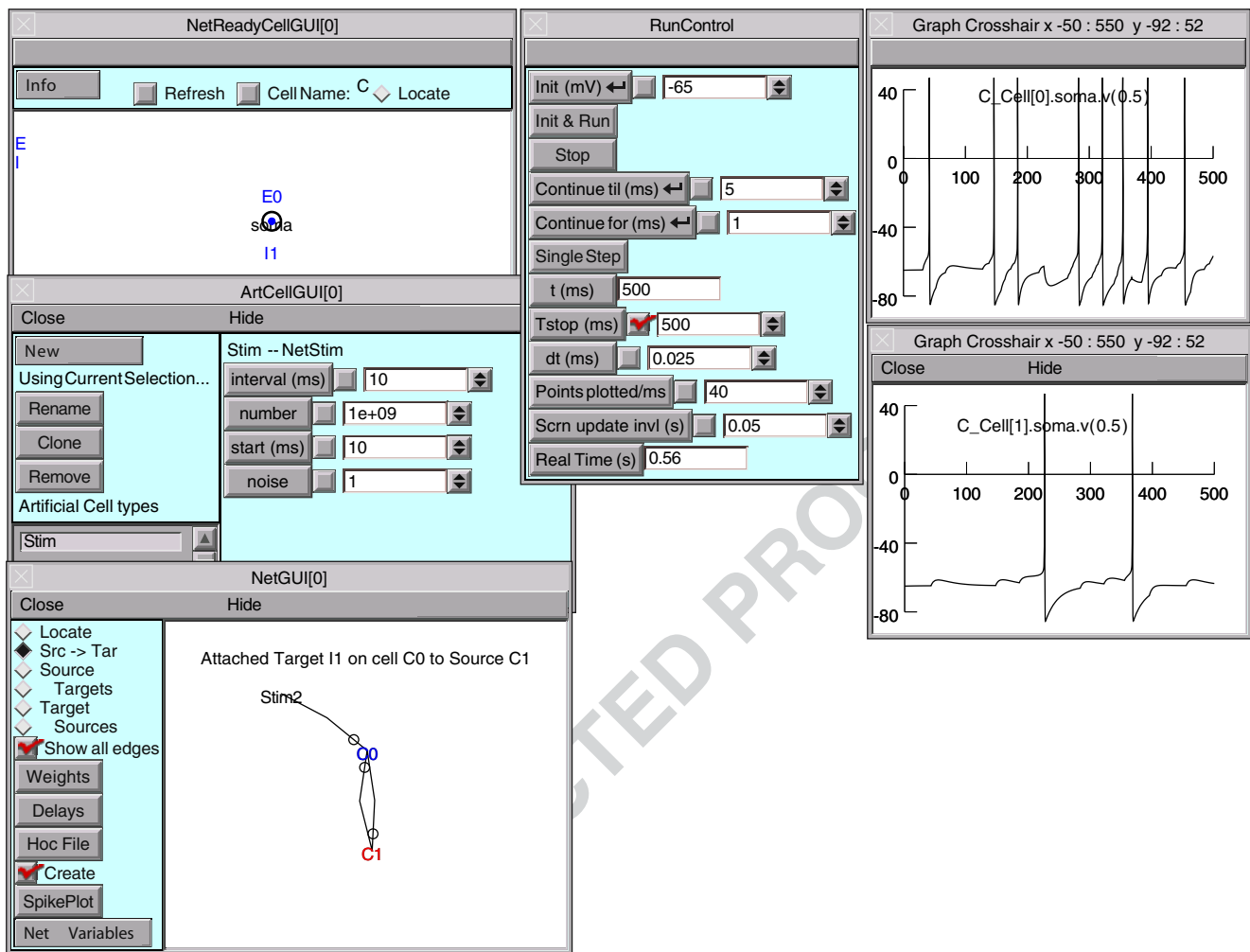


**Fig. 6** NEURON graphical user interface. In developing large scale networks, it is helpful to start by debugging small prototype nets. NEURON's GUI, especially its Network Builder (shown here), can simplify this task. Also, at the click of a button the

Network Builder generates hoc code that can be reused as the building blocks for large scale nets [see Chapter 11, "Modeling networks" in Carnevale and Hines (2006)]

B/W IN PRINT

991 including Borg–Graham formulation) and/or kine- 1005  
 992 tic schemes. Channel states and total conductance 1006  
 993 can be simulated as deterministic (continuous in 1007  
 994 time), or stochastic (countably many channels with 1008  
 995 independent state transitions, producing abrupt 1009  
 996 conductance changes).

997 Cell builder—manages anatomical and biophys- 1009  
 998 ical properties of model cells.

999 Network builder—prototypes small networks 1010  
 1000 that can be mined for reusable code to develop 1011  
 1001 large-scale networks (Chapter 11 in Carnevale and 1012  
 1002 Hines 2006).

1003 Linear circuit builder—specifies models in- 1015  
 1004 volving gap junctions, ephaptic interactions, dual-

electrode voltage clamps, dynamic clamps, and 1005  
 other combinations of neurons and electrical circuit 1006  
 elements. 1007

• Model analysis tools 1008

Import3D—converts detailed morphometric 1009  
 data (Eutectic, NeuroLucida, and SWC formats) 1010  
 into model cells. It automatically fixes many 1011  
 common errors, and helps users identify complex 1012  
 problems that require judgment. 1013

Model view—automatically discovers and 1014  
 presents a summary of model properties in a 1015  
 browsable textual and graphical form. This aids 1016  
 code development and maintenance, and is 1017  
 increasingly important as code sharing grows. 1018

1019 Impedance—compute and display voltage trans-  
 1020 fer ratios, input and transfer impedance, and the  
 1021 electrotonic transformation.  
 1022 • Simulation control tools  
 1023 Variable step control—automatically adjusts the  
 1024 state variable error tolerances that regulate adap-  
 1025 tive integration.  
 1026 Multiple run fitter—optimizes function and  
 1027 model parameters.

1028 *4.1.4 NEURON in a parallel environment*

1029 NEURON supports three kinds of parallel processing.

- 1030 1. Multiple simulations distributed over multiple  
 1031 processors, each processor executing its own sim-  
 1032 ulation. Communication between master processor  
 1033 and workers uses a bulletin-board method similar  
 1034 to Linda (Carriero and Gelernter 1989).
- 1035 2. Distributed network models with gap junctions.

- 1036 3. Distributed models of individual cells (each proces-  
 1037 sor handles part of the cell). At present, setting  
 1038 up distributed models of individual cells requires  
 1039 considerable effort; in the future it will be made  
 1040 much more convenient.

The four benchmark simulations of spiking neural  
 networks (see Appendix B) were implemented under  
 NEURON. Figure 7(a) demonstrates the speedup that  
 NEURON can achieve with distributed network mod-  
 els of the four types [COBA, current-based (CUBA),  
 HH, event-based—see Appendix B] on a Beowulf clus-  
 ter (dashed lines are “ideal” – run time inversely pro-  
 portional to number of CPUs – and solid symbols are  
 actual run times). Figure 7(b) shows that performance  
 improvement scales with the number of processors and  
 the size and complexity of the network; for this figure  
 we ran a series of tests using a NEURON implemen-  
 tation of the single column thalamocortical network  
 model described by Traub et al. (2005) on the Cray

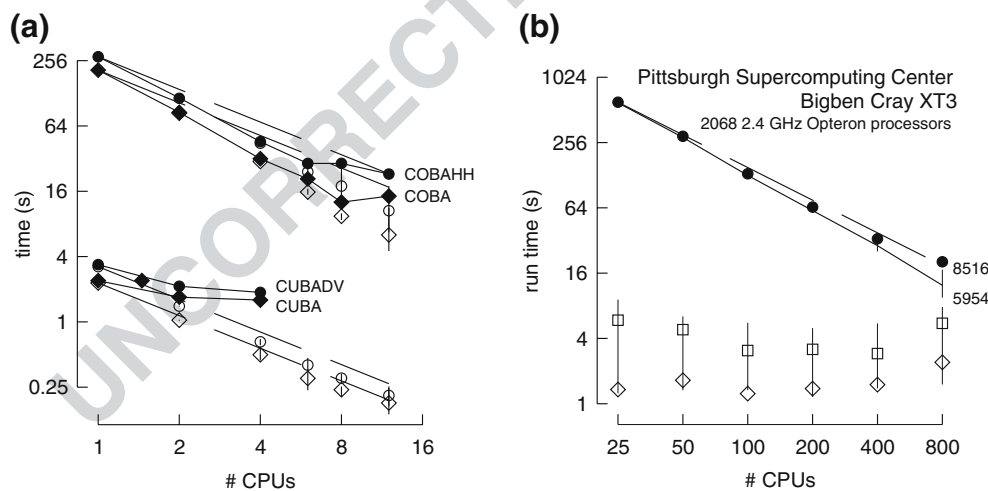


**Fig. 7** Parallel simulations using NEURON. **(a)** Four benchmark network models were simulated on 1, 2, 4, 6, 8, and 12 CPUs of a Beowulf cluster (6 nodes, dual CPU, 64-bit 3.2 GHz Intel Xeon with 1024 KB cache). *Dashed lines* indicate “ideal speedup” (run time inversely proportional to number of CPUs). *Solid symbols* are run time, *open symbols* are average computation time per CPU, and *vertical bars* indicate variation of computation time. The CUBA and CUBADV models execute so quickly that little is gained by parallelizing them. The CUBA model is faster than the more efficient CUBADV because the latter generates twice as many spikes (spike counts are COBAHH 92,219, COBA 62,349, CUBADV 39,280, CUBA 15,371). **(b)** The Pittsburgh Supercomputing Center’s Cray XT3 (2.4 GHz Opteron processors) was used to simulate a NEURON implementation of the thalamocortical network model of Traub et al. (2005). This model has 3,560 cells in 14 types, 3,500 gap junctions, 5,596,810 equa-

tions, and 1,122,520 connections and synapses, and 100 ms of model time it generates 73,465 spikes and 19,844,187 delivered spikes. The *dashed line* indicates “ideal speedup” and *solid circles* are the actual run times. The *solid black line* is the average computation time, and the *intersecting vertical lines* mark the range of computation times for each CPU. Neither the number of cell classes nor the number of cells in each class were multiples of the number of processors, so load balance was not perfect. When 800 CPUs were used, the number of equations per CPU ranged from 5954 to 8516. *Open diamonds* are average spike exchange times. *Open squares* mark average voltage exchange times for the gap junctions, which must be done at every time step; these lie on *vertical bars* that indicate the range of voltage exchange times. This range is large primarily because of synchronization time due to computation time variation across CPUs. The minimum value is the actual exchange time



1055 XT3 at the Pittsburgh Supercomputer Center. Similar  
 1056 performance gain has been documented in extensive  
 1057 tests on parallel hardware with dozens to thousands of  
 1058 CPUs, using published models of networks of conduc-  
 1059 tance based neurons (Migliore et al. 2006). Speedup is  
 1060 linear with the number of CPUs, or even superlinear  
 1061 (due to larger effective high speed memory cache), until  
 1062 there are so many CPUs that each one is solving fewer  
 1063 than 100 equations.

1064 *4.1.5 Future plans*

1065 NEURON undergoes a continuous cycle of improve-  
 1066 ment and revision, much of which is devoted to as-  
 1067 pects of the program that are not immediately obvious  
 1068 to the user, e.g. improvement of computational effi-  
 1069 ciency. More noticeable are new GUI tools, such as  
 1070 the recently added Channel Builder. Many of these  
 1071 tools exemplify a trend toward “form-based” model  
 1072 specification, which is expected to continue. The use of  
 1073 form-based GUI tools increases the ability to exchange  
 1074 model specifications with other simulators through the  
 1075 medium of Extensible Markup Language (XML). With  
 1076 regard to network modeling, the emphasis will shift  
 1077 away from developing simulation infrastructure, which  
 1078 is reasonably complete, to the creation of new tools for  
 1079 network design and analysis.

1080 *4.1.6 Software development, support,  
 1081 and documentation*

1082 Michael Hines directs the NEURON project, and  
 1083 is responsible for almost all code development. The  
 1084 other members of the development team have varying  
 1085 degrees of responsibility for activities such as docu-  
 1086 mentation, courses, and user support. NEURON has  
 1087 benefited from significant contributions of time and  
 1088 effort by members of the community of NEURON  
 1089 users who have worked on specific algorithms, written  
 1090 or tested new code, etc. Since 2003, user contributions  
 1091 have been facilitated by adoption of an “open source  
 1092 development model” so that source code, including the  
 1093 latest research threads, can be accessed from an on-line  
 1094 repository.<sup>2</sup>

1095 Support is available by email, telephone, and consul-  
 1096 tation. Users can also post questions and share informa-  
 1097 tion with other members of the NEURON community  
 1098 via a mailing list and The NEURON Forum.<sup>3</sup> Currently  
 1099 the mailing list has more than 700 subscribers with

“live” email addresses; the Forum, which was launched 1100  
 in May, 2005, has already grown to 300 registered users 1101  
 and 1700 posted messages. 1102

Tutorials and reference material are available.<sup>4</sup> The 1103  
 NEURON Book (Carnevale and Hines 2006) is the 1104  
 authoritative book on NEURON. Four books by 1105  
 other authors have made extensive use of NEURON 1106  
 (Destexhe and Sejnowski 2001; Johnston and Wu 1995; 1107  
 Lytton 2002; Moore and Stuart 2000), and several of 1108  
 them have posted their code online or provide it on CD 1109  
 with the book. 1110

Source code for published NEURON models is 1111  
 available at many WWW sites. The largest code archive 1112  
 is ModelDB,<sup>5</sup> which currently contains 238 models, 152 1113  
 of which were implemented with NEURON. 1114

*4.1.7 Software availability* 1115

NEURON runs under UNIX/Linux/OS X, MSWin 98 1116  
 or later, and on parallel hardware including Beowulf 1117  
 clusters, the IBM Blue Gene and Cray XT3. NEURON 1118  
 source code and installers are provided free of charge,<sup>6</sup> 1119  
 and the installers do not require “third party” software. 1120  
 The current standard distribution is version 5.9.39. The 1121  
 alpha version can be used as a simulator/controller 1122  
 in dynamic clamp experiments under real-time Linux<sup>7</sup> 1123  
 with a National Instruments M series DAQ card. 1124

4.2 GENESIS 1125

*4.2.1 GENESIS capabilities and design philosophy* 1126

GENESIS (the General Neural Simulation System) 1127  
 was given its name because it was designed, at the 1128  
 outset, be an extensible general simulation system 1129  
 for the realistic modeling of neural and biological 1130  
 systems (Bower and Beeman 1998). Typical simula- 1131  
 tions that have been performed with GENESIS range 1132  
 from subcellular components and biochemical reac- 1133  
 tions (Bhalla 2004) to complex models of single neu- 1134  
 rons (De Schutter and Bower 1994), simulations of 1135  
 large networks (Nenadic et al. 2003), and systems-level 1136  
 models (Stricanne and Bower 1998). Here, “realistic 1137  
 models” are defined as those models that are based on 1138  
 the known anatomical and physiological organization 1139  
 of neurons, circuits and networks (Bower 1995). For 1140  
 example, realistic cell models typically include dendritic 1141

<sup>2</sup><http://www.neuron.yale.edu/neuron/install.html>  
<sup>3</sup><https://www.neuron.yale.edu/phpBB2/index.php>

<sup>4</sup><http://www.neuron.yale.edu/neuron/docs/docs.html>  
<sup>5</sup><http://senselab.med.yale.edu/senselab/ModelDB>  
<sup>6</sup><http://www.neuron.yale.edu>  
<sup>7</sup><http://rtai.org>

1142 morphology and a large variety of ionic conductances,  
1143 whereas realistic network models attempt to duplicate  
1144 known axonal projection patterns.

1145 Parallel GENESIS (PGENESIS) is an extension  
1146 to GENESIS that runs on almost any parallel clus-  
1147 ter, SMP, supercomputer, or network of workstations  
1148 where MPI and/or PVM is supported, and on which  
1149 serial GENESIS itself is runnable. It is customarily  
1150 used for large network simulations involving tens of  
1151 thousands of realistic cell models (for example, see  
1152 Hereld et al. 2005).

1153 GENESIS has a well-documented process for users  
1154 themselves to extend its capabilities by adding new  
1155 user-defined GENESIS object types (classes), or script  
1156 language commands without the need to understand  
1157 or modify the GENESIS simulator code. GENESIS  
1158 comes already equipped with mechanisms to easily  
1159 create large scale network models made from sin-  
1160 gle neuron models that have been implemented with  
1161 GENESIS.

1162 While users have added, for example, the Izhikevich  
1163 (2003) simplified spiking neuron model (now built in to  
1164 GENESIS), and they could also add IF or other forms  
1165 of abstract neuron models, these forms of neurons are  
1166 not realistic enough for the interests of most GENESIS  
1167 modelers. For this reason, GENESIS is not normally  
1168 provided with IF model neurons, and no GENESIS  
1169 implementations have been provided for the IF model  
1170 benchmarks (see Appendix B). Typical GENESIS  
1171 neurons are multicompartmental models with a vari-  
1172 ety of HH type voltage- and/or calcium-dependent  
1173 conductances.

#### 1174 4.2.2 Modeling with GENESIS

1175 GENESIS is an object-oriented simulation system, in  
1176 which a simulation is constructed of basic building  
1177 blocks (GENESIS elements). These elements commu-  
1178 nicate by passing messages to each other, and each  
1179 contains the knowledge of its own variables (fields) and  
1180 the methods (actions) used to perform its calculations  
1181 or other duties during a simulation. GENESIS elements  
1182 are created as instantiations of a particular precompiled  
1183 object type that acts as a template. Model neurons  
1184 are constructed from these basic components, such  
1185 as neural compartments and variable conductance ion  
1186 channels, linked with messages. Neurons may be linked  
1187 together with synaptic connections to form neural cir-  
1188 cuits and networks. This object-oriented approach is  
1189 central to the generality and flexibility of the system, as  
1190 it allows modelers to easily exchange and reuse models  
1191 or model components. Many GENESIS users base their  
1192 simulation scripts on the examples that are provided

with GENESIS or in the GENESIS Neural Modeling 1193  
Tutorials package (Beeman 2005). 1194

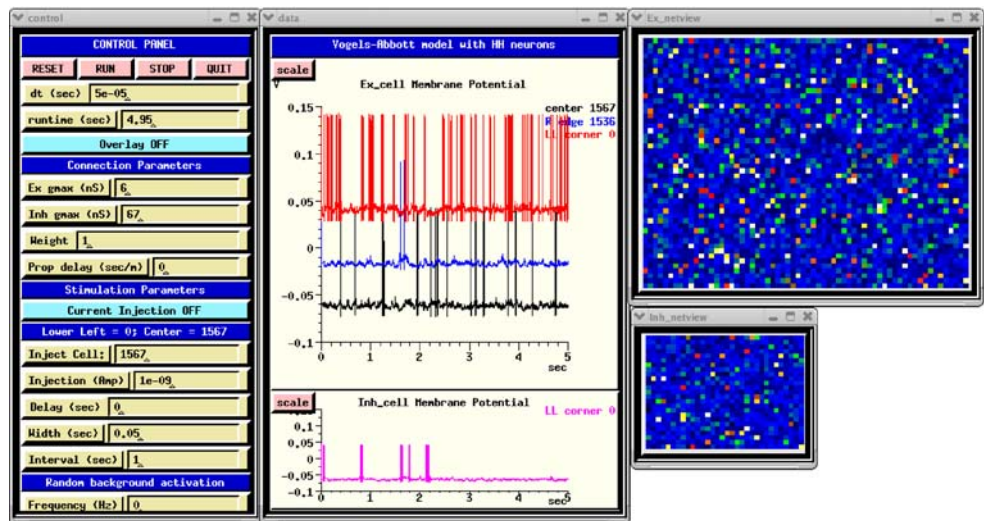
1195 GENESIS uses an interpreter and a high-level sim- 1195  
ulation language to construct neurons and their net- 1196  
works. This use of an interpreter with pre-compiled 1197  
object types, rather than a separate step to compile 1198  
scripts into binary machine code, gives the advantage of 1199  
allowing the user to interact with and modify a simula- 1200  
tion while it is running, with no sacrifice in simulation 1201  
speed. Commands may be issued either interactively 1202  
to a command prompt, by use of simulation scripts, 1203  
or through the graphical interface. The 268 scripting 1204  
language commands and the 125 object types provided 1205  
with GENESIS are powerful enough that only a few 1206  
lines of script are needed to specify a sophisticated 1207  
simulation. For example, the GENESIS “cell reader” 1208  
allows one to build complex model neurons by reading 1209  
their specifications from a data file. 1210

1211 GENESIS provides a variety of mechanisms to 1211  
model calcium diffusion and calcium-dependent con- 1212  
ductances, as well as synaptic plasticity. There are also 1213  
a number of “device objects” that may be interfaced 1214  
to a simulation to provide various types of input to 1215  
the simulation (pulse and spike generators, voltage 1216  
clamp circuitry, etc.) or measurements (peristimulus 1217  
and interspike interval histograms, spike frequency 1218  
measurements, auto- and cross-correlation histograms, 1219  
etc.). Object types are also provided for the modeling 1220  
of biochemical pathways (Bhalla and Iyengar 1999). 1221  
A list and description of the GENESIS object types, 1222  
with links to full documentation, may be found in the 1223  
“Objects” section of the hypertext *GENESIS Reference* 1224  
*Manual*, downloadable or viewable from the GENESIS 1225  
web site. 1226

#### 4.2.3 GENESIS graphical user interfaces 1227

1228 Very large scale simulations are often run with no 1228  
GUI, with the simulation output to either text or bi- 1229  
nary format files for later analysis. However, GENESIS 1230  
is usually compiled to include its graphical interface 1231  
XODUS, which provides object types and script-level 1232  
commands for building elaborate graphical interfaces, 1233  
such as the one shown in Fig. 8 for the dual ex- 1234  
ponential variation of the HH benchmark simulation 1235  
(Benchmark 3 in Appendix B). GENESIS also con- 1236  
tains graphical environments for building and run- 1237  
ning simulations with no scripting, such as Neurokit 1238  
(for single cells) and Kinetikit (for modeling bio- 1239  
chemical reactions). These are themselves created as 1240  
GENESIS scripts, and can be extended or modified. 1241  
This allows for the creation of the many educational 1242

**Fig. 8** The GUI for the GENESIS implementation of the HH benchmark, using the dual-exponential form of synaptic conductance



B/W IN PRINT

1243 tutorials that are included with the GENESIS distrib-  
1244 ution (Bower and Beeman 1998).

1245 *4.2.4 Obtaining GENESIS and user support*

1246 GENESIS and its graphical front-end XODUS are  
1247 written in C and are known to run under most Linux  
1248 or UNIX-based systems with the X Window System, as  
1249 well as Mac OS/X and MS Windows with the Cygwin  
1250 environment. The current release of GENESIS and  
1251 PGENESIS (ver. 2.3, March 17, 2006) is available from  
1252 the GENESIS web site<sup>8</sup> under the GNU General Pub-  
1253 lic License. The GENESIS source distribution contains  
1254 full source code and documentation, as well as a large  
1255 number of tutorial and example simulations. Documen-  
1256 tation for these tutorials is included along with online  
1257 GENESIS help files and the hypertext GENESIS Ref-  
1258 erence Manual. In addition to the source distribution,  
1259 precompiled binary versions are available for Linux,  
1260 Mac OS/X, and Windows with Cygwin. The GENESIS  
1261 Neural Modeling Tutorials (Beeman 2005) are a set  
1262 of HTML tutorials intended to teach the process of  
1263 constructing biologically realistic neural models with  
1264 the GENESIS simulator, through the analysis and mod-  
1265 ification of provided example simulation scripts. The  
1266 latest version of this package is offered as a separate  
1267 download from the GENESIS web site.

1268 Support for GENESIS is provided through email to  
1269 <http://www.genesis@genesis-sim.org>, and through the  
1270 GENESIS Users Group, BABEL. Members of BA-  
1271 BEL receive announcements and exchange informa-  
1272 tion through a mailing list, and are entitled to access the

BABEL web page. This serves as a repository for the 1273  
latest contributions by GENESIS users and developers, 1274  
and contains hypertext archives of postings from the 1275  
mailing list. 1276

Rallpacks are a set of benchmarks for evaluating 1277  
the speed and accuracy of neuronal simulators for 1278  
the construction of single cell models (Bhalla et al. 1279  
1992). However, it does not provide benchmarks for 1280  
network models. The package contains scripts for both 1281  
GENESIS and NEURON, as well as full specifications 1282  
for implementation on other simulators. It is included 1283  
within the GENESIS distribution, and is also available 1284  
for download from the GENESIS web site. 1285

1286 *4.2.5 GENESIS implementation of the HH benchmark*

The HH benchmark network model (Benchmark 3 in 1287  
Appendix B) provides a good example of the type of 1288  
model that should probably NOT be implemented with 1289  
GENESIS. The Vogels and Abbott (2005) IF network 1290  
on which it is based is an abstract model designed to 1291  
study the propagation of signals under very simplified 1292  
conditions. The identical excitatory and inhibitory neu- 1293  
rons have no physical location in space, and no distance- 1294  
dependent axonal propagation delays in the connections. 1295  
The benchmark model simply replaces the IF neurons 1296  
with single-compartment cells containing fast sodium 1297  
and delayed rectifier potassium channels that fire toni- 1298  
cally and display no spike frequency adaptation. Such 1299  
models offer no advantages over IF cells for the study 1300  
of the situation explored by Vogels and Abbott. 1301

Nevertheless, it is a simple matter to implement such 1302  
a model in GENESIS, using a simplification of exist- 1303  
ing example scripts for large network models, and the 1304

<sup>8</sup><http://www.genesis-sim.org/GENESIS>

1305 performance penalty for “using a sledge hammer to  
1306 crack a peanut” is not too large for a network of this  
1307 size. The simulation script for this benchmark illustrates  
1308 the power of the GENESIS scripting commands for  
1309 creating networks. Three basic commands are used for  
1310 filling a region with copies of prototype cells, making  
1311 synaptic connections with a great deal of control over  
1312 the connectivity, and setting propagation delays.

1313 The instantaneous rise in the synaptic conductances  
1314 makes this a very efficient model to implement with  
1315 a simulator specialized for IF networks, but such a  
1316 non-biological conductance is not normally provided  
1317 by GENESIS. Therefore, two implementations of the  
1318 benchmark have been provided. The Dual Exponential  
1319 VA HH Model script implements synaptic conduc-  
1320 tances with a dual exponential form having a 2 ms time-  
1321 to-peak, and the specified exponential decay times of  
1322 5 ms for excitatory connections and 10 ms for inhibitory  
1323 connections. The Instantaneous Conductance VA HH  
1324 Model script uses a user-added *isynchan* object type  
1325 that can be compiled and linked into GENESIS to  
1326 provide the specified conductances with an instanta-  
1327 neous rise time. There is little difference in the behavior  
1328 of the two versions of the simulation, although the  
1329 Instantaneous Conductance model executes somewhat  
1330 faster.

1331 Figure 8 shows the implementation of the Dual Ex-  
1332ponential VA HH Model with a GUI that was cre-  
1333ated by making small changes to the example *RSnet.g*,  
1334 *protodefs.g*, and *graphics.g* scripts, which are provided  
1335 in the *GENESIS Modeling Tutorial* (Beeman 2005)  
1336 section “Creating large networks with GENESIS”.

1337 These scripts and the tutorial specify a rectangu-  
1338lar grid of excitatory neurons. An exercise suggests  
1339adding an additional layer of inhibitory neurons. The  
1340 GENESIS implementations of the HH benchmark use

a layer of  $64 \times 50$  excitatory neurons and a layer of  
1341  $32 \times 25$  inhibitory neurons. A change of one line in  
1342 the example *RSnet.g* script allows the change from the  
1343 nearest-neighbor connectivity of the model to the re-  
1344 quired infinite-range connectivity with 2% probability.  
1345

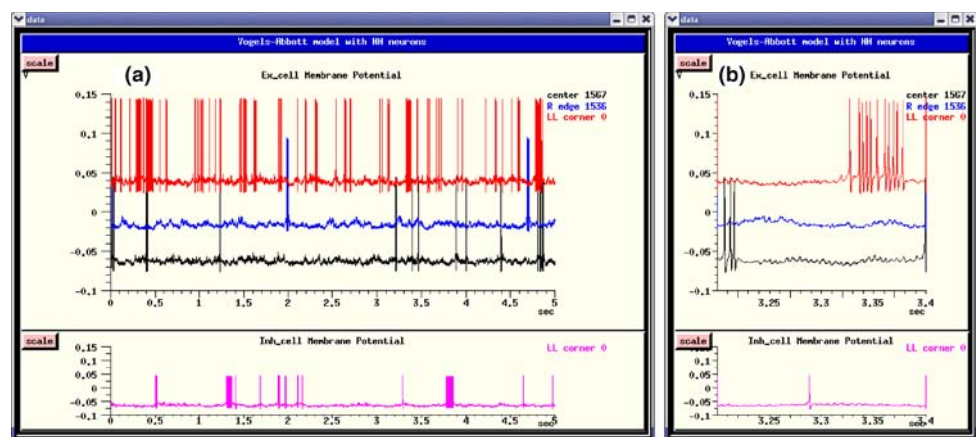
The identical excitatory and inhibitory neurons  
1346 used in the network are implemented as specified in  
1347 Appendix B. For both versions of the model, Poisson-  
1348 distributed random spike inputs with a mean frequency  
1349 of 70 Hz were applied to the excitatory synapses of the  
1350 all excitatory neurons. The the simulation was run for  
1351 0.05 s, the random input was removed, and it was then  
1352 run for an additional 4.95 s.  
1353

The Control Panel at the left is used to run the sim-  
1354 ulation and to set parameters such as maximal synaptic  
1355 conductances, synaptic weight scaling, and propagation  
1356 delays. There are options to provide current injection  
1357 pulses, as well as random synaptic activation. The plots  
1358 in the middle show the membrane potentials of three  
1359 excitatory neurons (0, 1536, and 1567), and inhibitory  
1360 neuron 0. The netview displays at the right show the  
1361 membrane potentials of the excitatory neurons (top)  
1362 and inhibitory neurons (bottom). With no propagation  
1363 delays, the positions of the neurons on the grid are  
1364 irrelevant. Nevertheless, this two-dimensional repre-  
1365 sentation of the network layers makes it easy to visu-  
1366 alize the number of cells firing at any time during the  
1367 simulation.  
1368

Figure 9 shows the plots for the membrane potential  
1369 of the same neurons as those displayed in Fig. 8, but  
1370 produced by the Instantaneous Conductance VA HH  
1371 Model script. The plot at the right shows a zoom of the  
1372 interval between 3.2 and 3.4 s.  
1373

In both figures, excitatory neuron 1536 has the  
1374 lowest ratio of excitatory to inhibitory inputs of the  
1375 four neurons plotted. It fires only rarely, whereas  
1376

**Fig. 9** Membrane potentials for four selected neurons of the Instantaneous Conductance VA HH Model in GENESIS. (a) The entire 5 s of the simulation. (b) Detail of the interval 3.2–3.4 s



1377 excitatory neuron 0, which has the highest ratio, fires  
1378 most frequently.

#### 1379 4.2.6 Future plans for GENESIS

1380 The GENESIS simulator is now undergoing a major  
1381 redevelopment effort, which will result in GENESIS  
1382 3. The core simulator functionality is being reim-  
1383 plemented in C++ using an improved scheme for  
1384 messaging between GENESIS objects, and with a  
1385 platform-independent and browser-friendly Java-based  
1386 GUI. This will result in not only improved perfor-  
1387 mance and portability to MS Windows and non-UNIX  
1388 platforms, but will also allow the use of alternate  
1389 script parsers and user interfaces, as well as the ability  
1390 to communicate with other modeling programs and  
1391 environments. The GENESIS development team is  
1392 participating in the NeuroML (Goddard et al. 2001;  
1393 Crook et al. 2005) project,<sup>9</sup> along with the devel-  
1394 opers of NEURON. This will enable GENESIS 3  
1395 to export and import model descriptions in a com-  
1396 mon simulator-independent XML format. Develop-  
1397 ment versions of GENESIS are available from the  
1398 Sourceforge GENESIS development site.<sup>10</sup>

#### 1399 4.3 NEST

##### 1400 4.3.1 The NEST initiative

1401 The problem of simulating neuronal networks of bi-  
1402 ologically realistic size and complexity has long been  
1403 underestimated. This is reflected in the limited num-  
1404 ber of publications on suitable algorithms and data  
1405 structures in high-level journals. The lack of awareness  
1406 of researchers and funding agencies of the need for  
1407 progress in simulation technology and sustainability of  
1408 the investments may partially originate from the fact  
1409 that a mathematically correct simulator for a particular  
1410 neuronal network model can be implemented by an  
1411 individual in a few days. However, this has routinely re-  
1412 sulted in a cycle of unscalable and unmaintainable code  
1413 being rewritten in unmaintainable fashion by novices,  
1414 with little progress in the theoretical foundations.

1415 Due to the increased availability of computational  
1416 resources, simulation studies are becoming ever more  
1417 ambitious and popular. Indeed, many neuroscientific  
1418 questions are presently only accessible through sim-  
1419 ulation. An unfortunate consequence of this trend is  
1420 that it is becoming ever harder to reproduce and verify

the results of these studies. The ad hoc simulation 1421  
tools of the past cannot provide us with the appro- 1422  
priate degree of comprehensibility. Instead we require 1423  
carefully crafted, validated, documented and expressive 1424  
neuronal network simulators with a wide user commu- 1425  
nity. Moreover, the current progress towards more re- 1426  
alistic models demands correspondingly more efficient 1427  
simulations. This holds especially for the nascent field 1428  
of studies on large-scale network models incorporating 1429  
plasticity. This research is entirely infeasible without 1430  
parallel simulators with excellent scaling properties, 1431  
which is outside the scope of ad hoc solutions. Fi- 1432  
nally, to be useful to a wide scientific audience over a 1433  
long time, simulators must be easy to maintain and to 1434  
extend. 1435

On the basis of these considerations, the NEST ini- 1436  
tiative was founded as a long term collaborative project 1437  
to support the development of technology for neural 1438  
systems simulations (Diesmann and Gewaltig 2002). 1439  
The NEST simulation tool is the reference implemen- 1440  
tation of this initiative. The software is provided to 1441  
the scientific community under an open source license 1442  
through the NEST initiative's website.<sup>11</sup> The license 1443  
requests researchers to give reference to the initiative in 1444  
work derived from the original code and, more impor- 1445  
tantly, in scientific results obtained with the software. 1446  
The website also provides references to material rel- 1447  
evant to neuronal network simulations in general and 1448  
is meant to become a scientific resource of network 1449  
simulation information. Support is provided through 1450  
the NEST website and a mailing list. At present NEST 1451  
is used in teaching at international summer schools and 1452  
in regular courses at the University of Freiburg. 1453

##### 4.3.2 The NEST simulation tool 1454

In the following we give a brief overview of the NEST 1455  
simulation tool and its capabilities. 1456

**4.3.2.1 Domain and design goals** The domain of 1457  
NEST is large neuronal networks with biologically re- 1458  
alistic connectivity. The software easily copes with the 1459  
threshold network size of  $10^5$  neurons (Morrison et 1460  
al. 2005) at which each neuron can be supplied with 1461  
the natural number of synapses and simultaneously a 1462  
realistic sparse connectivity can be maintained. Typical 1463  
neuron models in NEST have one or a small number of 1464  
compartments. The simulator supports heterogeneity 1465  
in neuron and synapse types. In networks of realistic 1466  
connectivity the memory consumption and work load 1467  
is dominated by the number of synapses. Therefore, 1468

<sup>9</sup><http://www.neuroml.org>

<sup>10</sup><http://sourceforge.net/projects/genesis-sim>

<sup>11</sup><http://www.nest-initiative.org>

1469 much emphasis is placed on the efficient representation  
1470 and update of synapses. In many applications network  
1471 construction has the same computational costs as the  
1472 integration of the dynamics. Consequently, NEST par-  
1473 allelizes both. NEST is designed to guarantee strict  
1474 reproducibility: the same network is required to gen-  
1475 erate the same results independent of the number of  
1476 machines participating in the simulation. It is consid-  
1477 ered an important principle of the project that the  
1478 development work is carried out by neuroscientists op-  
1479 erating on a joint code base. No developments are made  
1480 without the code being directly tested in neuroscien-  
1481 tific research projects. This implements an incremental  
1482 and iterative development cycle. Extensibility and long-  
1483 term maintainability are explicit design goals.

1484 **4.3.2.2 Infrastructure** The primary user interface is  
1485 a simulation language interpreter which processes a  
1486 rather high level expressive language with an extremely  
1487 simple syntax which incorporates heterogeneous ar-  
1488 rays, dictionaries, and pure (i.e. unnamed) functions  
1489 and is thus suited for interactive work. There is no  
1490 built-in graphical user interface as it would not be  
1491 particularly helpful in NEST's domain: network spec-  
1492 ification is procedural, and data analysis is generally  
1493 performed off-line for reasons of convenience and ef-  
1494 ficiency. The simulation language is used for data pre-  
1495 and post-processing, specification of parameters, and  
1496 for the compact description of the network structure  
1497 and the protocol of the virtual experiment. The neuron  
1498 models and synapse types are not expressed in the  
1499 simulation language as this would result in a slower  
1500 performance. They are implemented as derived classes  
1501 on the C++ level such that all models provide the same  
1502 minimal functionality and are thus easily interchange-  
1503 able on the simulation language level. A mechanism  
1504 for error handling propagates errors messages through  
1505 all levels of the software. Connections between nodes  
1506 (i.e. neurons, generators and recording devices) are  
1507 checked for consistency at the time of creation. User  
1508 level documentation is provided in a browsable for-  
1509 mat (the "helpdesk") and is generated directly from  
1510 source code.

1511 The code of NEST is modularized to facilitate the  
1512 development of new neuron models that can be loaded  
1513 at run time and to decouple the development of ex-  
1514 tensions from a specific NEST release. In the frame-  
1515 work of the FACETS project a Python interface and a  
1516 "facetsmodule" has been created. In addition to provid-  
1517 ing an interface between user-defined modules and the  
1518 core code, NEST can interface with other software - for  
1519 example, in order to provide a graphical user interface.  
1520 The primary strategy used is interpreter-interpreter

interaction, whereby each interpreter emits code that  
the other interpreter accepts as its native language. This  
approach minimizes the need to define protocols and  
the dependency of NEST on foreign libraries.

**4.3.2.3 Kernel** There is a common perception that  
event-driven algorithms are exact and time-driven al-  
gorithms are approximate. We have recently shown  
that both parts of this perception are generally false; it  
depends on the dynamics of the neuron model whether  
an event-driven algorithm can find an exact solution,  
just as it does for time-driven algorithms (Morrison et  
al. 2007). NEST is designed for large scale simulations  
where performance is a critical issue. We have there-  
fore argued that when comparing different integration  
strategies, one should evaluate the efficiency, i.e. the  
simulation time required to achieve a given integration  
error, rather than the plain simulation time (Morrison  
et al. 2007). This philosophy is reflected in the simula-  
tion kernel of NEST. Although it implements a glob-  
ally time-driven algorithm with respect to the ordering  
of neuron updates and the delivery of events, spike  
times are not necessarily constrained to the discrete  
time grid. Neuron implementations treating incoming  
and outgoing spikes in continuous time are seamlessly  
integrated into the time-driven infrastructure with no  
need for a central event queue. This permits a great  
flexibility in the range of neuron models which can  
be represented, including exactly solvable continuous  
time neuron models, models requiring approximation  
techniques to locate threshold passing and models with  
grid-constrained dynamics and spike times.

The simulation kernel of NEST supports paralleliza-  
tion by multi-threading and message passing, which  
allows distribution of a simulation over multiple proces-  
sors of an SMP machine or over multiple machines in  
a cluster. Communication overhead is minimized by  
only communicating in intervals of the minimum prop-  
agation delay between neurons, and communication  
bulk is minimized by storing synapses on the machine  
where the post-synaptic neuron is located (Morrison  
et al. 2005). This results in supra-linear speed-up in  
distributed simulations; scaling in multi-threaded sim-  
ulations is reasonable, but more research is required to  
understand and overcome present constraints. The user  
only needs to provide a serial script, as the distribution  
is performed automatically. Interactive usage of the  
simulator is presently only possible in purely multi-  
threaded operation. Reproducibility of results indepen-  
dent of the number of machines/processors is achieved  
by dividing a simulation task into a fixed number of ab-  
stract (virtual) processes which are distributed amongst  
the actual machines used (Morrison et al. 2005).

1573 4.3.3 Performance

1574 The supplementary material contains simulation scripts  
 1575 for all of the benchmarks specified in Appendix B.  
 1576 Considering the domain of NEST, the benchmarks can  
 1577 only demonstrate NEST's capabilities in a limited way.  
 1578 Therefore, a fifth benchmark is included which is not  
 1579 only significantly larger than the other benchmarks  
 1580 (three times as many neurons and forty times as many  
 1581 synapses), but also incorporates spike-timing dependent  
 1582 plasticity in its excitatory-excitatory synapses. The  
 1583 neuron model for this benchmark is the same as for  
 1584 Benchmark 2. All the benchmarks were simulated on  
 1585 a Sun Fire V40z equipped with four dual core AMD  
 1586 Opteron 875 processors at 2.2 GHz and 32 Gbytes  
 1587 RAM running Ubuntu 6.06.1 LTS with kernel 2.6.15-  
 1588 26-amd64-server. Simulation jobs were bound to specific  
 1589 cores using the *taskset* command. The simulations  
 1590 were performed with a synaptic propagation delay of  
 1591 0.1 ms and a computation time step of 0.1 ms unless  
 1592 otherwise stated.

1593 Figure 10(a) shows the simulation time for one biological  
 1594 second of Benchmarks 1 – 3. To compare the  
 1595 benchmarks fairly despite their different firing rates,  
 1596 the spiking was suppressed in all three benchmarks by  
 1597 removing the initial stimulus, and in the case of Benchmark  
 1598 2, the intrinsic firing was suppressed by setting  
 1599 the resting potential to be lower than the threshold.  
 1600 For networks of IF neurons of this size and activity,  
 1601 the delivery of spikes does not contribute significantly  
 1602 to the simulation times, which are dominated by the  
 1603 neuron updates. If the spiking is not suppressed, the  
 1604 simulation times for Benchmarks 1 and 2 are less than  
 1605 10% longer. The simulation time for Benchmark 3 is  
 1606 about 15% longer because of the computational cost  
 1607 associated with the integration of the action potential.  
 1608 Benchmark 2 (CUBA IF neuron model) is significantly  
 1609 faster than the other two as its linear subthreshold  
 1610 dynamics permits the use of exact integration techniques  
 1611 (see Rotter and Diesmann 1999). The non-linear  
 1612 dynamics of the conductance based IF neuron model  
 1613 in Benchmark 1 and the HH neuron in Benchmark 3  
 1614 are propagated by one global computation time step  
 1615 by one or more function calls to the standard adaptive  
 1616 time stepping method of the GNU Scientific Library  
 1617 (GSL; Galassi et al. 2001) with a required accuracy of  
 1618  $1 \mu V$ . The ODE-solver used is the embedded Runge-  
 1619 Kutta-Fehlberg (4, 5) provided by the GSL, but this  
 1620 is not a constraint of NEST - a neuron model may  
 1621 employ any method for propagating its dynamics. In  
 1622 a distributed simulation, processes must communicate  
 1623 in intervals of the minimum synaptic delay in order to  
 1624 preserve causality (Morrison et al. 2005). It is therefore

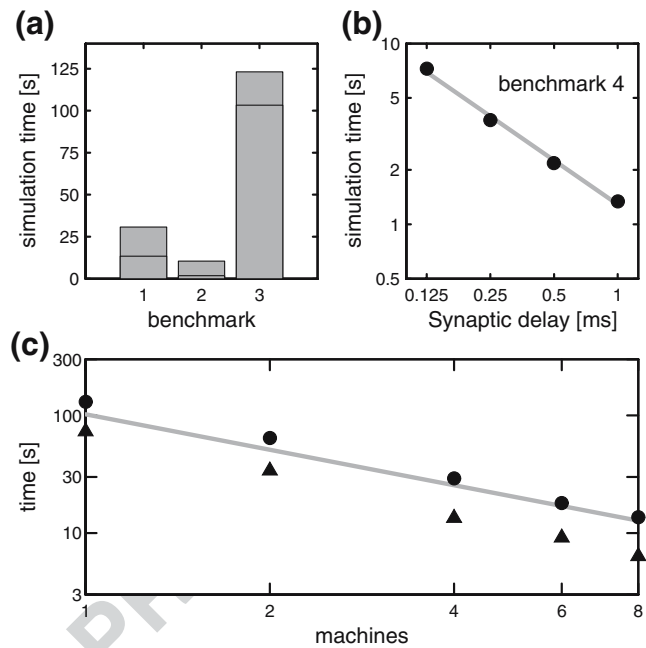


**Fig. 10** Performance of NEST on Benchmarks 1-4 and an additional benchmark (5) with STDP. (a) Simulation time for one biological second of Benchmarks 1-3 distributed over two processors, spiking suppressed, with a synaptic delay of 0.1 ms. The horizontal lines indicate the simulation times for the benchmarks with the synaptic delay increased to 1.5 ms. (b) Simulation time for one biological second of Benchmark 4 as a function of the minimum synaptic delay in double logarithmic representation. The gray line indicates a linear fit to the data (slope=-0.8). (c) Simulation time for one biological second of Benchmark 5, a network of 11250 neurons and connection probability of 0.1 (total number of synapses:  $12.7 \times 10^6$ ) as a function of the number of processors in double logarithmic representation. All synapses static, triangles; excitatory-excitatory synapses implementing multiplicative STDP with an all-to-all spike pairing scheme, circles. The gray line indicates a linear speed-up

more efficient to simulate with realistic synaptic delays 1625  
 than with unrealistically short delays, as can be seen 1626  
 in Fig. 10(a). The simulation times for the benchmark 1627  
 networks incorporating a synaptic delay of 1.5 ms are in 1628  
 all cases significantly shorter than the simulation times 1629  
 for the networks if the synaptic delay is assumed to 1630  
 be 0.1 ms. 1631

Benchmark 4 (IF neuron model with voltage jump 1632  
 synapses) is ideal for an event-driven simulation, as 1633  
 all spike times can be calculated analytically - they 1634  
 occur either when an excitatory spike is received, or 1635  
 due to the relaxation of the membrane potential to 1636  
 the resting potential, which is above the threshold. 1637  
 Therefore the size of the time steps in which NEST 1638  
 updates the neuron dynamics plays no role in determining 1639  
 the accuracy of the simulation. The primary 1640  
 constraint on the step size is that it must be less than 1641  
 or equal to the minimum synaptic delay between the 1642

1643 neurons in the network. Fig. 10(b) shows the simulation  
 1644 time for one biological second of Benchmark 4 on two  
 1645 processors as a function of the minimum synaptic delay.  
 1646 Clearly, the simulation time is strongly dependent on  
 1647 the minimum delay in this system. At a realistic value of  
 1648 1 ms, the network simulation is approximately a factor  
 1649 of 1.3 slower than real time; at a delay of 0.125 ms the  
 1650 simulation is approximately 7.3 times slower than real  
 1651 time. In the case of neuron models where the synaptic  
 1652 time course is not invertible, the computational time  
 1653 step determines the accuracy of the calculation of the  
 1654 threshold crossing. For a discussion of this case and the  
 1655 relevant quantitative benchmarks, see Morrison et al.  
 1656 (2007).

1657 Figure 10(c) shows the scaling of an application  
 1658 which lies in the domain of neural systems for which  
 1659 NEST is primarily designed. The simulated network  
 1660 contains 11250 neurons, of which 9000 are excitatory  
 1661 and 2250 inhibitory. Each neuron receives 900 inputs  
 1662 randomly chosen from the population of excitatory  
 1663 neurons and 225 inputs randomly chosen from the  
 1664 inhibitory population. The scaling is shown for the  
 1665 case that all the synapses are static, and for the case  
 1666 that the excitatory-excitatory synapses implement mul-  
 1667 tiplicative spike-timing dependent plasticity with an all-  
 1668 to-all spike pairing scheme (Rubin et al. 2001). For  
 1669 implementation details of the STDP, see Morrison et  
 1670 al. (2006), for further network parameters, see the  
 1671 supplementary material. The network activity is in the  
 1672 asynchronous irregular regime at 10 Hz. Both applica-  
 1673 tions scale supra-linearly due to the exploitation of fast  
 1674 cache memory. When using eight processors, the static  
 1675 network is a factor of 6.5 slower than real time and the  
 1676 plastic network is a factor of 14 slower. Compared to  
 1677 Benchmark 2, the network contains 3 times as many  
 1678 neurons, 40 times as many synapses and the firing rate  
 1679 is increased by a factor of 2. However, using the same  
 1680 number of processors (2), the static network simulation  
 1681 is only a factor of 17 slower, and the plastic network  
 1682 simulation is only a factor of 32 slower. This demon-  
 1683 strates that NEST is capable of simulating large, high-  
 1684 connectivity networks with computationally expensive  
 1685 synaptic dynamics with a speed suitable for interactive  
 1686 work. Although for this network the presence of the  
 1687 STDP synapses increases the simulation time by a fac-  
 1688 tor of two, this factor generally depends on the number  
 1689 of synapses and the activity.

1690 *4.3.4 Perspectives*

1691 Future work on NEST will focus on an interac-  
 1692 tive mode for distributed computing, an improvement  
 1693 of performance with respect to modern multi-core

computer clusters, and a rigorous test and validation  
 1694 suite. Further information on NEST and the current  
 1695 release can be found at the NEST web site.<sup>12</sup> 1696

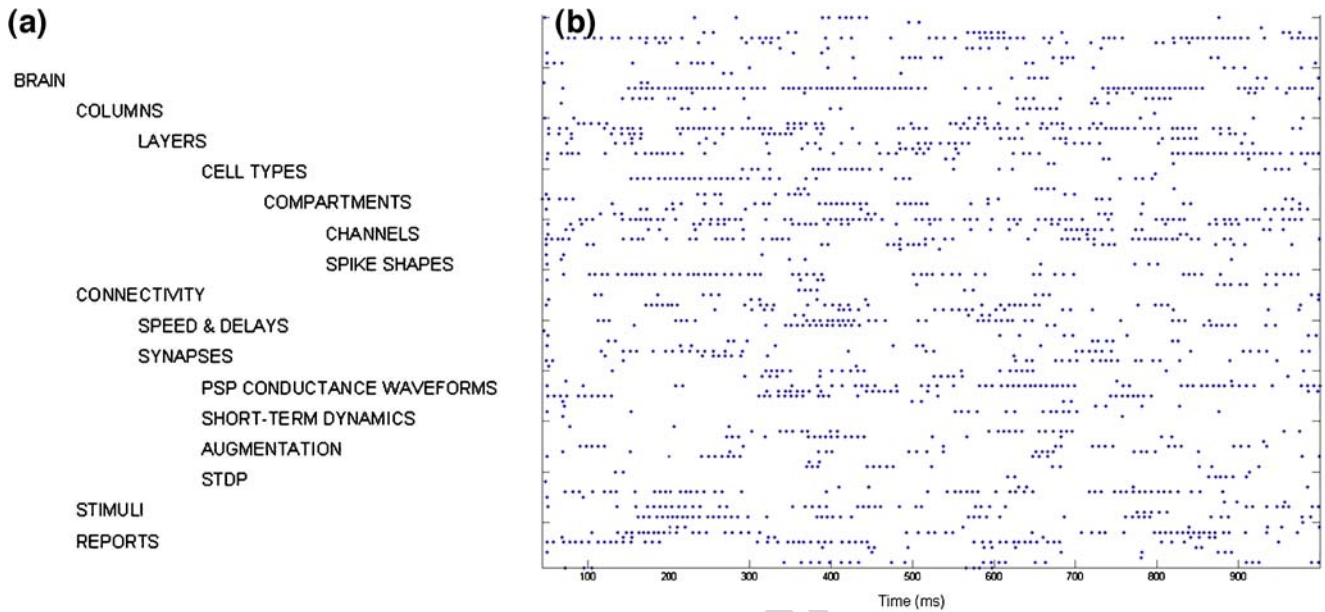
4.4 NeoCortical simulator 1697

The NeoCortical Simulator (NCS), as its name sug-  
 1698 gests, is optimized to model the horizontally dispersed,  
 1699 vertically layered distribution of neurons characteris-  
 1700 tic of the mammalian neocortex. NCS development  
 1701 began in 1997, a time at which fascinating details of  
 1702 synaptic plasticity and connectivity were being discov-  
 1703 ered (Markram et al. 1997a,b) yet available simula-  
 1704 tors such as GENESIS and NEURON did not offer  
 1705 parallel architectures nor the degree of neuronal com-  
 1706 partmental simplification required for reasonable per-  
 1707 formance times. Also emerging at the time were  
 1708 inexpensive clusters-of-workstations, also known as  
 1709 Beowulf clusters, operating under the LINUX operat-  
 1710 ing system. Following a 1997 neuroscience fellowship  
 1711 with Rodney Douglas and Kevan Martin at the Institute  
 1712 for Neuroinformatics in Zürich, Philip Goodman pro-  
 1713 grammed the first NCS using Matlab in collaboration  
 1714 with Henry Markram (then at the Weizmann Institute,  
 1715 now at the Swiss EPFL) and Thomas McKenna, Neural  
 1716 Computation Program Officer at the U.S. Office of  
 1717 Naval Research. Preliminary results led to ONR fund-  
 1718 ing (award N000140010420) in 1999, which facilitated  
 1719 the subsequent collaboration with UNR computer sci-  
 1720 entists Sushil Louis and Frederick Harris, Jr. This led  
 1721 to a C++ implementation of NCS using LINUX MPI  
 1722 on a Beowulf cluster. NCS was first made available  
 1723 to outside investigators beginning in 2000, with further  
 1724 development targeting the following specifications: 1725

1. Compartments: sampling frequency and membrane 1726  
 compartmental realism sufficient to capture bio- 1727  
 logical response properties, arbitrary voltage- and 1728  
 ion-sensitive channel behaviors, and multicompart- 1729  
 mental models distributed in 3-D (dendritic, so- 1730  
 matic, and axonal systems) 1731
2. Synapses: short-term depression and facilitation 1732  
 (Markram et al. 1998a), augmentation (Wang et al. 1733  
 2006) and Hebbian spike-timing dependent plastic- 1734  
 ity (Markram et al. 1997b) 1735
3. 3-D Connectionism: a layout to easily allocate neu- 1736  
 rons into subnetwork groupings, layers, column, 1737  
 and sheets separated by real micron- or millimeter 1738  
 spacings, with realistic propagation distances and 1739  
 axonal conduction speeds 1740

<sup>12</sup><http://www.nest-initiative.org>





Q18 **Fig. 11** NCS file specifications and example of simulation. (a) Hierarchy of the NCS Command File Objects. The file is ASCII-based with simple object delimiters. Brainlab scripting tools are

available for repetitive structures (Drewes 2005). (b) 1-s spike rastergram of 100 arbitrarily selected neurons in the benchmark simulation

- 1741 4. Parallelism: an inherently parallel, efficient method  
1742 of passing messages of synaptic events among  
1743 neurons
- 1744 5. Reporting: an efficient way to collect, sample  
1745 and analyze selected compartmental and neuronal  
1746 behaviors
- 1747 6. Stimulation: ability to (a) specify fixed, standard  
1748 neurophysiological stimulation protocols, (b) port  
1749 signals from an external device, and (c) export neu-  
1750 ronal responses and await subsequent replies from  
1751 external systems (e.g., dynamic clamps, in vitro or  
1752 in vivo preparations, robotic emulations)
- 1753 7. Freeze/resume system state: the ability to stop a  
1754 simulation and hibernate all hardware and software  
1755 parameters into a binary blob, for unpacking and  
1756 resuming in later experiments
- 1757 8. Command files: simplicity in generating and modi-  
1758 fying scripts

1759 As of 2005, NCS developers achieved all the ob-  
1760 jectives above, using an ASCII file based command  
1761 input file to define a hierarchy of reusable brain objects  
1762 (Fig. 11(a)). NCS uses a clock-based IF neurons whose  
1763 compartments contain COBA synaptic dynamics and  
1764 Hodgkin–Huxley formulations of ionic channel gating  
1765 particles.<sup>13</sup> Although a user-specified active spike tem-

plate is usually used for our large simulations, HH 1766  
channel equations can be specified for the rapid sodium 1767  
and delayed rectifier spike behavior. No nonlinear sim- 1768  
plifications, such as the Izhikevich formulation, are sup- 1769  
ported. Compartments are allocated in 3-D space, and 1770  
are connected by forward and reverse conductances 1771  
without detailed cable equations. Synapses are COBA, 1772  
with phenomenological modeling of depression, facilitation, 1773  
augmentation, and STDP. 1774

NCS runs on any LINUX cluster. We run NCS on 1775  
our 200-CPU hybrid of Pentium and AMD processors, 1776  
and also on the 8,000-CPU Swiss EPFL IBM Blue 1777  
Brain. NCS can run in single-PC mode under LINUX 1778  
or LINUX emulation (e.g., Cygwin) and on the new 1779  
Pentium-based Macintosh. 1780

Although NCS was motivated by the need to model 1781  
the complexity of the neocortex and hippocampus, lim- 1782  
bic and other structures can be modeled by variably col- 1783  
lapsing layers and specifying the relevant 3-D layouts. 1784  
Large-scale models often require repetitive patterns 1785  
of interconnecting brain objects, which can be tedious 1786  
using only the basic ASCII command file. We therefore 1787  
developed a suite of efficient Python-based scripting 1788  
tools called Brainlab (Drewes 2005). An Internet-based 1789  
library and control system was also developed (Waikul 1790  
et al. 2002). 1791

NCS delivers reports on any fraction of neuronal 1792  
cell groups, at any specified interval. Reports inclu- 1793  
de membrane voltage (current clamp mode), current 1794

<sup>13</sup><http://brain.unr.edu/publications/thesis.ecw01.pdf>

1795 (voltage clamp), spike-event-only timings (event-  
 1796 triggered), calcium concentrations, synaptic dynamics  
 1797 parameter states, and any HH channel parameter. Al-  
 1798 though NCS does not provide any direct visualization  
 1799 software, report files are straightforward to view in any  
 1800 graphics environment. Two such Matlab-based tools  
 1801 are available for download from the lab's web site.<sup>14</sup>

1802 **Benchmark.** We ran the Vogels and Abbott (2005)  
 1803 benchmark under the conditions specified for the  
 1804 COBA IF model (see Benchmark 1 in Appendix B),  
 1805 and obtained the expected irregularly-bursting sus-  
 1806 tained pattern (first second shown in Fig. 11(b)). At  
 1807 the default 10:1 ratio of inhibitory to excitatory synaptic  
 1808 conductances, the overall mean firing rate was 15.9 Hz.

1809 The largest simulations to-date have been on the  
 1810 order of a million single-compartment neurons using  
 1811 membrane AHP, M, A-type channels. Neurons were  
 1812 connected by 1 trillion synapses using short-term and  
 1813 STDP dynamics; this required about 30 min on 120  
 1814 CPUs to simulate one biological second (Ripplinger  
 1815 et al. 2004). Intermediate-complexity simulations have  
 1816 examined multimodal sensory integration and informa-  
 1817 tion transfer,<sup>15</sup> and genetic algorithm search for para-  
 1818 meter sets which support learning of visual patterns  
 1819 (Drewes et al. 2004). Detailed work included evalu-  
 1820 ation of interneuronal membrane channels (Maciokas  
 1821 et al. 2005) underlying the spectrum of observed firing  
 1822 behaviors (Gupta et al. 2000), and potential roles in  
 1823 speech recognition (Blake and Goodman 2002) and  
 1824 neuropathology (Kellogg et al. 1999; Wills et al. 1999;  
 1825 Wiebers et al. 2003; Opitz and Goodman 2005). Re-  
 1826 cent developments focus on IP port-based real time  
 1827 input-output of the "brain" to remotely behaving and  
 1828 learning robots.<sup>16</sup>The UNR Brain Computation Lab-  
 1829 oratory is presenting collaborating with the Brain  
 1830 Mind Institute of the Swiss EPFL. Their 8,000-CPU  
 1831 Blue Brain cluster<sup>17</sup> currently runs NCS alone or  
 1832 as in a hybrid configuration as an efficient synap-  
 1833 tic messaging system with CPU-resident instances of  
 1834 NEURON. The Reno and Swiss teams are explor-  
 1835 ing ways to better calibrate simulated to living mi-  
 1836 crocircuits, and to effect real-time robotic behaviors.  
 1837 Under continuing ONR support, the investigators and  
 1838 two graduate students provide part-time assistance to

external users at no cost through e-mail and online 1839  
 documentation. User manual and programmer specifi- 1840  
 cations with examples are available.<sup>18</sup> 1841

4.5 Circuit simulator 1842

4.5.1 Feature overview 1843

The *circuit simulator* (CSIM) is a tool for simulating 1844  
 heterogeneous networks composed of (spike emitting) 1845  
 point neurons. CSIM is intended to simulate networks 1846  
 containing a few neurons, up to networks with a few 1847  
 thousand neurons and on the order of 100000 synapses. 1848  
 It was written to do modeling at the network level in 1849  
 order to analyze the computational effects which can 1850  
 not be observed at the single cell level. To study single 1851  
 cell computations in detail we give the advice to use 1852  
 simulators like GENESIS or NEURON. 1853

*Easy to use Matlab interface* : The core of CSIM is writ- 1854  
 ten in C++ which is controlled by means of Matlab 1855  
 (there is no standalone version of CSIM). We have 1856  
 chosen Matlab since it provides very powerful graphics 1857  
 and analysis capabilities and is a widely used program- 1858  
 ming language in the scientific community. Hence it is 1859  
 not necessary to learn yet another script language to 1860  
 set up and run simulations with CSIM. Furthermore 1861  
 the results of a simulation are directly returned as 1862  
 Matlab arrays and hence any plotting and analysis tools 1863  
 available in Matlab can easily be applied. 1864

Until now CSIM does not provide a GUI. However 1865  
 one can easily use Matlab powerful GUI builder to 1866  
 make a GUI for a specific application based on CSIM. 1867

*Object oriented design* : We adopted an object oriented 1868  
 design for CSIM which is similar to the approaches 1869  
 taken in GENESIS and NEURON. That is there are 1870  
 objects (e.g. a *LifNeuron* object implements the stan- 1871  
 dard LIF model) which are interconnected by means 1872  
 of well defined signal channels. The creation of objects, 1873  
 the connection of objects and the setting of parame- 1874  
 ters of the objects is controlled at the level of Matlab 1875  
 whereas the actual simulation is done in the C++ core. 1876

*Fast C++ core* : Since CSIM is implemented in C++ 1877  
 and is not as general as e.g. GENESIS simulations 1878  
 are performed quite fast. We also implemented some 1879  
 ideas from event driven simulators which result in a 1880  
 considerable speedup (up to a factor of three for low 1881

<sup>14</sup><http://brain.unr.edu/publications/neuroplot.m>; <http://brain.unr.edu/publications/EVALCELLTRACINGS.zip>

<sup>15</sup>[http://brain.unr.edu/publications/Maciokas\\_Dissertation\\_final.zip](http://brain.unr.edu/publications/Maciokas_Dissertation_final.zip)

<sup>16</sup>[http://brain.unr.edu/publications/jcm.hierarch\\_robotics.unr\\_ms\\_thesis03.pdf](http://brain.unr.edu/publications/jcm.hierarch_robotics.unr_ms_thesis03.pdf); <http://brain.unr.edu/publications/JGKingThesis.pdf> (Macera-Rios et al. 2004)

<sup>17</sup><http://bluebrainproject.epfl.ch>

<sup>18</sup><http://brain.unr.edu/ncsDocs>

1882 firing rates; see the subsection about implementation  
1883 aspects below).

1884 *Runs on Windows and Linux (Unix)*: CSIM is devel-  
1885 oped on Linux (Matlab 6.5 and 7.2, gcc 4.0.2). From the  
1886 site [www.lsm.tugraz.at/csm](http://www.lsm.tugraz.at/csm) precompiled versions  
1887 for Linux and Windows are available. Since CSIM is  
1888 pure C++ it should not be hard to port it to other  
1889 platforms for which Matlab is available.

1890 *Different levels of modeling*: By providing different  
1891 neuron models CSIM allows to investigate networks  
1892 at different levels of abstraction: sigmoidal neurons  
1893 with analog output, linear and non-linear LIF neurons  
1894 and compartmental based (point) neurons with  
1895 spiking output. A broad range of synaptic models  
1896 is also available for both spiking and non-spiking  
1897 neuron models: starting from simple static synapses  
1898 ranging over synapses with short-term plasticity to  
1899 synapse models which implement different models for  
1900 long-term plasticity.

1901 *4.5.2 Built-in models*

1902 *Neuron models*: CSIM provides two different classes  
1903 of neurons: neurons with analog output and neurons  
1904 with spiking output. Neurons with analog output are  
1905 useful for analyzing population responses in larger cir-  
1906 cuits. For example CSIM provides a sigmoidal neuron  
1907 with leaky integration. However, there are much more  
1908 different objects available to build models of spiking  
1909 neurons:

- 1910 • Standard (linear) LIF neurons
- 1911 • Non-linear LIF neurons based on the models of  
1912 Izhikevich
- 1913 • Conductance based point neurons with and without  
1914 a spike template. There are general conductance  
1915 based neurons where the user can insert any num-  
1916 ber of available ion-channel models to build the  
1917 neuron model. On the other hand there is a rich  
1918 set of predefined point neurons available used in  
1919 several studies.

1920 *Spiking synapses*: As for the neurons CSIM also im-  
1921 plements synapses which transmit analog values and  
1922 spike transmitting synapses. Two types of synapses are  
1923 implemented: static and dynamic synapses. While for  
1924 static synapses the amplitude of each postsynaptic re-  
1925 sponse (current of conductance change) is the same,  
1926 the amplitude of an postsynaptic response in the case  
1927 of a dynamic synapse depends on the spike train that  
1928 it has seen so far, i.e. dynamic synapses implement a

form of short term plasticity (depression, facilitation). 1929  
For synapses transmitting spikes the time course of a 1930  
postsynaptic response is modeled by  $A \times \exp(-t/\tau_{syn})$ , 1931  
where  $\tau_{syn}$  is the synaptic time constant and  $A$  is the 1932  
synaptic strength which is constant for static synapses 1933  
and given by the model described in Markram et al. 1934  
(1998b) for dynamic synapses. 1935

Note that static as well as dynamic synapses are 1936  
available as current supplying or conductance based 1937  
models. 1938

*Analog synapses*: For synapses transmitting analog 1939  
values, such as the output of a sigmoidal neuron, static 1940  
synapses are simply defined by their strength (weight), 1941  
whereas for dynamic synapses we implemented a con- 1942  
tinuous version of the dynamic synapse model for spik- 1943  
ing neurons (Tsodyks et al. 1998). 1944

*Synaptic plasticity*: CSIM also supports spike time de- 1945  
pendent plasticity, STDP, applying a similar model as in 1946  
Song et al. (2000). STDP can be modeled most easily by 1947  
making the assumption that each pre- and postsynaptic 1948  
spike pair contributes to synaptic modification indepen- 1949  
dently and in a similar manner. Depending on the time 1950  
difference  $\Delta t = t_{pre} - t_{post}$  between pre- and postsynap- 1951  
tic spike the absolute synaptic strength is changed by an 1952  
amount  $L(\Delta t)$ . The typical shape for the function  $L(\Delta t)$  1953  
as found for synapses in neocortex layer 5 (Markram 1954  
et al. 1997a,b) is implemented. Synaptic strengthening 1955 Q4  
and weakening are subject to constraints so that the 1956  
synaptic strength does not go below zero or above a cer- 1957  
tain maximum value. Furthermore additional variants 1958  
as suggested in Froemke and Dan (2002) and Gütig et 1959  
al. (2003) are also implemented. 1960

1961 *4.5.3 Implementation aspects*

*Network input and output*: There are two forms of in- 1962  
puts which can be supplied to the simulated neural 1963  
microcircuit: spike trains and analog signals. To record 1964  
the output of the simulated model special objects called 1965  
*Recorder* are used. A recorder can be connected to any 1966  
object to record any field of that object. 1967

*Simulation Strategy*: CSIM employees a clock based 1968  
simulation strategy with a fixed simulation step width 1969  
 $dt$ . Typically the exponential Euler integration method 1970  
is used. A spike which occurs during a simulation 1971  
time step is assumed to occur at the end of that time 1972  
step. That implies that spikes can only occur at multi- 1973  
ples of  $dt$ . 1974

1975 *Efficient processing of spikes*: In a typical simulation  
 1976 of a neural circuit based on simple neuron models  
 1977 the CPU time spent in advancing *all* the synapses  
 1978 may be larger than the time needed to integrate the  
 1979 neuron equations. However if one considers the fact  
 1980 that synapses are actually “idle” most of the time (at  
 1981 least in low firing rate scenarios) it makes sense to  
 1982 update during one time step only those synapses whose  
 1983 postsynaptic response is not zero, i.e. are active. CSIM  
 1984 implements this idea by dividing synapses into a list of  
 1985 idle and a list of active synapses where only the latter  
 1986 is updated during a simulation time step. A synapse  
 1987 becomes active (i.e. is moved from the idle list to the  
 1988 active list) if a spike arrives. After its postsynaptic  
 1989 response has vanished the synapse becomes idle again  
 1990 (i.e. is moved back from the active list to the idle list).  
 1991 This trick can result in considerable speed up for low  
 1992 firing rate scenarios.

1993 *4.5.4 Further information*

1994 CSIM is distributed under the GNU General Public  
 1995 License and is available for download.<sup>19</sup> Support for  
 1996 CSIM (and its related tools) can be obtained by writing  
 1997 email to [lsm@igi.tu-graz.ac.at](mailto:lsm@igi.tu-graz.ac.at).

1998 At the site <http://www.lsm.tugraz.at> one can  
 1999 find besides the download area for CSIM (including the  
 2000 user manual and an object reference manual) a list of  
 2001 publications which used CSIM (and its related tools)  
 2002 and also the code of published models.

2003 *Related tools*: Furthermore the site <http://www.lsm.tugraz.at>  
 2004 provides two sets of Matlab scripts  
 2005 and objects which heavily build on CSIM. The *circuit*  
 2006 *tool* supports the construction of multi-column circuits  
 2007 by providing functionality to connect pools of neurons  
 2008 to pools of neurons. The *learning tool* was developed  
 2009 to analyze neural circuits in the spirit of the liquid  
 2010 state machine (LSM) approach Maass et al. 2002 and  
 2011 therefore contains several machine learning methods  
 2012 (see Natschläger et al. 2003, for more information about  
 2013 this tools).

2014 As of this writing resources are devoted to develop  
 2015 a parallel version of CSIM called PCSIM which allows  
 2016 distributed simulation of large scale networks. PCSIM  
 2017 will have a python interface which allows an easy  
 2018 implementation of the upcoming PyNN application  
 2019 programming interface (see Appendix A). The current

development version of PCSIM can be obtained from 2020  
 the SourceForge site.<sup>20</sup> 2021

4.5.5 *CSIM implementations of the benchmark 2022*  
*simulations 2023*

We implemented the benchmark networks 1 to 3 as 2024  
 specified in Appendix B. 2025

The IF benchmark networks (Benchmark 1 and 2) 2026  
 are well suited to be simulated with CSIM and can be 2027  
 implemented by only using built-in objects: *CbNeuron* 2028  
 and *StaticSpikingCbSynapse* as the neuron and synapse 2029  
 model for the COBA network and *LifNeuron* and *Stat-* 2030  
*icSpikingSynapse* as neuron and synapse model for the 2031  
 CUBA network. 2032

To implement Benchmark 3 (HH network) it is 2033  
 necessary to add the desired channel dynamics to 2034  
 CSIM by implementing it at the C++ level. The 2035  
 user defined neuron model (*TraubsHHNeuron*) is 2036  
 easily implemented in C++ (see the files `traubs_` 2037  
`hh_channels.[cpp|h]` and `TraubsHHNeuron.` 2038  
`[cpp|h]`). After these files are compiled and linked to 2039  
 CSIM they are available for use in the simulation. We 2040  
 refer the user to the CSIM manual for details on how to 2041  
 add user defined models at C++ level to CSIM. 2042

For each benchmark network we provide two im- 2043  
 plementations: the first implementation uses the plain 2044  
 CSIM interface only while the second implementation 2045  
 makes use of the *circuit tool* mentioned in the previous 2046  
 subsection (filename suffix `*_circuit.m`). 2047

To provide the initial stimulation during the first 2048  
 50ms of the simulation we set up a pool of input 2049  
 neurons (*SpikingInputNeuron* objects) which provide 2050  
 random spikes to the network. 2051

Results of CSIM simulations of all implemented 2052  
 benchmarks are depicted in Fig. 12. This figures were 2053  
 produced by the simulation scripts provided for each 2054  
 benchmark using Matlab’s powerful graphics capabilities 2055  
 (see the file `make_figures.m`) and illustrate the 2056  
 sustained irregular activity described by Vogels and 2057  
 Abbott (2005) for such networks. 2058

The current development version of PCSIM has 2059  
 been used to perform scalability tests based on the 2060  
 CUBA benchmark (Benchmark 2). The results are 2061  
 summarized in Fig. 13. For the small 4000 neuron net- 2062  
 work the speedup for more than four machines vanishes 2063  
 while for the larger networks a more than expected 2064  
 speedup occurs up to six machines. This shows that 2065  
 PCSIM is scalable with regard to the problem size and 2066

<sup>19</sup><http://www.lsm.tugraz.at/csim>

<sup>20</sup><http://sourceforge.net/projects/pcsim>

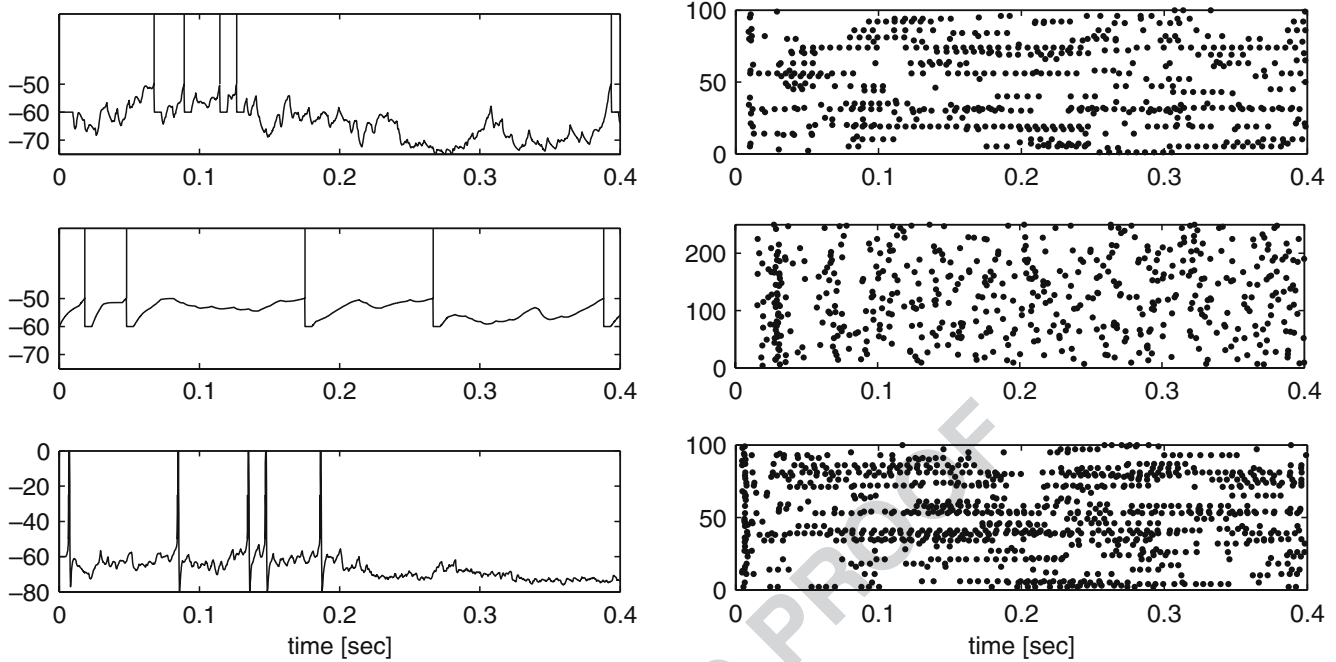


**Fig. 12** Results of CSIM simulations of the Benchmarks 1 to 3 (top to bottom). The left panels show the voltage traces (in mV) of a selected neuron. For Benchmark 1 (COBA) and Benchmark 2 (CUBA) models (top two rows), the spikes superimposed as vertical lines. The right panels show the spike raster for randomly selected neurons for each of the three benchmarks

2067 the number of available machines. The development  
 2068 version of PCSIM together with the python script  
 2069 for the CUBA benchmark can be obtained from the  
 2070 SourceForge site.<sup>21</sup>

2071 4.6 XPPAUT

2072 *XPPAUT* is a general numerical tool for simulating,  
 2073 animating, and analyzing dynamical systems. These can  
 2074 range from discrete finite state models (McCulloch–  
 2075 Pitts) to stochastic Markov models, to discretization  
 2076 of partial differential and integrodifferential equations.  
 2077 *XPPAUT* was not specifically developed for neural  
 2078 simulations but because of its ability to provide a complete  
 2079 numerical analysis of the dependence of solutions  
 2080 on parameters (“bifurcation diagrams”) it is widely  
 2081 used by the community of computational and theoretical  
 2082 neuroscientists. There are many online tutorials  
 2083 many of which are geared to neuroscience. While it  
 2084 can be used for modest sized networks, it is not specifically  
 2085 designed for this purpose and due to its history,  
 2086 there are limits on the size of problems which can be  
 2087 solved (about 2000 differential equations is the current  
 2088 limit). The benchmarks were not performed due to

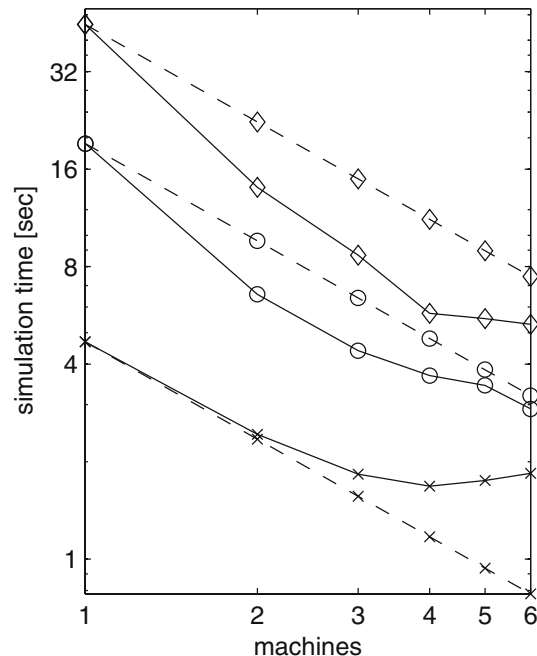
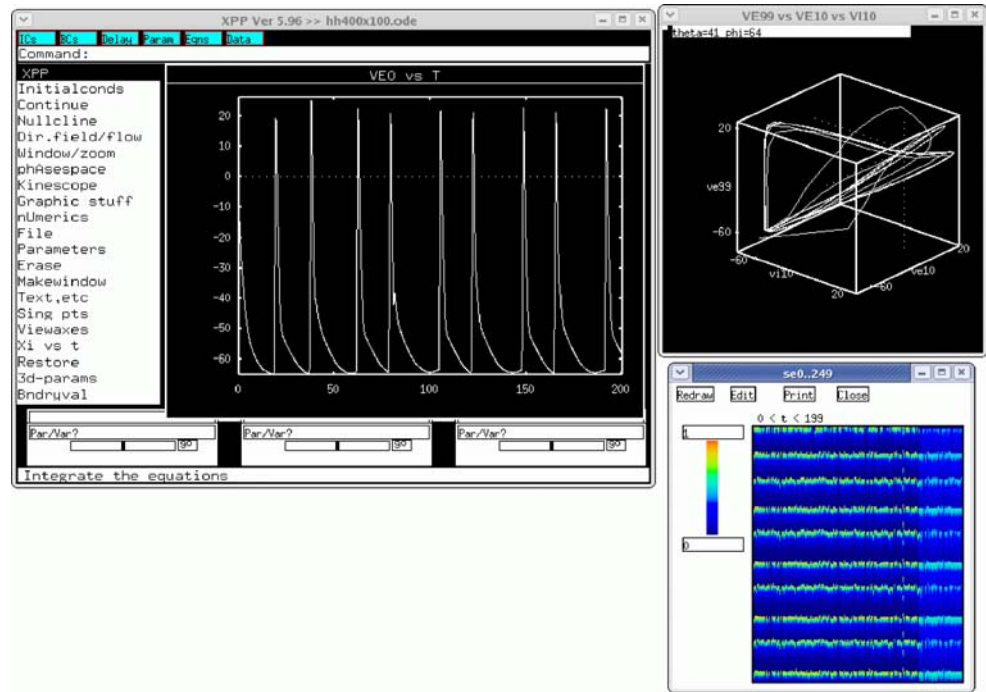


**Fig. 13** Performance of PCSIM. The time needed to simulate the Benchmark 2 (CUBA) network (1 ms synaptic delay, 0.1 ms time step) for 1 s of biological time (solid line) as well as the expected times (dashed line) are plotted against the number of machines (Intel Xeon, 3.4 Ghz, 2 Mb cache). The CUBA model was simulated for three different sizes: 4000 neurons and  $3.2 \times 10^5$  synapses (stars), 10000 neurons and  $2 \times 10^6$  synapses (circles), and 20000 neurons and  $20 \times 10^6$  synapses (diamonds)

<sup>21</sup><http://sourceforge.net/projects/pcsim>

**Fig. 14** *XPPAUT* interface for a network of 200 excitatory and 50 inhibitory HH neurons with random connectivity, COBA dynamical synapses. Each neuron is also given a random drive. Main window, a three-dimensional phase plot, and an array plot are shown

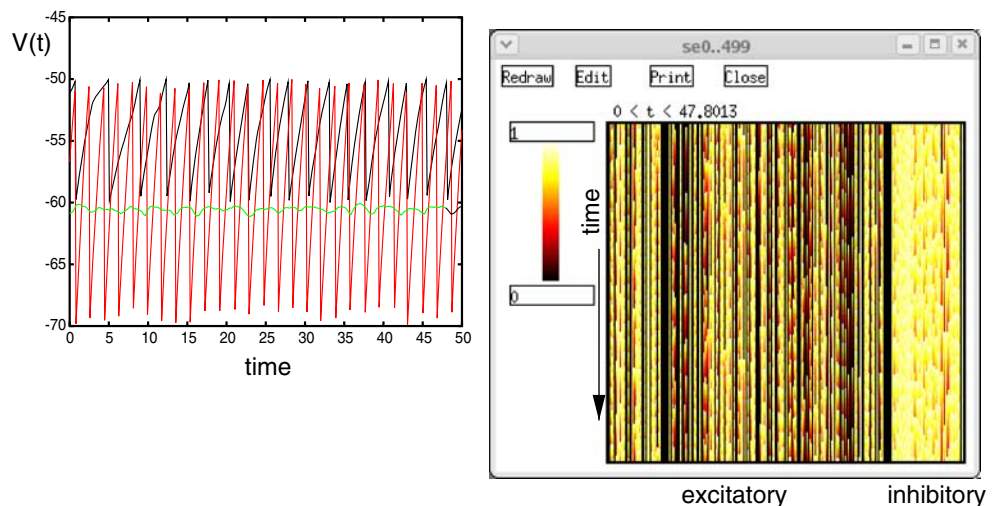


2089 this limitation in size, however, a reduced version is  
 2090 included. Rather than a pure simulator, *XPPAUT* is  
 2091 a tool for understanding the equations and the results  
 2092 of simulating the equations. *XPPAUT* uses a highly  
 2093 optimized parser to produce a pseudocode which is in-  
 2094 terpreted and runs very fast – at about half the speed of  
 2095 directly compiled code. Since no compiler is required,  
 2096 *XPPAUT* is a stand alone program and runs on all  
 2097 platforms which have an X-windows interface available  
 2098 (UNIX, MAC OSX, Windows, etc.) The program is

open source and available as source and various binary 2099  
 versions (Figs. 14 and 15). 2100

*XPPAUT* can be run interactively (the preferred 2101  
 method) but can also be run in batch mode with no 2102  
 GUI with the results dumped to one or more files. 2103  
 Graphical output in postscript, GIF, PBM, and ani- 2104  
 mated GIF is possible. (There are codecs available for 2105  
 AVI format but these are not generally included in the 2106  
 compiled versions.) Numerous packages for controlling 2107  
*XPPAUT* have been written, some stand-alone such as 2108

**Fig. 15** Persistent state in an IF network with 400 excitatory and 100 inhibitory cell. *XPPAUT* simulation with exponential COBA synapses, sparse coupling and random drive. Excitatory and inhibitory synapses are shown as well as voltages traces from 3 neurons



2109 JigCell and others using Matlab or PERL. Data from  
 2110 simulations can be saved for other types of analysis  
 2111 and or plotting with other packages. The “state” of the  
 2112 program can be saved as well so that users can come  
 2113 back where they let off.

2114 There are no limits as far as the form of the equations  
 2115 is concerned since the actual equations that you desire  
 2116 to solve are written down like you would write them in  
 2117 a paper. For example the voltage equation for a COBA  
 2118 model would be written as:

$$2119 \quad dv/dt = (-g_l * (v - e_l) - g_{na} * m^3 * h * (v - e_{na}) \\ 2120 \quad \quad - g_k * n^4 * (v - e_k)) / cm$$

2121 There is a method for writing indexed networks as  
 2122 well, so that one does not have to write every equa-  
 2123 tion. Special operators exist for speeding up network  
 2124 functions like discrete convolutions and implementa-  
 2125 tion of the stochastic Gillespie algorithm. Furthermore,  
 2126 the user can link the right-hand sides of differential  
 2127 equations to external C libraries to solve complex equa-  
 2128 tions [for example, equation-free firing rate models,  
 2129 (Laing 2007)]. Because it is a general purpose solver,  
 2130 the user can mix different types of equations for ex-  
 2131 ample stochastic discrete time events with continuous  
 2132 ODEs. Event driven simulations are also possible and  
 2133 can be performed in such a way that output occurs  
 2134 only when an event happens. There are many ways to  
 2135 display the results of simulations including color-coded  
 2136 plots showing space-time behavior, a built-in animation  
 2137 language, and one- two- and three-dimensional phase-  
 2138 space plots.

2139 *XPPAUT* provides a variety of numerical meth-  
 2140 ods for solving differential equations, stochastic sys-  
 2141 tems, delay equations, Volterra integral equations, and  
 2142 boundary-value problems (BVP). The numerical in-  
 2143 tegrators are very robust and vary from the simple  
 2144 Euler method to the standard method for solving stiff  
 2145 differential equations, CVODE. The latter allows the  
 2146 user to specify whether the system is banded and thus  
 2147 can improve calculation speed by up to two orders of  
 2148 magnitude. The use of BVP solvers is rare in neuro-  
 2149 science applications but they can be used to solve, for  
 2150 example, the steady-state behavior of Fokker–Planck  
 2151 equations for noisy neurons and to find the speed of  
 2152 traveling waves in spatially distributed models.

2153 Tools for analysis dynamical properties such as  
 2154 equilibria, basins of attraction, Lyapunov exponents,  
 2155 Poincare maps, embedding, and temporal averaging  
 2156 are all available via menus. Some statistical analysis of  
 2157 simulations is possible such as power spectra, mean and  
 2158 variance, correlation analysis and histograms are also

included in the package. There is a very robust para- 2159  
 meter fitting algorithm (Marquardt–Levenburg) which 2160  
 allows the user to find parameters and initial conditions 2161  
 which best approximate specified data. 2162

One part of *XPPAUT* which makes it very popular is 2163  
 the inclusion of the continuation package, AUTO. This 2164  
 package allows the user to track equilibria, limit cycles, 2165  
 and solutions to boundary-value problems as parame- 2166  
 ters vary. The stability of the solutions is irrelevant so 2167  
 that users can track the entire qualitative behavior of 2168  
 a differential equation. *XPPAUT* provides a simple to 2169  
 use GUI for AUTO which allows the user to seam- 2170  
 lessly switch back and forth between simulation and 2171  
 analysis. 2172

*XPPAUT* is used in many different courses and 2173  
 workshops including the Methods in Computational 2174  
 Neuroscience course at the Marine Biological Labo- 2175  
 ratory (where it was developed 15 years ago), various 2176  
 European CNS courses as well as in classroom settings. 2177  
 Since equations are written for the software as you 2178  
 would write them on paper, it is easy to teach students 2179  
 how to use *XPPAUT* for their own problems. There 2180  
 are many features for the qualitative analysis of dif- 2181  
 ferential equations such as direction fields, nullclines 2182  
 and color coding of solutions by some property (such 2183  
 as energy or speed). 2184

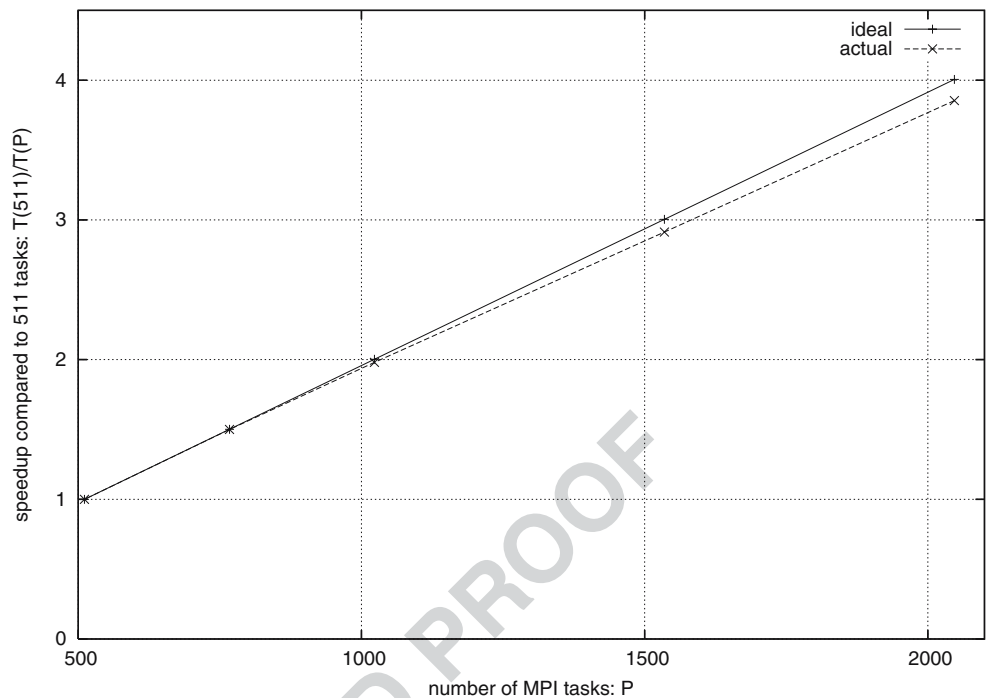
*XPPAUT* can be considered a stable mature pack- 2185  
 age. It is developed and maintained by the author. 2186  
 While a list of users is not maintained, a recent Google 2187  
 search revealed 38500 hits and a search on Google 2188  
 Scholar showed over 250 papers citing the software. In 2189  
 the future, the parser will be rewritten so that there will 2190  
 be no limit to the number of equations and methods 2191  
 for implementing large spatially distributed systems 2192  
 will also be incorporated. Parts of the analysis code in 2193  
*XPPAUT* may possibly be included in NEURON in 2194  
 the near future. A book has been written on the use 2195  
 of the program (Ermentrout 2004) and it comes with 2196  
 120 pages of documentation and dozens of examples. 2197

4.7 SPLIT 2198

4.7.1 Parallel simulators 2199

The development of parallel simulation in computa- 2200  
 tional neuroscience has been relatively slow. Today 2201  
 there are a few publicly available parallel simula- 2202  
 tors, but they are far from as general, flexible, and 2203  
 documented as commonly used serial simulators such 2204  
 as Neuron (Hines and Carnevale 1997) and Genesis 2205  
 (Bower and Beeman 1998). For Genesis there is PGE- 2206  
 NESIS and the development of a parallel version of 2207  
 Neuron has started. In addition there exists simulators 2208

**Fig. 16** Speedup for model with 4 million cells and 2 billion synapses simulated with SPLIT on BG/L (from Djurfeldt et al. 2005)



Q7 2209 like NCS<sup>22</sup> (see Frye 2005), NEST (Morrison et al. 2210 2005), and our own parallelizing simulator SPLIT 2211 (Hammarlund and Ekeberg 1998). However, they are 2212 in many ways still on the experimental and develop- 2213 mental stage (Fig. 16).

2214 4.7.2 The simulator

2215 SPLIT is a tool specialized for efficiently simulating 2216 large-scale multicompartmental models based on HH 2217 formalism. It should be regarded as experimental soft- 2218 ware for demonstrating the possibility and usefulness 2219 of very large scale biophysically detailed neuronal net- 2220 work simulations. Recently, this tool was used for 2221 one of the largest cortex simulations ever performed 2222 (Djurfeldt et al. 2005). It supports massive parallelism 2223 on cluster computers using MPI. The model is specified 2224 by a C++ program written by the SPLIT user. This pro- 2225 gram is then linked with the SPLIT library to obtain the 2226 simulator executable. Currently, there is no supported 2227 graphical interface, although an experimental Java/QT- 2228 based graphical interface has been developed. There 2229 is no built-in support for analysis of results. Rather, 2230 SPLIT should be regarded as a pure, generic, neural 2231 simulation kernel with the user program adapting it into 2232 a simulator specific to a certain model. Although this

approach is in some sense “raw”, this means that the 2233 model specification benefits from the full power of a 2234 general purpose programming language. 2235

SPLIT provides COBA synaptic interactions with 2236 short-term plasticity (facilitation and depression). 2237 Long-term plasticity (such as STDP) and IF formal- 2238 ism have not yet been implemented, although this is 2239 planned for the future. 2240

The user program specifies the model through the 2241 SPLIT API which is provided by the class *split*. The 2242 user program is serial and parallelism is hidden from 2243 the user. The program can be linked with either a 2244 serial or parallel version of SPLIT. In the parallel case, 2245 some or all parts of the program run in a master node 2246 on the cluster while SPLIT internally sets up parallel 2247 execution on a set of slave nodes. As an option, parts 2248 of the user program can execute distributed onto each 2249 slave via a callback interface. However, SPLIT provides 2250 a set of tools which ensures that also such distrib- 2251 uted code can be written without explicit reference to 2252 parallelism. 2253

The SPLIT API provides methods to dynamically 2254 inject spikes to an arbitrary subset of cells during a 2255 simulation. Results of a simulation are logged to file. 2256 Most state variables can be logged. This data can be 2257 collected into one file at the master node or written 2258 down at each slave node. In the latter case, a separate 2259 program might be used to collect the files at each node 2260 after the simulation terminates. 2261

<sup>22</sup><http://brain.cse.unr.edu/ncsdocs>



2262 4.7.3 Large scale simulations

2263 Recently, Djurfeldt et al. (2005) have described an  
 2264 effort to optimize SPLIT for the Blue Gene/L super-  
 2265 computer. BG/L (Gara et al. 2005) represents a new  
 2266 breed of cluster computers where the number of pro-  
 2267 cessors, instead of the computational performance of  
 2268 individual processors, is the key to higher total perfor-  
 2269 mance. By using a lower clock frequency, the amount  
 2270 of heat generated decreases dramatically. Therefore,  
 2271 CPU chips can be mounted more densely and need less  
 2272 cooling equipment. A node in the BG/L cluster is a  
 2273 true “system on a chip” with two processor cores, 512  
 2274 MiB of on chip memory and integrated network logic.  
 2275 A BG/L system can contain up to 65536 processing  
 2276 nodes.

2277 During this work, simulations of a neuronal network  
 2278 model of layers II/III of the neocortex were per-  
 2279 formed using COBA multicompartmental model neu-  
 2280 rons based on HH formalism. These simulations  
 2281 comprised up to 8 million neurons and 4 billion  
 2282 synapses. After a series of optimization steps, perfor-  
 2283 mance measurements showed linear scaling behavior  
 2284 both on the Blue Gene/L supercomputer (see Fig. 1)  
 2285 and on a more conventional cluster computer. Opti-  
 2286 mizations included parallelization of model setup and  
 2287 domain decomposition of connectivity meta data. Com-  
 2288 putation time was dominated by the synapses which  
 2289 allows for a “free” increase of cell model complex-  
 2290 ity. Furthermore, communication time was hidden by  
 2291 computation.

2292 4.7.4 Implementation aspects

2293 SPLIT has so far been used to model neocortical net-  
 2294 works (Fransén and Lansner 1998; Lundqvist et al.  
 2295 2007), the Lamprey spinal cord (Kozlov et al. 2003,  
 Q192296 submitted for publication) and the olfactory cortex  
 2297 (Sandström et al. 2007).

2298 The library exploits data locality for better cache-  
 2299 based performance. In order to gain performance on  
 2300 vector architectures, state variables are stored as se-  
 2301 quences. It uses techniques such as adjacency lists  
 2302 for compact representation of projections and Ad-  
 2303 dress Event Representation (Bailey and Hammerstrom  
 2304 1988) for efficient communication of spike events.

2305 Perhaps the most interesting concept in SPLIT is its  
 2306 asynchronous design: On a parallel architecture, each  
 2307 slave process has its own simulation clock which runs  
 2308 asynchronously with other slaves. Any pair of slaves  
 2309 only need to communicate at intervals determined by  
 2310 the smallest axonal delay in connections crossing from  
 2311 one slave to the other.

The neurons in the model can be distributed arbi- 2312  
 trarily over the set of slaves. This gives great freedom 2313  
 in optimizing communication so that densely connected 2314  
 neurons reside on the same CPU and so that axonal 2315  
 delays between neurons simulated on different slaves 2316  
 are maximized. The asynchronous design, where a slave 2317  
 process does not need to communicate with all other 2318  
 slaves at each time step, gives two benefits: (1) By com- 2319  
 municating more seldom, the communication overhead 2320  
 is reduced. (2) By allowing slave processes to run out of 2321  
 phase, to a degree determined by the mutually smallest 2322  
 axonal delay, the waiting time for communication is 2323  
 decreased. 2324

4.7.5 Benchmark 2325

The SPLIT implementation of the HH benchmark 2326  
 (Benchmark 3 in Appendix B) consists of a C++ pro- 2327  
 gram which specifies what entities are to be part of 2328  
 the simulation (cell populations, projections, noise- 2329  
 generators, plots), makes a call which distributes these 2330  
 objects onto the cluster slaves (in the parallel case), 2331  
 sets the parameters of the simulation objects, initializes, 2332  
 and simulates. While writing the code, close attention 2333  
 needs to be paid to which parameters are scalar and 2334  
 which are vectorized over the sets of cells or axons. 2335  
 Channel equations are pre-compiled into the library, 2336  
 and a choice of which set of equations to use needs to 2337  
 be made. Parameters are specified using SI units. 2338

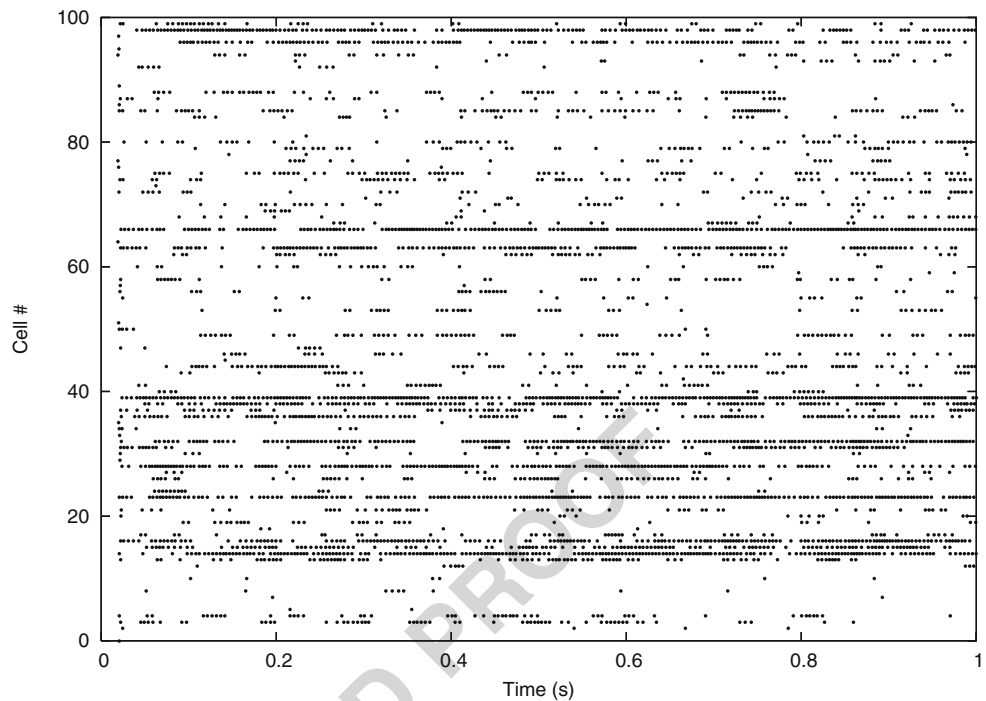
The Benchmark 3 simulation (4000 cells, 5 s of simu- 2339  
 lated time) took 386 s on a 2 GHz Pentium M machine 2340  
 (Dell D810). Outputs are written in files on disk and 2341  
 can easily be displayed using *gnuplot*. Figure 17 shows 2342  
 a raster of spiking activity in 100 cells during the first 2343  
 second of activity. Figure 18 shows membrane potential 2344  
 traces of 3 of the cells during 5 s (left) and 100 ms 2345  
 (right). 2346

4.7.6 Future plans 2347

Ongoing and possible future developments of SPLIT 2348  
 include: 2349

- A revision of the simulation kernel API 2350
- The addition of a Python interpreter interface 2351
- Compatibility with channel models used in popular 2352  
 simulators such as Neuron and Genesis, enabling 2353  
 easy transfer of neuron models 2354
- Gap junctions 2355
- Graded transmitter release 2356
- Better documentation and examples 2357

**Fig. 17** Raster plot showing spikes of 100 cells during the first second of activity (SPLIT simulation of Benchmark 3)



2358 Currently, SPLIT is developed, in part time, by two  
 2359 people. There exists some limited documentation and  
 2360 e-mail support.

2361 4.8 Mvaspike

2362 4.8.1 Modelling with events

2363 It has been argued many times that action potentials as  
 2364 produced by many types of neurones can be considered  
 2365 as *events*: they consist of stereotypical impulses that  
 2366 appear superimposed on the internal voltage dynamics  
 2367 of the neurones. As a result, many models of neurones  
 2368 offer ways of defining event times associated with each  
 2369 emitted action potential, often through the definition  
 2370 of a firing threshold.<sup>23</sup> Neural simulation tools have  
 2371 taken advantage of this for a long time, through the  
 2372 use of *event driven algorithms* (see Section 2). Indeed,  
 2373 when one speaks of *events* in the context of simulation  
 2374 of neural networks, *event-driven* algorithms come to  
 2375 mind and it is the authors' impression that the use of  
 2376 events upstream, during the modeling stage, is often  
 2377 understated.

Mvaspike was designed as an event-based modeling  
 and simulation framework. It is grounded on a well  
 established set-theoretic modeling approach [discrete  
 event system specification (DEVS) (Zeigler and Vahie  
 1993; Zeigler et al. 2000)]. Target models are discrete  
 events systems: their dynamics can be described by  
 changes of state variables at arbitrary moments in  
 time.<sup>24</sup> One aspect of Mvaspike is to bridge the gap  
 between the more familiar expression of continuous  
 dynamics, generally in use in the neuroscience commu-  
 nity, and the event-centric use of models in the simu-  
 lator (see Fig. 19). This is conveniently easy for many  
 simple models that represent the models of choice in  
 Mvaspike (mostly IF or phase models, and SRMs).  
 Watts (1994) already noted that many neuronal proper-  
 ties can be explicitly and easily represented in discrete  
 event systems. Think of absolute refractory *periods*,  
 rising *time* of PSPs, axonal propagation *delays*, these are  
 notions directly related to time intervals (and therefore,  
 events) that are useful to describe many aspects of  
 the neuronal dynamics. This being obviously quite far  
 from the well established, more electro-physiologically  
 correct conductance based models, another aim of

<sup>23</sup>The firing threshold here has to be taken in a very broad sense, from a simple spike detection threshold in a continuous model (e.g. HH) to an active threshold that is used in the mathematical expression of the dynamics (IF model).

<sup>24</sup>As opposed to discrete time systems, in which state changes occurs periodically, and continuous systems where state changes continuously.

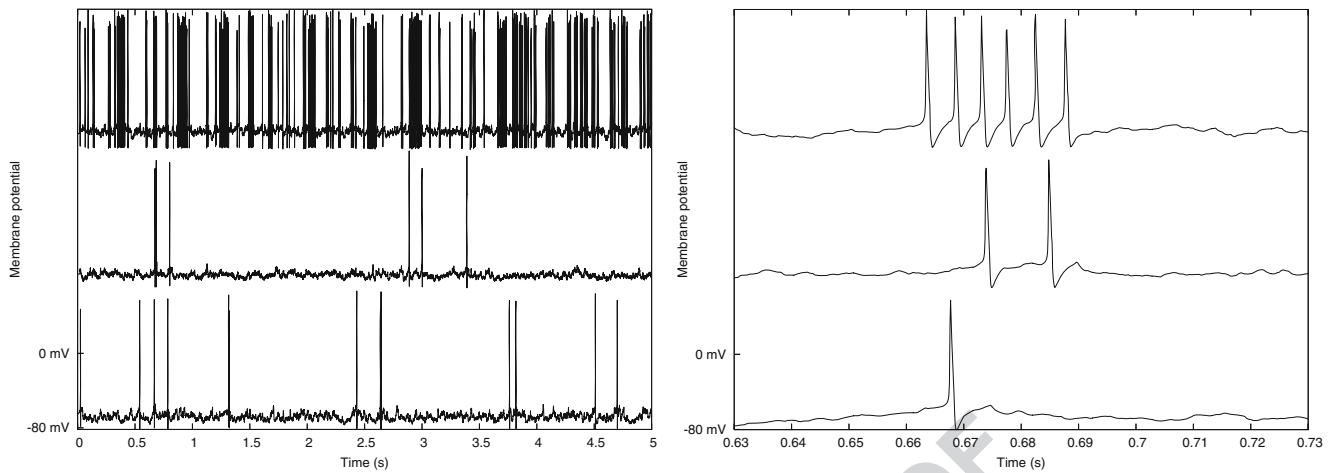


**Fig. 18** Plots of the membrane potential for 3 of the 4000 cells. The right plot shows a subset of the data in the left plot, with higher time resolution (SPLIT simulation of Benchmark 3)

2401 Mvaspike is therefore to take into account as much as  
 2402 possible of these more complex models, through the  
 2403 explicit support of discrete-time events, and, possibly,  
 2404 state space discretization for the integration of contin-  
 2405 uous or hybrid dynamics.

2406 The DEVS formalism makes also possible the mod-  
 2407 eling of large, hierarchical or modular systems (e.g.  
 2408 networks of coupled populations of neurons, or micro-  
 2409 circuits, cortical columns etc.), through a well-defined  
 2410 coupling and composition system. This helps model-  
 2411 ing large and complex networks, but also favor code  
 2412 reusability, prototyping, and the use of different levels  
 2413 of modeling. Additional tools have been implemented  
 2414 in Mvaspike to take into account e.g. synaptic or axo-  
 2415 nal propagation delays, the description of structured  
 2416 or randomly connected networks in an efficient way,  
 2417 through the use of generic iterators to describe the  
 2418 connectivity (Rochel and Martinez 2003).

4.8.2 The simulator

2419

The core simulation engine in Mvaspike is event- 2420  
 driven, meaning that it is aimed at simulating networks 2421  
 of neurons where event-times can be computed effi- 2422  
 ciently. Firing times will then be calculated exactly (in 2423  
 fact, to the precision of the machine). This does not 2424  
 mean however that it is restricted to models that offer 2425  
 analytical expressions of the firing times, as numerical 2426  
 approximations can be used in many situations. 2427

Mvaspike consists of a core C++ library, implement- 2428  
 ing a few generic classes to describe networks, neu- 2429  
 rons and additional input/output systems. It has been 2430  
 designed to be easy to access from other program- 2431  
 ming languages (high level or scripting languages, e.g. 2432  
 Python) and extensible. Well established simulation al- 2433  
 gorithms are provided, based on state of the art priority 2434  
 queue data structures. They have been found to be 2435

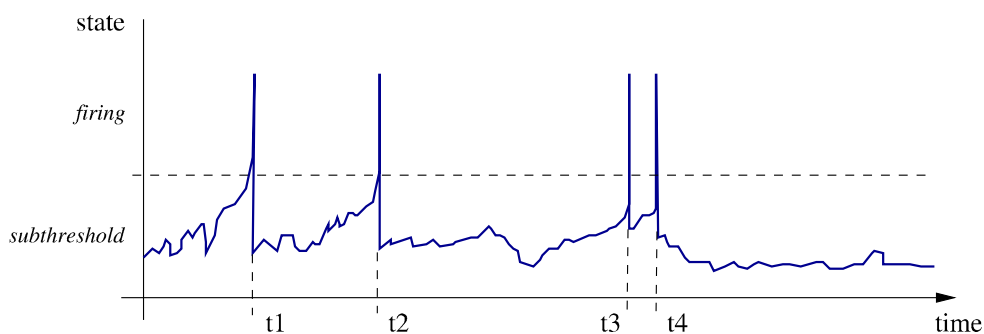
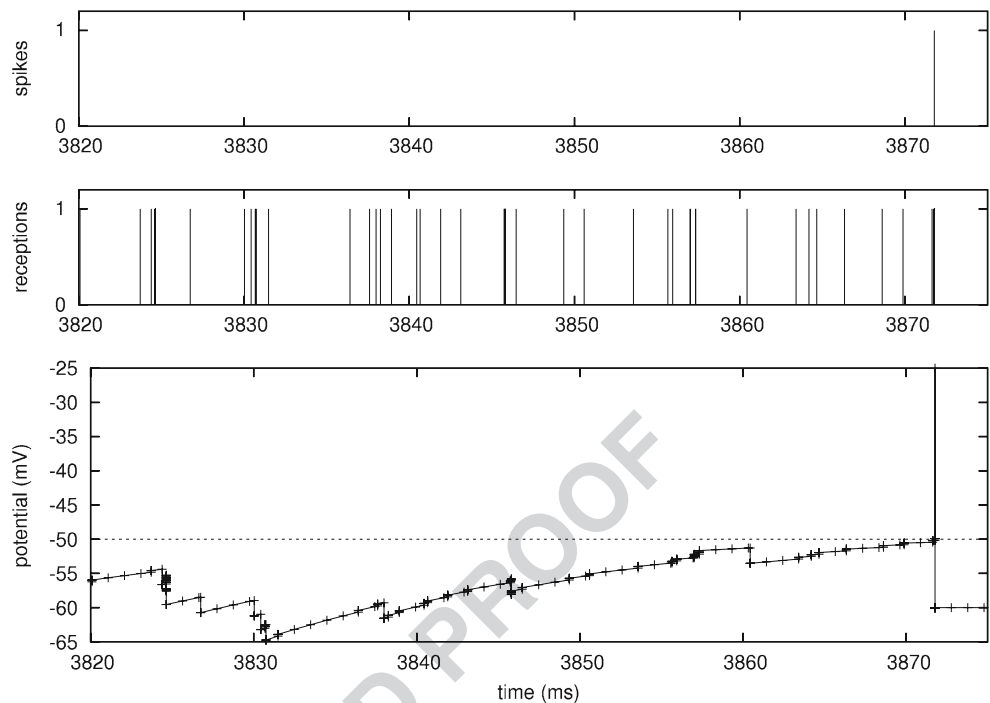


**Fig. 19** Neuronal dynamics from a discrete-event dynamical systems perspective. Events (t1-t4), corresponding to the state variable switching from the sub-threshold to the firing dynamics, can occur at any arbitrary point in time. They correspond here

to change of the neuron output that can be passed to the rest of the systems (e.g. other neurons). Internal changes (e.g. end of the refractory period) can also be described in a similar way

**Fig. 20** Membrane potential of a single neuron, from a Mvaspike implementation of Benchmark 4.

Top: membrane potential dynamics (impulses have been superimposed at firing time to make them more apparent). Bottom: Mvaspike simulation result typically consists of lists of events (here, spiking and reception time, top and middle panels) and the corresponding state variables at these instants (not shown). In order to obtain the full voltage dynamics, a post-processing stage is used to add new intermediary values between events (bottom trace)



2436 sufficiently efficient on average; however, the object-  
 2437 oriented approach has been designed to permit the use  
 2438 of dedicated, optimized sub-simulators when possible.  
 2439 On top of the core engine lies a library that includes  
 2440 a few common models of neurons, including linear or  
 2441 quadratic IF (or SRM) neurons, with Dirac synaptic  
 2442 interactions, or various forms of piecewise linear and  
 2443 exponential PSPs. Other available ingredients include  
 2444 plasticity mechanisms (STDP), refractory periods, in-  
 2445 put spike trains generation (Poisson). Some connectiv-  
 2446 ity patterns (e.g. all-to-all, ring, etc.) are also included.  
 2447 There is no graphical user interface, nor pre- and  
 2448 post-processing tools included, as these are elements of  
 2449 the modeling and simulation work-flow that we believe  
 2450 to be easy to handle using third-party environments or  
 2451 high level languages, tailored to the needs and habits of  
 2452 the user.

2453 *4.8.3 Benchmarks*

2454 The simplest model available in Mvaspike corresponds  
 2455 to the one defined for Benchmark 4 (see Appendix B).  
 2456 A straightforward implementation of the correspond-  
 2457 ing network can be done using only available objects  
 2458 from the library.  
 2459 The typical output of a Mvaspike simulation is a  
 2460 list of events, corresponding e.g. to spikes emitted (or  
 2461 received) by the neurons. In particular, the membrane  
 2462 potential is not available directly. In order to obtain

the voltage trace presented in Fig. 20, a simple post-  
 processing stage was necessary in order to obtain val-  
 ues for the membrane potential at different instants  
 between the event times. To this aim, the differential  
 equation governing the dynamics between events is  
 used (in a integrated form), together with the values  
 already available at each event times, to find new in-  
 intermediary values. Here, this is as simple as computing  
 the effect of the leak (exponential) and the refractory  
 period. As this only has to be done between events,  
 each neuron can be treated independently of the others.  
 In a sense, this illustrates how the hybrid formalism (as  
 presented in Section 2.1) is handled in Mvaspike: the  
 flow of discrete events is the main point of interest,  
 continuous dynamics come second.

2478 *4.8.4 Current status and further perspectives*

Mvaspike is currently usable for the modeling of  
 medium to large scale networks of spiking neurons.  
 It is released under the GPL license, maintained and  
 supported by its main author and various contributors.  
 It has been used to model networks of IF neurons,  
 for e.g. modeling the early stages of the visual sys-  
 tem (see e.g. Hugues et al. 2002; Wohrer et al. 2006),  
 and more theoretical research on computing paradigms  
 offered by spiking neurons (for instance, Rochel and  
 Cohen 2005; Rochel and Vieville 2006). A partial par-  
 allel implementation was developed and successfully

t1.1 **Table 1** Comparison of features of the different simulators

t1.2 Question	NEURON	GENESIS	NEST	NCS	CSIM	XPP	SPLIT	Mvaspike
t1.3 HH	B.I.	B.I.	YES	B.I.	B.I.	YES	B.I.	POSS
t1.4 LIF	B.I.	POSS	YES	B.I.	B.I.	YES	POSS**	B.I.
t1.5 Izhikevich IF	YES	B.I.	YES	NO	B.I.	YES	POSS**	POSS**
t1.6 Cable eqs	B.I.	B.I.	NO	NO	NO	YES	B.I.	NO
t1.7 ST plasticity	YES	B.I.	YES	B.I.	B.I.	YES	B.I.	YES
t1.8 LT Plasticity	YES	YES	YES	B.I.	B.I.	YES	NO**	YES
t1.9 Event-based	B.I.	NO	YES	NO	NO	YES	NO	YES
t1.10 Exact	B.I.	–	YES	–	–	NO	–	YES
t1.11 Clock-based	B.I.	B.I.	YES	B.I.	YES	YES	YES	POSS**
t1.12 Interpolated	B.I.	NO	YES	NO	NO	YES	B.I.	POSS
t1.13 G synapses	B.I.	B.I.	YES	B.I.	B.I.	YES	B.I.	POSS**
t1.14 Parallel	B.I.	YES	B.I.	B.I.	NO**	NO	B.I.	NO**
t1.15 Graphics	B.I.	B.I.	NO(*)	NO(*)	NO(*)	YES	NO	NO
t1.16 Simple analysis	B.I.	B.I.	YES	NO(*)	NO(*)	YES	NO	NO
t1.17 Complx analysis	B.I.	YES	NO(*)	NO(*)	NO(*)	YES	NO	NO
t1.18 Development	YES	YES	YES	YES	YES	YES	YES	YES
t1.19 How many p.	3	2–3	4	2–3	2	1	2	1
t1.20 Support	YES	YES	YES	YES	YES	YES	YES	YES
t1.21 Type	e,p,c	e	e	e	e	e	e	e
t1.22 User forum	YES	YES	YES	NO	NO	YES	YES	NO
t1.23 Publ list	YES	YES	YES	YES	YES	NO	NO	NO
t1.24 Codes	YES	YES	YES	YES	YES	YES	NO	NO
t1.25 Online manual	YES	YES	YES	YES	YES	YES	YES	YES
t1.26 Book	YES	YES	NO	NO	NO	YES	NO	NO
t1.27 XML import	NO**	POSS	NO**	NO**	NO	YES	NO	NO**
t1.28 XML export	B.I.	NO**	NO**	NO**	NO	NO	NO	NO**
t1.29 Web site	YES	YES	YES	YES	YES	YES	YES	YES
t1.30 LINUX	YES	YES	YES	YES	YES	YES	YES	YES
t1.31 Windows	YES	YES	YES	YES	YES	YES	NO	NO
t1.32 Mac-Os	YES	YES	YES	NO	NO	YES	NO	NO
t1.33 Interface	B.I.	B.I.	POSS	B.I.	YES	POSS	POSS	POSS
t1.34 Save option	B.I.	YES	NO**	B.I.	NO	NO	NO	NO

t1.35 Different questions were asked (see below), and for each question, the answer is either: B.I. = Built-in feature, incorporated in the simulator without need to load additional mechanisms; YES = feature very easy to simulate or implement (ie., a few minutes of programming); POSS = feature possible to implement, but requires a bit of user programming; or NO = feature not implemented, would require modifying the code. The list of questions were: HH: can it simulate HH models? LIF: can it simulate LIF models? Izhikevich IF: can it simulate multivariable IF models, for example Izhikevich type? Cable eqs: can it simulate compartmental models with dendrites? ST plasticity: can it simulate short-term synaptic plasticity? (facilitation, depression) LT Plasticity: can it simulate long-term synaptic plasticity? (LTP, LTD, STDP) Event-based: can it simulate event-based strategies? exact: in this case, is the integration scheme exact? Clock-based: can it simulate clock-based strategies? (e.g., Runge–Kutta) interpolated: in this case, does it use interpolation for spike times? G synapses: can it simulate COBA synaptic interactions? parallel: does it support parallel processing? graphics: does it have a graphical interface? simple analysis: is it possible to use the interface for simple analysis? (spike count, correlations, etc) complx analysis: can more complex analysis be done? (parameter fitting, fft, matrix operations, ...) development: is it currently developed? how many p.: if yes, how many developers are working on it? support: is it supported? (help for users) type: what type of support (email, phone, consultation?) user forum: is there a forum of users or mailing list? publ list: is there a list of publications of articles that used it? codes: are there codes available on the web of published models? online manual: are there tutorials and reference material available on the web? book: are there published books on the simulator? XML import: can it import model specifications in XML? XML export: can it export model specifications in XML? web site: is there a web site of the simulator where all can be found? (including help and source codes) LINUX: does it run on LINUX? Windows: does it run on Windows? (98, 2K, XP) Mac-Os: does it run on Mac-OS X? Interface: Is there a possibility to interface the simulator to outside signals? (such as a camera, or a real neuron) Save option: Does it have a “save option,” (different than ctrl-z), allowing the user to interrupt a simulation, and continue it later on? (this feature is important on a cluster when simulations must be interrupted) \* Graphical interface and analysis possible via front-ends like Python or MATLAB \*\* Feature planned to be implemented in a future version of the simulator

2490 tested on small clusters of PCs and parallel machines  
 2491 (16 processors max), and should be completed to take  
 2492 into account all aspects of the framework and more  
 2493 ambitious hardware platforms.

2494 Work is ongoing to improve the interface of the  
 2495 simulator regarding input and output data formatting,  
 2496 through the use of structured data language (XML).  
 2497 While a proof-of-concept XML extension has already  
 2498 been developed, this is not a trivial task, and further  
 2499 work is needed in the context of existing initiatives  
 2500 (such as NeuroML).

2501 Meanwhile, it is expected that the range of models  
 2502 available to the user will be extended, for instance  
 2503 through the inclusion of models of stochastic point  
 2504 processes, and generic implementation of state space  
 2505 discretization methods.

2506 **5 Discussion**

2507 We have presented here an overview of different  
 2508 strategies and algorithms for simulating spiking neural  
 2509 networks, as well as an overview of most of the  
 2510 presently available simulation environment to imple-  
 2511 ment such simulations. We also have conceived a set  
 2512 of benchmark simulations of spiking neural networks  
 2513 (Appendix B) and provide as supplementary material  
 2514 (linked to ModelDB) the codes for implementing the  
 2515 benchmarks in the different simulators. We believe this  
 2516 should constitute a very useful resource, especially for  
 2517 new researchers in the field of computational neuro-  
 2518 science.

2519 We voluntarily did not approach the difficult prob-  
 2520 lem of simulation speed and comparison of different  
 2521 simulators in this respect. In Table 1 we have tried to  
 2522 enumerate the features of every simulator, in partic-  
 2523 ular regarding the models that are implemented, the  
 2524 possibility of distributed simulation and the simulation  
 2525 environment. In summary, we can classify the simu-  
 2526 lators presented in Section 4 into four categories ac-  
 2527 cording to their most relevant range of application: (1)  
 2528 single-compartment models: CSIM, NEST and NCS;  
 2529 (2) multi-compartment models: NEURON, GENESIS,  
 2530 SPLIT; (3) event-driven simulation: MVASPIKE; (4)  
 2531 dynamical system analysis: XPP. The simulators NEST,  
 2532 NCS, PCSIM (the new parallel version of CSIM)  
 2533 and SPLIT are specifically designed for distributed  
 2534 simulations of very large networks. Three simulators  
 2535 (NEURON, GENESIS and XPP) constitute a com-  
 2536 plete simulation environment which includes a graphi-  
 2537 cal interface and sophisticated tools for representation  
 2538 of model structure and analysis of the results, as well  
 2539 as a complete book for documentation. In other sim-

ulators, analysis and graphical interface are obtained  
 through the use of an external front-end (such as  
 MATLAB or Python).

2543 It is interesting to note that the different simula-  
 2544 tion environments are often able to simulate the same  
 2545 models, but unfortunately the codes are not compatible  
 2546 with each-other. This underlines the need for a more  
 2547 transparent communication channel between simula-  
 2548 tors. Related to this, the present efforts with simulator-  
 2549 independent codes (such as NeuroML, see Appendix  
 2550 A) constitutes the main advance for a future inter-  
 2551 operability. We illustrated here that, using a Python-  
 2552 based interface, one of the benchmarks can be run in  
 2553 either NEURON or NEST using the same code (see  
 2554 Fig. 24 and Appendix A).

2555 Thus, future work should focus on obtaining a full  
 2556 compatibility between simulation environments and  
 2557 XML-based specifications. Importing and exporting  
 2558 XML should enable to convert simulation codes be-  
 2559 tween simulators, and thereby provide very efficient  
 2560 means of combining existing models. A second direc-  
 2561 tion for future investigations is to adapt simulation  
 2562 environments to current hardware constraints, such as  
 2563 parallel computations on clusters. Finally, more work  
 2564 is also needed to clarify the differences between simu-  
 2565 lation strategies and integration algorithms, which may  
 2566 considerably differ for cases where the timing of spikes  
 2567 is important (Fig. 4).

2568 **Acknowledgements** Research supported by the European  
 2569 Community (FACETS project, IST 15879), NIH (NS11613),  
 2570 CNRS, ANR and HFSP. We are also grateful for the feedback  
 2571 and suggestions from users that have led to improvements of the  
 2572 simulators reviewed here.

2573 **Appendix A: Simulator-independent model**  
 2574 **specification**

2575 As we have seen, there are many freely-available, open-  
 2576 source and well-documented tools for simulation of  
 2577 networks of spiking neurons. There is considerable  
 2578 overlap in the classes of network that each is able to  
 2579 simulate, but each strikes a different balance between  
 2580 efficiency, flexibility, scalability and user-friendliness,  
 2581 and the different simulators encompass a range of simu-  
 2582 lation strategies. This makes the choice of which tool  
 2583 to use for a particular project a difficult one. Moreover,  
 2584 we argue that using just one simulator is an undesirable  
 2585 state of affairs. This follows from the general principle  
 2586 that scientific results must be reproducible, and that any  
 2587 given instrument may have flaws or introduce a system-  
 2588 atic bias. The simulators described here are complex  
 2589 software packages, and may have hidden bugs or

2590 unexamined assumptions that may only be apparent in  
 2591 particular circumstances. Therefore it is desirable that  
 2592 any given model should be simulated using at least two  
 2593 different simulators and the results cross-checked.  
 2594 This is, however, more easily said than done. The  
 2595 configuration files, scripting languages or graphical in-  
 2596 terfaces used for specifying model structure are very  
 2597 different for the different simulators, and this, to-  
 2598 gether with subtle differences in the implementation  
 2599 of conceptually-identical ideas, makes the conversion  
 2600 of a model from one simulation environment to an-  
 2601 other an extremely non-trivial task; as such it is rarely  
 2602 undertaken.  
 2603 We believe that the field of computational neuro-  
 2604 science has much to gain from the ability to easily  
 2605 simulate a model with multiple simulators. First, it  
 2606 would greatly reduce implementation-dependent bugs,  
 2607 and possible subtle systematic biases due to use of  
 2608 an inappropriate simulation strategy. Second, it would  
 2609 facilitate communication between investigators and re-  
 2610 duce the current segregation into simulator-specific  
 2611 communities; this, coupled with a willingness to publish  
 2612 actual simulation code in addition to a model descrip-  
 2613 tion, would perhaps lead to reduced fragmentation of  
 2614 research effort and an increased tendency to build on  
 2615 existing models rather than redevelop them de novo.  
 2616 Third, it would lead to a general improvement in  
 2617 simulator technology since bugs could be more easily  
 2618 identified, benchmarking greatly simplified, and hence  
 2619 best-practice more rapidly propagated.  
 2620 This goal of simulator independent model specifica-  
 2621 tion is some way off, but some small steps have been  
 2622 taken. There are two possible approaches (which will  
 2623 probably prove to be complementary) to developing  
 2624 simulator-independent model specification, which mir-  
 2625 ror the two approaches taken to model specification by  
 2626 individual simulators: declarative and programmatic.  
 2627 Declarative model specification is exemplified by the  
 2628 use of configuration files, as used for example by NCS.  
 2629 Here there is a fixed library of neuron models, synapse  
 2630 types, plasticity mechanisms, connectivity patterns, etc.,  
 2631 and a particular model is specified by choosing from this  
 2632 library. This has the advantages of simplicity in setting  
 2633 up a model, and of well-defined behaviors for individual  
 2634 components, but has less flexibility than the alternative,  
 2635 programmatic model specification. Most simulators re-  
 2636 viewed here use a more or less general purpose pro-  
 2637 gramming language, usually an interpreted one, which  
 2638 has neuroscience specific functions and classes together  
 2639 with more general control and data structures. As  
 2640 noted, this gives the flexibility to generate new struc-  
 2641 tures beyond those found in the simulator's standard  
 2642 library, but at the expense of the very complexity that

we identified above as the major roadblock in convert- 2643  
 ing models between simulators. 2644

A.1 Declarative model specification using NeuroML 2645

The NeuroML project<sup>25</sup> is an open-source collabora- 2646  
 tion<sup>26</sup> whose stated aims are: 2647

1. To support the use of declarative specifications for 2648  
 models in neuroscience using XML 2649
2. To foster the development of XML standards 2650  
 for particular areas of computational neuroscience 2651  
 modeling 2652

The following standards have so far been developed: 2653

- MorphML: specification of neuroanatomy (i.e. neu- 2654  
 ron morphology) 2655
- ChannelML: specification of models of ion chan- 2656  
 nels and receptors (see Fig. 21 for an example) 2657
- Biophysics: specification of compartmental cell 2658  
 models, building on MorphML and ChannelML 2659
- NetworkML: specification of cell positions and con- 2660  
 nections in a network. 2661

The common syntax of these specifications is XML.<sup>27</sup> 2662  
 This has the advantages of being both human- and 2663  
 machine-readable, and standardized by an interna- 2664  
 tional organization, which in turn has led to wide up- 2665  
 take and developer participation. 2666

Other XML-based specifications that have been de- 2667  
 veloped in neuroscience and in biology more gener- 2668  
 ally include BrainML<sup>28</sup> for exchanging neuroscience 2669  
 data, CellML<sup>29</sup> for models of cellular and subcellular 2670  
 processes and SBML<sup>30</sup> for representing models of bio- 2671  
 chemical reaction networks. 2672

Although XML has become the most widely used 2673  
 technology for the electronic communication of hier- 2674  
 archically structured information, the real standardiza- 2675  
 tion effort is orthogonal to the underlying technology, 2676  
 and concerns the structuring of domain-specific knowl- 2677  
 edge, i.e. a listing of the objects and concepts of interest 2678  
 in the domain and of the relationships between them, 2679  
 using a standardized terminology. To achieve this, Neu- 2680  
 roML uses the XML Schema Language<sup>31</sup> to define the 2681

<sup>25</sup><http://www.neuroml.org> (Crook et al. 2005)

<sup>26</sup><http://sourceforge.net/projects/neuroml>

<sup>27</sup><http://www.w3.org/XML>

<sup>28</sup><http://brainml.org>

<sup>29</sup><http://www.cellml.org>

<sup>30</sup><http://sbml.org>

<sup>31</sup><http://www.w3.org/XML/Schema>

**Fig. 21** Example of Hodgkin-Huxley K<sup>+</sup> conductance specified in ChannelML, a component of NeuroML

```
<?xml version="1.0" encoding="UTF-8"?>
<channelml xmlns="http://morphml.org/channelml/schema"
  xmlns:xsi="http://www.w3.org/2001/XMLSchema-instance"
  xmlns:meta="http://morphml.org/metadata/schema"
  xsi:schemaLocation="http://morphml.org/channelml/schema
    ../Schemata/v1.1/Level2/ChannelML_v1.1.xsd"
  units="Physiological Units">

  <ion name="k" default_erev="-77.0" charge="1"/> <!-- phys units: mV -->

  <channel_type name="KChannel" density="yes">

    <meta:notes>Simple example of K conductance in squid giant axon.
      Based on channel from Hodgkin and Huxley 1952</meta:notes>

    <current_voltage_relation>
      <ohmic ion="k">
        <conductance default_gmax="36"> <!-- phys units: mS/cm2-->
          <gate power="4">
            <state name="n" fraction="1">
              <transition>
                <voltage_gate>
                  <alpha>
                    <parameterised_hh type="linoid" expr="A*(k*(v-d))/(1 - exp(-(k*(v-d))))">
                      <parameter name="A" value="0.1"/>
                      <parameter name="k" value="0.1"/>
                      <parameter name="d" value="-55"/>
                    </parameterised_hh>
                  </alpha>
                  <beta>
                    <parameterised_hh type="exponential" expr="A*exp(k*(v-d))">
                      <parameter name="A" value="0.125"/>
                      <parameter name="k" value="-0.0125"/>
                      <parameter name="d" value="-65"/>
                    </parameterised_hh>
                  </beta>
                </voltage_gate>
              </transition>
            </state>
          </gate>
        </conductance>
      </ohmic>
    </current_voltage_relation>
  </channel_type>
</channelml>
```

2682 allowed elements and structure of a NeuroML docu-  
 2683 ment. The validity of a NeuroML document may be  
 2684 checked with reference to the schema definitions. The  
 2685 NeuroML Validation service<sup>32</sup> provides a convenient  
 2686 way to do this.

2687 *A.1.1 Using NeuroML for specifying network models*

2688 In order to use NeuroML to specify spiking neuronal  
 2689 network models we require detailed descriptions of

- 2690 1. Point spiking neurons (IF neurons and generaliza-  
 2691 tions thereof)
- 2692 2. Compartmental models with HH-like biophysics

- 3. Large networks with structured internal connec- 2693  
 tivity related to a network topology (e.g., full- 2694  
 connectivity, 1D or 2D map with local connectivity, 2695  
 synfire chains patterns, with/without randomness) 2696  
 and structured map to map connectivity (e.g., 2697  
 point-to-point, point-to-many, etc.) 2698

At the time of writing, NeuroML supports the sec- 2699  
 ond and third items, but not the first. However, an 2700  
 extension to support specification of IF-type neuron 2701  
 models is currently being developed, and will hopefully 2702  
 be incorporated into the NeuroML standard in the near 2703  
 future. 2704

Specification of HH-type models uses the MorphML, 2705  
 ChannelML and Biophysics standards of NeuroML 2706  
 (see Fig. 21 for an example. We focus here only on spec- 2707  
 ification of networks, using the NetworkML standard. 2708

<sup>32</sup><http://morphml.org:8080/NeuroMLValidator>



2709 A key point is that a set of neurons and network con-  
 2710 nectivity may be defined either by *extension* (providing  
 2711 the list of all neurons, parameters and connections), for  
 2712 example:

---

```
<population name="PopulationA">
  <cell_type>CellA</cell_type>
  <instances>
    <instance id="0"><location x="0" y="0" z="0"/></instance>
    <instance id="1"><location x="0" y="10" z="0"/></instance>
    <instance id="2"><location x="0" y="20" z="0"/></instance>
    . . .
  </instances>
</population>
```

---

2713 (note that *CellA* is a cell model described earlier in  
 2714 the NeuroML document), or by *specification*, i.e. an  
 2715 implicit enumeration, for example:

---

```
<population name="PopulationA">
  <cell_type>CellA</cell_type>
  <pop_location>
    <random_arrangement>
      <population_size>200</population_size>
      <spherical_location>
        <meta:center x="0" y="0" z="0" diameter="100"/>
      </spherical_location>
    </random_arrangement>
  </pop_location>
</population>
```

---

2716 Similarly, for connectivity, one may define an explicit  
 2717 list of connections,

---

```
<projection name="NetworkConnection1">
  <source>PopulationA</source>
  <target>PopulationB</target>
  <connections>
    <connection id="0">
      <pre cell_id="0" segment_id = "0"/>
      <post cell_id="1" segment_id = "1"/>
    </connection>
    <connection id="1">
      <pre cell_id="2" segment_id = "0"/>
      <post cell_id="1" segment_id = "0"/>
    </connection>
    . . .
  </connections>
</projection>
```

---

2718 or specify an algorithm to determine the connections:  
 2719 <projection name="NetworkConnection1">  
 2720 <source>PopulationA</source>  
 2721 <target>PopulationB</target>  
 2722 <connectivity\_pattern>  
 2723 <num\_per\_source>3</num\_per\_source>  
 2724 <max\_per\_target>2</max\_per\_target>  
 2725 </connectivity\_pattern>  
 2726 </projection>

2727 *A.1.2 Using NeuroML with a specific simulator*

2728 One very interesting feature of XML is that any lan-  
 2729 guage such as NeuroML is not fixed for ever:

- 2730 • It may be adapted to your own<sup>33</sup> way of presenting  
 2731 data and models (e.g. words may be written in  
 2732 your own native language) as soon as the related  
 2733 logical-structure can be translated to/from standard  
 2734 NeuroML
- 2735 • add-ons are always easily defined, as soon as  
 2736 they are compatible with the original NeuroML  
 2737 specifications.

2738 Then using NeuroML simply means editing such  
 2739 data-structures using a suitable XML editor, validating  
 2740 them (i.e. verify that the related logical-structures are  
 2741 well-formed and valid with respect to the specification,  
 2742 conditions, etc.) and normalizing them (i.e. translate it  
 2743 to an equivalent logical-structure but without redun-  
 2744 dancy, while some factorization simplifies subsequent  
 2745 manipulation).

2746 Translation from this validated normalized form  
 2747 is efficient and safe. Translation can be achieved by

<sup>33</sup>Pragmatic generic coding-rules. There are always several ways to represent information as a logical-structure. Here are a few key ideas to make such choices:

- Maximizing atomicity. i.e. structure the data with a maximal decomposition (e.g. atomic values must only contain “words” else there is still a “structure” and is thus to be decomposed itself in terms of elements).
- Maximizing factorization, i.e. prohibit data redundancy, but use references to index a data fragment from another part of the data. This saves place and time, but also avoid data inconsistency.
- Maximizing flat representation, i.e. avoid complex tree structures, when the data can be represented as uniform lists of data, i.e. tables with simple records, such as a field-set.
- Maximizing generic description, i.e. abstract representation, without any reference to file format or operating-system syntax: independent of how the data is going to be used.
- Maximizing parameterization of functionality, i.e. specify, as much as possible, the properties (i.e. characteristics / parameters / options) of a software module or a function as a static set of data (instead of “putting-it-in-the-code”).

one of two methods: Either a simulator may accept 2748  
 a NeuroML document as input, and translation from 2749  
 NeuroML elements to native simulator objects is per- 2750  
 formed by the simulator, or the XSL Transformation 2751  
 language<sup>34</sup> may be used to generate native simulator 2752  
 code (e.g. *hoc* or *NMODL* in the case of NEURON). 2753  
 For example, the NeuroML Validator service provides 2754  
 translation of ChannelML and MorphML files to NEU- 2755  
 RON and GENESIS formats. 2756

The process of editing, validating, normalizing and 2757  
 translating NeuroML data-structures is summarized in 2758  
 Fig. 22. 2759

*A.1.3 Future extensions* 2760

The NetworkML standard is at an early stage of devel- 2761  
 opment. Desirable future extensions include: 2762

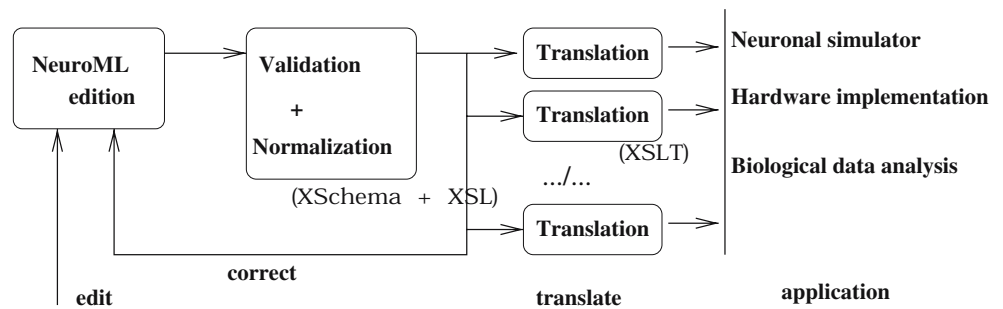
- Specification of point spiking models, such as the IF 2763  
 model. 2764
- More flexible specification of numerical parame- 2765  
 ters. Numerical parameter values are not simple 2766  
 “numbers” but satisfy certain standard conditions 2767  
 (parameter values are physical quantities with a 2768  
 unit, may take a default value, have values bounded 2769  
 within a certain range with minimal/maximal values 2770  
 and are defined up to a certain precision) or specific 2771  
 conditions defined by a boolean expression, and 2772  
 may have their default value not simply defined 2773  
 by a constant but from an algebraic expression. 2774  
 In the current NeuroML standards all numerical 2775  
 parameters are simple numbers, and all units must 2776  
 be consistent with either a “physiological units” 2777  
 system or the SI system (they may not be mixed in 2778  
 a single NeuroML document). 2779
- Specifying parameter values as being drawn from a 2780  
 defined random distribution. 2781

*A.2 Programmatic model specification using Python* 2782

For network simulations, we may well require more 2783  
 flexibility than can easily be obtained using a declar- 2784  
 ative model specification, but we still wish to obtain 2785  
 simple conversion between simulators, i.e. to be able 2786  
 to write the simulation code for a model only once, 2787  
 then run the same code on multiple simulators. This 2788  
 requires first the definition of an API (Application 2789  
 Programming Interface) or meta-language, a set of 2790  
 functions/classes which provides a superset of the 2791

<sup>34</sup><http://www.w3.org/TR/xslt>

**Fig. 22** From NeuroML to simulator



2792 capabilities of the simulators we wish to run on.<sup>35</sup> Hav- 2823  
 2793 ing defined an API, there are two possible next stages:  
 2794 (1) each simulator implements a parser which can 2825  
 2795 interpret the meta-language; (2) a separate program 2826  
 2796 either translates the meta-language into simulator- 2827  
 2797 specific code or controls the simulator directly, giving 2828  
 2798 simulator-specific function calls.

2799 In our opinion, the second of these possibilities is the 2829  
 2800 better one, since 2830

- 2801 1. it avoids replication of effort in writing parsers,
- 2802 2. we can then use a general purpose, state-of-the-art 2833  
 2803 interpreted programming language, such as Python 2834  
 2804 or Ruby, rather than a simulator-specific language, 2835  
 2805 and thus leverage the effort of outside developers 2836  
 2806 in areas that are not neuroscience specific, such as 2837  
 2807 data analysis and visualization<sup>36</sup> 2838

2808 The PyNN project<sup>37</sup> has begun to develop both the 2831  
 2809 API and the binding to individual simulation engines, 2832  
 2810 for both purposes using the Python programming lan- 2833  
 2811 guage. The API has two parts, a low-level, procedural 2834  
 2812 API (functions *create()*, *connect()*, *set()*, *record()*), and 2835  
 2813 a high-level, object-oriented API (classes *Population* 2836  
 2814 and *Projection*, which have methods like *set()*, *record()*, 2837  
 2815 *setWeights()*, etc.). The low-level API is good for small 2838  
 2816 networks, and perhaps gives more flexibility. The high- 2839  
 2817 level API is good for hiding the details and the book- 2840  
 2818 keeping, and is intended to have a one-to-one mapping 2841  
 2819 with NeuroML, i.e. a *population* element in NeuroML 2842  
 2820 will correspond to a *Population* object in PyNN.

2821 The other thing that is required to write a model 2843  
 2822 once and run it on multiple simulators is standard cell 2844

2823 models. PyNN translates standard cell-model names 2824  
 2825 and parameter names into simulator-specific names, 2826  
 2827 e.g. standard model *IF\_curr\_alpha* is *iaf\_neuron* 2828  
 2828 in NEST and *StandardIF* in NEURON, while 2829  
 2829 *SpikeSource Poisson* is a *poisson\_generator* in NEST 2830  
 2830 and a *NetStim* in NEURON.

2831 An example of the use of the API to specify a simple 2832  
 2832 network is given in Fig. 23. 2833

2834 Python bindings currently exist to control NEST 2835  
 2835 (PyNEST<sup>38</sup>) and Mvaspike, and Python can be used as 2836  
 2836 an alternative interpreter for NEURON (nrnpython), 2837  
 2837 although the level of integration (how easy it is to access 2838  
 2838 the native functionality) is variable. Currently PyNN 2839  
 2839 supports PyNEST and NEURON (via nrnpython), and 2840  
 2840 there are plans to add support for other simulators with 2841  
 2841 Python bindings, initially Mvaspike and CSIM, and to 2842  
 2842 add support for the distributed simulation capabilities 2843  
 2843 of NEURON and NEST. 2844

A.2.1 Example simulations 2845

2846 Benchmarks 1 and 2 (see Appendix B) have been 2847  
 2847 coded in PyNN and run using both NEURON and 2848  
 2848 NEST (Fig. 24). The results for the two simulators are 2849  
 2849 not identical, since we used different random number 2850  
 2850 sequences when determining connectivity, but the dis- 2851  
 2851 tributions of inter-spike intervals (ISIs) and of the co- 2852  
 2852 efficient of variation of ISI are almost indistinguishable. 2853  
 2853 All the cell and synapse types used in the benchmarks 2854  
 2854 are standard models in PyNN. Where these models 2855  
 2855 do not come as standard in NEURON or NEST, the 2856  
 2856 model code is distributed with PyNN (in the case of 2857  
 2857 NEURON) or with PyNEST (in the case of NEST). We 2858  
 2858 do not report simulation times, as PyNN has not been 2859  
 2859 optimized for either simulator. 2860

<sup>35</sup>Note that since we choose a superset, the system must emit a warning/error if the underlying simulator engine does not support a particular feature.

<sup>36</sup>For Python, examples include efficient data storage and transfer (HDF5, ROOT), data analysis (SciPy), parallelization (MPI), GUI toolkits (GTK, QT).

<sup>37</sup>pronounced “pine”

<sup>38</sup>a Python interface to NEST

**Fig. 23** Example of the use of the PyNN API to specify a network that can then be run on multiple simulators

```

cell_params = { 'tau_m' : 20.0, 'tau_syn' : 2.0, 'tau_refrac': 1.0,
                'v_rest': -65.0, 'v_thresh': -50.0, 'cm': 1.0}

populationA = Population((10,), "IF_curr_alpha", cell_params)
populationB = Population((5,5), "IF_curr_alpha", cell_params)
populationA.randomInit('uniform', v_reset, v_thresh)

connAtoB = Projection(populationA, populationB, 'fixedProbability', 0.2)
connAtoA = Projection(populationA, populationA, 'distanceDependentProbability', "exp(-abs(d))")
connBtoA = Projection(populationB, populationA, 'allToAll')

connAtoB.setWeights(w_AB)
connAtoA.setWeights(w_AA)
connBtoA.setWeights(w_BA)

populationA.record()
populationB.record()

run(1000.0)

populationA.printSpikes("populationA.spiketimes")
populationB.printSpikes("populationA.spiketimes")
    
```

2856 **Appendix B: Benchmark simulations**

2857 In this appendix, we present a series of “benchmark”  
 2858 network simulations using both IF or HH type neurons.  
 2859 They were chosen such that at least one of the bench-  
 2860 mark can be implemented in the different simulators  
 2861 (the code corresponding to these implementations will  
 2862 be provided in the ModelDB database).<sup>39</sup>

2863 The models chosen were networks of excitatory  
 2864 and inhibitory neurons inspired from a recent study  
 2865 (Vogels and Abbott 2005). This paper considered two  
 2866 types of networks of LIF neurons, one with CUBA  
 2867 synaptic interactions (CUBA model), and another one  
 2868 with COBA synaptic interactions (CUBA model; see  
 2869 below). We also introduce here a HH-based version of  
 2870 the COBA model, as well as a fourth model consisting  
 2871 of IF neurons interacting through voltage deflections  
 2872 (“voltage-jump” synapses).

2873 B.1 Network structure

2874 Each model consisted of 4,000 IF neurons, which were  
 2875 separated into two populations of excitatory and in-  
 2876 hibitory neurons, forming 80% and 20% of the neurons,  
 2877 respectively. All neurons were connected randomly us-  
 2878 ing a connection probability of 2%.

2879 B.2 Passive properties

2880 The membrane equation of all models was given by:

$$C_m \frac{dV}{dt} = -g_L(V - E_L) + S(t) + G(t), \quad (5)$$

where  $C_m = 1 \mu\text{F}/\text{cm}^2$  is the specific capacitance,  $V$  2881  
 is the membrane potential,  $g_L = 5 \times 10^{-5} \text{ S}/\text{cm}^2$  is the 2882  
 leak conductance density and  $E_L = -60 \text{ mV}$  is the 2883  
 leak reversal potential. Together with a cell area of 2884  
 20,000  $\mu\text{m}^2$ , these parameters give a resting membrane 2885  
 time constant of 20 ms and an input resistance at rest 2886  
 of 100 M $\Omega$ . The function  $S(t)$  represents the spiking 2887  
 mechanism and  $G(t)$  stands for synaptic interactions 2888  
 (see below). 2889

B.3 Spiking mechanisms 2890

B.3.1 IF neurons 2891

In addition to passive membrane properties, IF neurons 2892  
 had a firing threshold of  $-50 \text{ mV}$ . Once the  $V_m$  reaches 2893  
 threshold, a spike is emitted and the membrane poten- 2894  
 tial is reset to  $-60 \text{ mV}$  and remains at that value for a 2895  
 refractory period of 5 ms. 2896

B.3.2 HH neurons 2897

HH neurons were modified from Traub and Miles 2898  
 (1991) and were described by the following equations: 2899

$$\begin{aligned}
 C_m \frac{dV}{dt} &= -g_L(V - E_L) - \bar{g}_{Na} m^3 h (V - E_{Na}) \\
 &\quad - \bar{g}_{Kd} n^4 (V - E_K) + G(t) \\
 \frac{dm}{dt} &= \alpha_m(V) (1 - m) - \beta_m(V) m \\
 \frac{dh}{dt} &= \alpha_h(V) (1 - h) - \beta_h(V) h \\
 \frac{dn}{dt} &= \alpha_n(V) (1 - n) - \beta_n(V) n, \quad (6)
 \end{aligned}$$

<sup>39</sup><http://senselab.med.yale.edu/senselab/ModelDB>

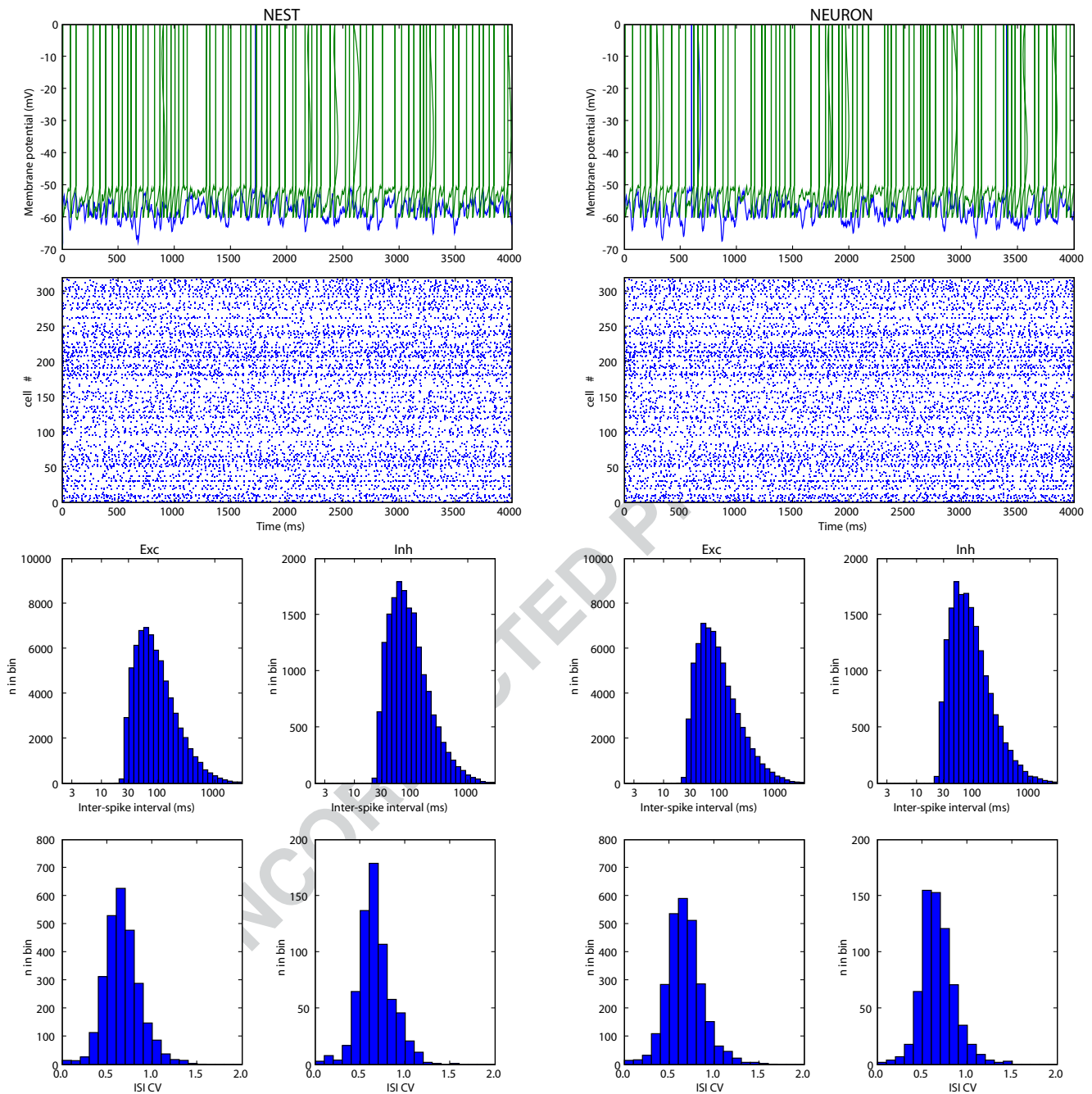


**Fig. 24** Same network model run on two different simulators using the same source code. The model considered was the Vogels-Abbott integrate-and-fire network with CUBA synapses and displaying self-sustained irregular activity states (Benchmark 2 in Appendix B). This network implemented with the PyNN simulator-independent network modelling API, and simulated using NEST (left column) and NEURON (right column) as the simulation engines. The same sequence of random numbers was used for each simulator, so the connectivity patterns were rigorously identical. The membrane potential trajectories of indi-

vidual neurons simulated in different simulators rapidly diverge, as small numerical differences are rapidly amplified by the large degree of recurrency of the circuit, but the interspike interval (ISI) statistics of the populations are almost identical for the two simulators. (Top row) Voltage traces for two cells chosen at random from the population. (Second row) Spike raster plots for the first 320 neurons in the population. (Third row) Histograms of ISIs for the excitatory and inhibitory cell populations. (Bottom row) Histograms of the coefficient of variation (CV) of the ISIs

B/W IN PRINT

2900 where  $\bar{g}_{Na} = 100 \text{ mS/cm}^2$  and  $\bar{g}_{Kd} = 30 \text{ mS/cm}^2$  are  
 2901 the maximal conductances of the sodium current and  
 2902 delayed rectifier with reversal potentials of  $E_{Na} =$   
 2903  $50 \text{ mV}$  and  $E_K = -90 \text{ mV}$ .  $m$ ,  $h$ , and  $n$  are the acti-  
 2904 vation variables which time evolution depends on the  
 2905 voltage-dependent rate constants  $\alpha_m$ ,  $\beta_m$ ,  $\alpha_h$ ,  $\beta_h$ ,  $\alpha_n$   
 2906 and  $\beta_n$ . The voltage-dependent expressions of the rate  
 2907 constants were modified from the model described by  
 2908 Traub and Miles (1991):

$$\begin{aligned} \alpha_m &= 0.32 * (13 - V + V_T) / [\exp((13 - V + V_T) / 4) - 1] \\ \beta_m &= 0.28 * (V - V_T - 40) / [\exp((V - V_T - 40) / 5) - 1] \\ \alpha_h &= 0.128 * \exp((17 - V + vV_T) / 18) \\ \beta_h &= 4 / [1 + \exp((40 - V + V_T) / 5)] \\ \alpha_n &= 0.032 * (15 - V + V_T) / [\exp((15 - V + V_T) / 5) - 1] \\ \beta_n &= 0.5 * \exp((10 - V + V_T) / 40), \end{aligned}$$

2909 where  $V_T = -63 \text{ mV}$  adjusts the threshold (which was  
 2910 around  $-50 \text{ mV}$  for the above parameters).

2911 **B.4 Synaptic interactions**

2912 *B.4.1 COBA synapses*

2913 For COBA synaptic interactions, the membrane equa-  
 2914 tion of neuron  $i$  was given by:

$$C_m \frac{dV_i}{dt} = -g_L(V_i - E_L) + S(t) - \sum_j g_{ji}(t)(V_i - E_j), \tag{7}$$

2915 where  $V_i$  is the membrane potential of neuron  $i$ ,  $g_{ji}(t)$   
 2916 is the synaptic conductance of the synapse from neuron  
 2917  $j$  to neuron  $i$ , and  $E_j$  is the reversal potential of that  
 2918 synapse.  $E_j$  was of  $0 \text{ mV}$  for excitatory synapses, or  
 2919  $-80 \text{ mV}$  for inhibitory synapses.

2920 Synaptic interactions were implemented as follows:  
 2921 when a spike occurred in neuron  $j$ , the synaptic conduc-  
 2922 tance  $g_{ji}$  was instantaneously incremented by a quan-  
 2923 tum value ( $6 \text{ nS}$  and  $67 \text{ nS}$  for excitatory and inhibitory  
 2924 synapses, respectively) and decayed exponentially with  
 2925 a time constant of  $5 \text{ ms}$  and  $10 \text{ ms}$  for excitation and  
 2926 inhibition, respectively.

*B.4.2 CUBA synapses* 2927

For implementing CUBA synaptic interactions, the fol- 2928  
 2929 lowing equation was used:

$$C_m \frac{dV_i}{dt} = -g_L(V_i - E_L) + S(t) - \sum_j g_{ji}(t)(\bar{V} - E_j), \tag{8}$$

where  $\bar{V} = -60 \text{ mV}$  is the mean membrane potential. 2930  
 The conductance quanta were of  $0.27 \text{ nS}$  and  $4.5 \text{ nS}$  2931  
 for excitatory and inhibitory synapses, respectively. 2932  
 The other parameters are the same as for COBA 2933  
 interactions. 2934

*B.4.3 Voltage-jump synapses* 2935

For implementing voltage-jump type of synaptic inter- 2936  
 actions, the membrane potential was abruptly increased 2937  
 by a value of  $0.25 \text{ mV}$  for each excitatory event, and it 2938  
 was decreased by  $2.25 \text{ mV}$  for each inhibitory event. 2939

**B.5 Benchmarks** 2940

Based on the above models, the following four bench- 2941  
 2942 marks were implemented.

*Benchmark 1: COBA IF network.* This benchmark 2943  
 consists of a network of IF neurons 2944  
 connected with COBA synapses, ac- 2945  
 cording to the parameters above. It is 2946  
 equivalent to the COBA model de- 2947  
 scribed in Vogels and Abbott (2005). 2948

*Benchmark 2: CUBA IF network.* This second bench- 2949  
 mark simulates a network of IF neu- 2950  
 rons connected with CUBA synapses, 2951  
 which is equivalent to the CUBA 2952  
 model described in Vogels and Abbott 2953  
 (2005). It has the same parameters as 2954  
 above, except that every cell needs to 2955  
 be depolarized by about  $10 \text{ mV}$ , which 2956  
 was implemented by setting  $E_L =$  2957  
 $-49 \text{ mV}$  (see Vogels and Abbott 2005). 2958

*Benchmark 3: COBA HH network.* This benchmark 2959  
 is equivalent to Benchmark 1, except 2960  
 that the HH model was used. 2961

*Benchmark 4: IF network with voltage-jump synapses.* 2962  
 This fourth benchmark used voltage- 2963  
 jump synapses, and has a membrane 2964

2965 equation which is analytically solvable,  
 2966 and can be implemented using event-  
 2967 driven simulation strategies.

2968 For all four benchmarks, the models simulate a self-  
 2969 sustained irregular state of activity, which is easy to  
 2970 identify: all cells fire irregularly and are characterized  
 2971 by important subthreshold voltage fluctuations. The  
 2972 neurons must be randomly stimulated during the first  
 2973 50 ms in order to set the network in the active state.

2974 **B.6 Supplementary material**

2975 The supplementary material to the paper contains the  
 2976 codes for implementing those benchmarks in the differ-  
 2977 ent simulators reviewed here (see Section 4 for details  
 2978 on specific implementations). We provide the codes  
 2979 for those benchmarks, implemented in each simula-  
 2980 tor, and this code is made available in the ModelDB  
 2981 database.<sup>40</sup>

2982 In addition, we provide a clock-driven implemen-  
 2983 tation of Benchmarks 1 and 2 with Scilab, a free  
 2984 vector-based scientific software. In this case, Bench-  
 2985 mark 1 is integrated with Euler method, second order  
 2986 Runge–Kutta and Euler with spike timing interpolation  
 2987 (Hansel et al. 1998), while Benchmark 2 is integrated  
 2988 exactly (with spike timings aligned to the time grid).  
 2989 The event-driven implementation (Benchmark 4) is  
 2990 also possible with Scilab but very inefficient because  
 2991 the programming language is interpreted, and since the  
 2992 algorithms are asynchronous, the operations cannot be  
 2993 vectorized. Finally, we also provide a C++ implementa-  
 2994 tion of Benchmark 2 and of a modified version of the  
 2995 COBA model (Benchmark 1, with identical synaptic  
 2996 time constants for excitation and inhibition).

2997 **References**

2998 Abbott, L. F., & Nelson, S. B. (2000). Synaptic plasticity: taming  
 2999 the beast. *Nature Neuroscience*, 3(Suppl), 1178–1283.  
 3000 Arnold, L. (1974). *Stochastic differential equations: Theory and*  
 3001 *applications*. New York: J. Wiley and Sons.  
 3002 Azouz, R. (2005). Dynamic spatiotemporal synaptic integra-  
 3003 tion in cortical neurons: neuronal gain, revisited. *Journal of*  
 3004 *Neurophysiology*, 94, 2785–2796.  
 3005 Badoual, M., Rudolph, M., Piwkowska, Z., Destexhe, A., &  
 3006 Bal, T. (2005). High discharge variability in neurons driven  
 3007 by current noise. *Neurocomputing*, 65, 493–498.

Bailey, J., & Hammerstrom, D. (1988). Why VLSI implemen- 3008  
 tations of associative VLCNs require connection multiplex- 3009  
 ing. *International Conference on Neural Networks (ICNN 88,* 3010  
*IEEE)* (pp. 173–180). San Diego. 3011  
 Banitt, Y., Martin, K. A. C., & Segev, I. (2005). Depressed res- 3012  
 sponses of facilitatory synapses. *Journal of Neurophysiology*, 3013  
 94, 865–870. 3014  
 Beeman, D. (2005). GENESIS Modeling Tutorial. Brains, Minds, 3015  
 and Media. 1: bmm220 (urn:nbn:de:0009-3-2206). 3016  
 Bernard, C., Ge, Y. C., Stockley, E., Willis, J. B., & Wheal, H. V. 3017  
 (1994). Synaptic integration of NMDA and non-NMDA re- 3018  
 ceptors in large neuronal network models solved by means 3019  
 of differential equations. *Biological Cybernetics*, 70(3), 3020  
 267–73. 3021  
 Bhalla, U., Bilitch, D., & Bower, J. M. (1992). Rallpacks: A set 3022  
 of benchmarks for neuronal simulators. *Trends in Neuro-* 3023  
*sciences*, 15, 453–458. 3024  
 Bhalla, U. S., & Iyengar, R. (1999). Emergent properties of 3025  
 networks of biological signaling pathways. *Science*, 283, 3026  
 381–387. 3027  
 Bhalla, U. S. (2004). Signaling in small subcellular volumes: II. 3028  
 Stochastic and diffusion effects on synaptic network proper- 3029  
 ties. *Biophysical Journal*, 87, 745–753. 3030  
 Blake, J. L., & Goodman, P. H. (2002). Speech perception simu- 3031  
 lated in a biologically-realistic model of auditory neocortex 3032  
 (abstract). *Journal of Investigative Medicine*, 50, 193S. 3033  
 Bower, J. M. (1995). Reverse engineering the nervous system: An 3034  
 in vivo, in vitro, and in computo approach to understand- 3035  
 ing the mammalian olfactory system. In: S. F. Zornetzer, 3036  
 J. L. Davis, & C. Lau (Eds.), *An introduction to neural* 3037  
*and electronic networks, second edn* (pp. 3–28). New York: 3038  
 Academic Press. 3039  
 Bower, J. M., & Beeman, D. (1998). *The book of GENESIS:* 3040  
*Exploring realistic neural models with the General Neural* 3041  
*Simulation System, second edn*. New York: Springer. 3042  
 Brette, R. (2006). Exact simulation of integrate-and-fire mod- 3043  
 els with synaptic conductances. *Neural Computation*, 18, 3044  
 2004–2027. 3045  
 Brette, R. (2007). Exact simulation of integrate-and-fire models 3046  
 with exponential currents. *Neural Computation* (in press). 3047  
 Brette, R., & Gerstner, W. (2005). Adaptive exponential 3048  
 integrate-and-fire model as an effective description of neu- 3049  
 ronal activity. *Journal of Neurophysiology*, 94, 3637–3642. 3050  
 Brown, R. (1988). Calendar queues: A fast 0(1) priority queue 3051  
 implementation for the simulation event set problem. *Jour-* 3052  
*nal of Communication ACM*, 31(10), 1220–1227. 3053  
 Carnevale, N. T., & Hines, M. L. (2006). *The NEURON book*. 3054  
 Cambridge: Cambridge University Press. 3055  
 Carriero, N., & Gelernter, D. (1989). Linda in context. *Commu-* 3056  
*nications of the ACM*, 32, 444–458. 3057  
 Claverol, E., Brown, A., & Chad, J. (2002). Discrete simula- 3058  
 tion of large aggregates of neurons. *Neurocomputing*, 47, 3059  
 277–297. 3060  
 Connolly, C., Marian, I., & Reilly, R. (2003). Approaches to 3061  
 efficient simulation with spiking neural networks. In WSPC. 3062  
 Cormen, T., Leiserson, C., Rivest, R., & Stein, C. (2001). *Intro-* 3063  
*duction to algorithms, second edn*. Cambridge: MIT Press. 3064  
 Crook, S., Beeman, D., Gleeson, P., & Howell, F. (2005). XML 3065  
 for model specification in neuroscience. Brains, Minds and 3066  
 Media 1: bmm228 (urn:nbn:de:0009-3-2282). 3067  
 Daley, D., & Vere-Jones, D. (1988). *An introduction to the theory* 3068  
*of point processes*. New York: Springer. 3069  
 Day, M., Carr, D. B., Ulrich, S., Ilijic, E., Tkatch, T., & Surmeier, 3070  
 D. J. (2005). Dendritic excitability of mouse frontal cortex 3071  
 pyramidal neurons is shaped by the interaction among 3072

<sup>40</sup><https://senselab.med.yale.edu/senselab/modeldb/ShowModel.asp?model=83319> (if necessary, use “reviewme” as password)

- 3073 HCN, Kir2, and k(leak) channels. *Journal of Neuroscience*,  
3074 25, 8776–8787.
- 3075 Delorme, A., & Thorpe, S. J. (2003). Spikenet: An event-driven  
3076 simulation package for modelling large networks of spiking  
3077 neurons. *Network*, 14(4), 613–627.
- 3078 De Schutter, E., & Bower, J. M. (1994). An active membrane  
3079 model of the cerebellar Purkinje cell. I. Simulation of current  
3080 clamps in slice. *Journal of Neurophysiology*, 71, 375–400.
- 3081 Destexhe, A., Mainen, Z., & Sejnowski, T. (1994a). An efficient  
3082 method for computing synaptic conductances based on a  
3083 kinetic model of receptor binding. *Neural Computation*, 6,  
3084 14–18.
- 3085 Destexhe, A., Mainen, Z., & Sejnowski, T. (1994b). Synthesis  
3086 of models for excitable membranes, synaptic transmission  
3087 and neuromodulation using a common kinetic formalism.  
3088 *Journal of Computational Neuroscience*, 1, 195–230.
- 3089 Destexhe, A., & Sejnowski, T. J. (2001). *Thalamocortical assem-*  
3090 *blies*. New York: Oxford University Press.
- 3091 Diesmann, M., & Gewaltig, M.-O. (2002). NEST: An envi-  
3092 ronment for neural systems simulations. In T. Plesser &  
3093 V. Macho (Eds.), *Forschung und wissenschaftliches*  
3094 *Rechnen, Beitrage zum Heinz-Billing-Preis 2001, Volume 58*  
3095 *of GWDG-Bericht*, (pp. 43–70). Gottingen: Ges. fur Wiss.  
3096 Datenverarbeitung.
- 3097 Djurfeldt, M., Johansson, C., Ekeberg, Ö., Rehn, M., Lundqvist,  
3098 M., & Lansner, A. (2005). *Massively parallel simulation*  
3099 *of brain-scale neuronal network models. Technical Report*  
3100 *TRITA-NA-P0513*. Stockholm: School of Computer Science  
3101 and Communication.
- 3102 Drewes, R., Maciokas, J. B., Louis, S. J., & Goodman, P. H.  
3103 (2004). An evolutionary autonomous agent with visual cor-  
3104 tex and recurrent spiking columnar neural network. *Lecture*  
3105 *Notes in Computer Science*, 3102, 257–258.
- 3106 Drewes, R. (2005). Modeling the brain with NCS and  
3107 Brainlab. *LINUX Journal online*. <http://www.linuxjournal.com/article/8038>.
- 3108 Ermentrout, B. (2002). Simulating, analyzing, and animating dy-  
3109 namical systems: A guide to XPPAUT for researchers and  
3110 students. SIAM.
- 3111 Ermentrout, B., & Kopell, N. (1986). Parabolic bursting in an ex-  
3112 citable system coupled with a slow oscillation. *Siam Journal*  
3113 *on Applied Mathematics*, 46, 233–253.
- 3114 Ferscha, A. (1996). Parallel and distributed simulation of discrete  
3115 event systems. In A. Y. Zomaya (Ed.), *Parallel and Dis-*  
3116 *tributed Computing Handbook* (pp. 1003–1041). New York:  
3117 McGraw-Hill.
- 3118 Fransén, E., & Lansner, A. (1998). A model of cortical as-  
3119 sociative memory based on a horizontal network of con-  
3120 nected columns. *Network: Computation in Neural Systems*, 9,  
3121 235–264.
- 3122 Froemke, R. C., & Dan, Y. (2002). Spike-timing-dependent  
3123 synaptic modification induced by natural spike trains.  
3124 *Nature*, 416, 433–438.
- 3125 Fujimoto, R. M. (2000). *Parallel and distributed simulation sys-*  
3126 *tems*. New York: Wiley.
- 3127 Galassi, M., Davies, J., Theiler, J., Gough, B., Jungman, G.,  
3128 Booth, M., et al. (2001). *Gnu scientific library: Reference*  
3129 *manual*. Bristol: Network Theory Limited.
- 3130 Gara, A., Blumrich, M. A., Chen, D., Chiu, G. L.-T.,  
3131 Coteus, P., Giampapa, M. E., et al. (2005). Overview of the  
3132 Blue Gene/L system architecture. *IBM Journal of Research*  
3133 *and Development*, 49, 195–212.
- 3134 Gerstner, W., & Kistler, W. M. (2002). Mathematical for-  
3135 mulations of hebbian learning. *Biological Cybernetics*, 87,  
3136 404–415.
- 3137 Giugliano, M. (2000). Synthesis of generalized algorithms for  
the fast computation of synaptic conductances with markov  
kinetic models in large network simulations. *Neural Compu-*  
*tation*, 12, 903–931.
- 3140 Giugliano, M., Bove, M., & Grattarola, M. (1999). Fast calcula-  
3141 tion of short-term depressing synaptic conductances. *Neural*  
3142 *Computation*, 11, 1413–1426.
- 3143 Goddard, N., Hucka, M., Howell, F., Cornelis, H., Shankar, K., &  
3144 Beeman, D. (2001). Towards NeuroML: Model description  
3145 methods for collaborative modelling in neuroscience. *Philo-*  
3146 *sophical Transactions of the Royal Society of London. Series*  
3147 *B, Biological Sciences*, 356, 1209–1228.
- 3148 Gupta, A., Wang, Y., & Markram, H. (2000). Organizing princi-  
3149 ples for a diversity of GABAergic interneurons and synapses  
3150 in the neocortex. *Science*, 287, 273–278.
- 3151 Gütig, R., Aharonov, R., Rotter, S., & Sompolinsky, H. (2003).  
3152 Learning input correlations through non-linear asymmetric  
3153 hebbian plasticity. *Journal of Neuroscience*, 23, 3697–3714.
- 3154 Gütig, R., & Sompolinsky, H. (2006). The tempotron: A neu-  
3155 ron that learns spike timing-based decisions. *Nature Neuro-*  
3156 *science*, 9, 420–428.
- 3157 Hammarlund, P., & Ekeberg, Ö. (1998). Large neural network  
3158 simulations on multiple hardware platforms. *Journal of*  
3159 *Computational Neuroscience*, 5, 443–459.
- 3160 Hansel, D., Mato, G., Meunier, C., & Neltner, L. (1998). On  
3161 numerical simulations of integrate-and-fire neural networks.  
3162 *Neural Computation*, 10, 467–483.
- 3163 Hereld, M., Stevens, R. L., Teller, J., & van Drongelen, W. (2005).  
3164 Large neural simulations on large parallel computers. *Inter-*  
3165 *national Journal of Bioelectromagnetism*, 7, 44–46.
- 3166 Hindmarsh, A. C., Brown, P. N., Grant, K. E., Lee, S. L., Serban,  
3167 R., Shumaker, D. E., et al. (2005). SUNDIALS: Suite of  
3168 nonlinear and differential/algebraic equation solvers. *ACM*  
3169 *Transactions on Mathematical Software*, 31, 363–396.
- 3170 Hines, M. (1984). Efficient computation of branched nerve equa-  
3171 tions. *International Journal of Bio-Medical Computing*, 15,  
3172 69–76.
- 3173 Hines, M. (1989). A program for simulation of nerve equations  
3174 with branching geometries. *International Journal of Bio-*  
3175 *Medical Computing*, 24, 55–68.
- 3176 Hines, M., & Carnevale, N. T. (1997). The neuron simulation  
3177 environment. *Neural Computation*, 9, 1179–1209.
- 3178 Hines, M. L., & Carnevale, N. T. (2000). Expanding NEURON's  
3179 repertoire of mechanisms with NMODL. *Neural Computa-*  
3180 *tion*, 12, 995–1007.
- 3181 Hines, M. L., & Carnevale, N. T. (2001). NEURON: A tool for  
3182 neuroscientists. *The Neuroscientist*, 7, 123–135.
- 3183 Hines, M. L., & Carnevale, N. T. (2004). Discrete event simula-  
3184 tion in the NEURON environment. *Neurocomputing*, 58–60,  
3185 1117–1122.
- 3186 Hirsch, M., & Smale, S. (1974). *Differential equations, dynamical*  
3187 *systems, and linear algebra. Pure and applied mathematics*.  
3188 New York: Academic Press.
- 3189 Hodgkin, A. L., & Huxley, A. F. (1952). A quantitative descrip-  
3190 tion of membrane current and its application to conduction  
3191 and excitation in nerve. *Journal of Physiology*, 117(4), 500–  
3192 544.
- 3193 Honeycutt, R. L. (1992). Stochastic Runge–Kutta algorithms.  
3194 I. White noise. *Physical Review A*, 45, 600–603.
- 3195 Houweling, A. R., Bazhenov, M., Timofeev, I., Steriade, M.,  
3196 & Sejnowski, T. J. (2005). Homeostatic synaptic plasticity  
3197 can explain post-traumatic epileptogenesis in chronically iso-  
3198 lated neocortex. *Cerebral Cortex*, 15, 834–845.
- 3199 Hugues, E., Guilleux, F., & Rochel, O. (2002). Contour detection  
3200 by synchronization of integrate-and-fire neurons. *Proceed-*  
3201



- ings of the 2nd workshop on biologically motivated computer vision—BMCV 2002, TÄijbingen, Germany. *Lecture Notes in Computer Science*, 2525, 60–69.
- Izhikevich, E. M. (2003). Simple model of spiking neurons. *IEEE Transactions on Neural Networks*, 14, 1569–1572.
- Jahnke, A., Roth, U., & Schoenauer, T. (1998). Digital simulation of spiking neural networks. In W. Maass & C. M. Bishop (Eds.), *Pulsed neural networks*. Cambridge: MIT Press.
- Johnston, D., & Wu, S. M.-S. (1995). *Foundations of Cellular Neurophysiology*. Cambridge: MIT Press.
- Kanold, P. O., & Manis, P. B. (2005). Encoding the timing of inhibitory inputs. *Journal of Neurophysiology*, 93, 2887–2897.
- Kellogg, M. M., Wills, H. R., & Goodman, P. H. (1999). Cumulative synaptic loss in aging and Alzheimer's dementia: A biologically realistic computer model (abstract). *Journal of Investigative Medicine*, 47(17S).
- Kernighan, B. W., & Pike, R. (1984). Appendix 2: Hoc manual. In *The UNIX programming environment* (pp. 329–333). Englewood Cliffs: Prentice-Hall.
- Kohn, J., & Wörgötter, F. (1998). Employing the Z-transform to optimize the calculation of the synaptic conductance of NMDA and other synaptic channels in network simulations. *Neural Computation*, 10, 1639–1651.
- Kozlov, A., Lansner, A., & Grillner, S. (2003). Burst dynamics under mixed nmda and ampa drive in the models of the lamprey spinal cpg. *Neurocomputing*, 52–54, 65–71.
- Laing, C. R. (2007). On the application of “equation-free” modelling to neural systems. *Journal of Computational Neuroscience* (in press).
- Lee, G., & Farhat, N. H. (2001). The double queue method: A numerical method for integrate-and-fire neuron networks. *Neural Networks*, 14, 921–932.
- Lundqvist, M., Rehn, M., Djurfeldt, M., & Lansner, A. (2007). Attractor dynamics in a modular network model of neocortex. *Network* (in press).
- Lytton, W. W. (1996). Optimizing synaptic conductance calculation for network simulations. *Neural Computation*, 8, 501–509.
- Lytton, W. W. (2002). *From computer to brain*. New York: Springer-Verlag.
- Lytton, W. W., & Hines, M. L. (2005). Independent variable time-step integration of individual neurons for network simulations. *Neural Computation*, 17, 903–921.
- Macara-Rios, J. C., Goodman, P. H., Drewes, R., & Harris, F. C. Jr (2004). Remote-neocortex control of robotic search and threat identification. *Robotics and Autonomous Systems*, 46, 97–110.
- Maciokas, J. B., Goodman, P. H., Kenyon, J. L., Toledo-Rodriguez, M., & Markram, H. (2005). Accurate dynamical model of interneuronal GABAergic channel physiologies. *Neurocomputing*, 65, 5–14.
- Makino, T. (2003). A discrete-event neural network simulator for general neuron models. *Neural Computing and Applications*, 11, 210–223.
- Marian, I., Reilly, R., & Mackey, D. (2002). Efficient event-driven simulation of spiking neural networks. In *Proceedings of the 3rd WSEAS International Conference on Neural Networks and Applications*.
- Markram, H., Lubke, J., Frotscher, M., Roth, A., & Sakmann, B. (1997a). Physiology and anatomy of synaptic connections between thick tufted pyramidal neurones in the developing rat neocortex. *Journal of Physiology*, 500, 409–440.
- Markram, H., Lubke, J., Frotscher, M., & Sakmann, B. (1997b). Regulation of synaptic efficacy by coincidence of postsynaptic APs and EPSPs. *Science*, 275, 213–215.
- Markram, H., Dimitri, P., Gupta, A., & Tsodyks, M. (1998a). Potential for multiple mechanisms, phenomena and algorithms for synaptic plasticity at single synapses. *Neuropharmacology*, 37, 489–500.
- Markram, H., Wang, Y., & Tsodyks, M. (1998b). Differential signaling via the same axon of neocortical pyramidal neurons. *Proceedings of the National Academy of Sciences of the United States of America*, 95, 5323–5328.
- Mattia, M., & Del Giudice, P. (2000). Efficient event-driven simulation of large networks of spiking neurons and dynamical synapses. *Neural Computation*, 12, 2305–2329.
- Markaki, M., Orphanoudakis, S., & Poirazi, P. (2005). Modelling reduced excitability in aged CA1 neurons as a calcium-dependent process. *Neurocomputing*, 65, 305–314.
- Mayrhofer, R., Affenzeller, M., Prähofer, H., Hfer, G., & Fried, A. (2002). Devs simulation of spiking neural networks. In *Proceedings of Cybernetics and Systems (EMCSR)*, (Vol. 2, pp. 573–578). Austrian Society for Cybernetic Studies.
- Migliore, M., Hines, M. L., & Shepherd, G. M. (2005). The role of distal dendritic gap junctions in synchronization of mitral cell axonal output. *Journal of Computational Neuroscience*, 18, 151–161.
- Migliore, M., Cannia, C., Lytton, W. W., Markram, H., & Hines, M. L. (2006). Parallel network simulations with NEURON. *Journal of Computational Neuroscience*, 21, 119–129.
- Moffitt, M. A., & McIntyre, C. C. (2005). Model-based analysis of cortical recording with silicon microelectrodes. *Clinical Neurophysiology*, 116, 2240–2250.
- Moore, J. W., & Stuart, A. E. (2000). *Neurons in action: computer simulations with NeuroLab*. Sunderland: Sinauer Associates.
- Morrison, A., Aertsen, A., & Diesmann, M. (2007). Spike-timing dependent plasticity in balanced random networks. *Neural Computation* (in press).
- Morrison, A., Mehring, C., Geisel, T., Aertsen, A., & Diesmann, M. (2005). Advancing the boundaries of high connectivity network simulation with distributed computing. *Neural Computation*, 17, 1776–1801.
- Morrison, A., Straube, S., Plesser, H. E., & Diesmann, M. (2006). Exact subthreshold integration with continuous spike times in discrete time neural network simulations. *Neural Computation*, 19, 47–79.
- Natschläger, T., Markram, H., & Maass, W. (2003). Computer models and analysis tools for neural microcircuits. In R. Kötter (Ed.), *Neuroscience databases. A practical guide* (pp. 123–138). Boston: Kluwer Academic Publishers.
- Nenadic, Z., Ghosh, B. K., & Ulinski, P. (2003). Propagating waves in visual cortex: A large scale model of turtle visual cortex. *Journal of Computational Neuroscience*, 14, 161–184.
- Olshausen, B. A., & Field, D. J. (2005). How close are we to understanding V1? *Neural Computation*, 17, 1665–1699.
- Opitz, B. A., & Goodman, P. H. (2005). In silico knockin/knockout in model neocortex suggests role of Ca-dependent K<sup>+</sup> channels in spike-timing information (abstract). *Journal of Investigative Medicine*, 53, 193S.
- Prescott, S. A., & De Koninck, Y. (2005). Integration time in a subset of spinal lamina I neurons is lengthened by sodium and calcium currents acting synergistically to prolong subthreshold depolarization. *Journal of Neuroscience*, 25, 4743–4754.
- Press, W. H., Flannery B. P., Teukolsky S. A., & Vetterling W. T. (1993). *Numerical recipes in C: The art of scientific computing*. Cambridge: Cambridge University Press.
- Reutimann, J., Giugliano, M., & Fusi, S. (2003). Event-driven simulation of spiking neurons with stochastic dynamics. *Neural Computation*, 15, 811–830.

- 3335 Ripplinger, M. C., Wilson, C. J., King, J. G., Frye, J., Drewes,  
3336 R., Harris, F. C., et al. (2004). Computational model of inter-  
3337 acting brain networks (abstract). *Journal of Investigative*  
3338 *Medicine*, 52, 155S.
- 3339 Rochel, O., & Martinez, D. (2003). An event-driven frame-  
3340 work for the simulation of networks of spiking neurons. In  
3341 *Proceedings of the 11th European Symposium on Artificial*  
3342 *Neural Networks - ESANN'2003* (pp. 295–300). Bruges.
- 3343 Rochel, O., & Vieville, T. (2006). One step towards an abstract  
3344 view of computation in spiking neural networks (abstract).  
3345 *10th International Conference on Cognitive and Neural*  
3346 *Systems*. Boston.
- 3347 Rochel, O., & Cohen, N. (2007). Real time computation:  
3348 Zooming in on population codes. *Biosystems* (in press)  
Q15 3349 (doi:10.1016/j.biosystems.2006.09.021).
- 3350 Rotter, S., & Diesmann, M. (1999). Exact digital simulation of  
3351 time-invariant linear systems with applications to neuronal  
3352 modeling. *Biological Cybernetics*, 81, 381–402.
- 3353 Rubin, J., Lee, D., & Sompolinsky, H. (2001). Equilibrium prop-  
3354 erties of temporally asymmetric Hebbian plasticity. *Physical*  
3355 *Review Letters*, 86, 364–367.
- 3356 Rudolph, M., & Destexhe, A. (2006). Analytical integrate-and-  
3357 fire neuron models with conductance-based dynamics for  
3358 event-driven simulation strategies. *Neural Computation*, 18,  
3359 2146–2210.
- 3360 Rudolph, M., & Destexhe, A. (2007). How much can we trust  
Q16 3361 neural simulation strategies? *Neurocomputing* (in press).
- 3362 Saghatelian, A., Roux, P., Migliore, M., Rochefort, C.,  
3363 Desmaisons, D., Charneau, P., et al. (2005). Activity-  
3364 dependent adjustments of the inhibitory network in the ol-  
3365 factory bulb following early postnatal deprivation. *Neuron*,  
3366 46, 103–116.
- 3367 Sanchez-Montanez, M. (2001). Strategies for the optimiza-  
3368 tion of large scale networks of integrate and fire neu-  
3369 rons. In J. Mira & A. Prieto (Eds.), *IWANN, Volume*  
3370 *2004/2001 of Lecture Notes in Computer Science*. New York:  
3371 Springer-Verlag.
- 3372 Sandström, M., Kotaleski, J. H., & Lansner, A. (2007). Scaling  
3373 effects in a model of the olfactory bulb. *Neurocomputing*  
Q17 3374 (in press).
- 3375 Shelley, M. J., & Tao, L. (2001). Efficient and accurate time-  
3376 stepping schemes for integrate-and-fire neuronal networks.  
3377 *Journal of Computational Neuroscience*, 11, 111–119.
- 3378 Sleator, D., & Tarjan, R. (1983). Self-adjusting binary trees.  
3379 In *Proceedings of the 15th ACM SIGACT Symposium on*  
3380 *Theory of Computing* (pp. 235–245).
- 3381 Sloot, A., Kaandorp, J. A., Hoekstra, G., & Overeinder, B. J.  
3382 (1999). Distributed simulation with cellular automata: Ar-  
3383 chitecture and applications. In J. Pavelka, G. Tel, & M.  
3384 Bartosek (Eds.), *SOFSEM'99, LNCS* (pp. 203–248). Berlin:  
3385 Springer-Verlag.
- 3386 Song, S., & Abbott, L. F. (2001). Cortical development  
3387 and remapping through spike timing-dependent plasticity.  
3388 *Neuron*, 32, 339–350.
- 3389 Song, S., Miller, K. D., & Abbott, L. F. (2000). Competitive  
3390 hebbian learning through spike-timing-dependent synaptic  
3391 plasticity. *Nature Neuroscience*, 3, 919–926.
- 3392 Stricanne, B., & Bower, J. M. (1998). A network model of the  
3393 somatosensory system cerebellum, exploring recovery from  
3394 peripheral lesions at various developmental stages in rats  
3395 (abstract). *Society of Neuroscience Abstracts*, 24, 669.
- 3396 Traub, R. D., & Miles, R. (1991). *Neuronal Networks of the Hip-*  
3397 *pocampus*. Cambridge UK: Cambridge University Press.
- Traub, R. D., Contreras, D., Cunningham, M. O., Murray, H., 3398  
LeBeau, F. E. N., Roopun, A., et al. (2005). Single-column 3399  
thalamocortical network model exhibiting gamma oscillations, 3400  
sleep spindles, and epileptogenic bursts. *Journal of* 3401  
*Neurophysiology*, 93, 2194–2232. 3402
- Tsodyks, M., Pawelzik, K., & Markram, H. (1998). Neural net- 3403  
works with dynamic synapses. *Neural Computation*, 10, 821– 3404  
835. 3405
- Tuckwell, H. (1988). *Introduction to theoretical neurobiology,* 3406  
*volume 1: Linear cable theory and dendritic structure.* 3407  
Cambridge: Cambridge University Press. 3408
- van Emde Boas, P., Kaas, R., & Zijlstra, E. (1976). Design and 3409  
implementation of an efficient priority queue. *Theory of* 3410  
*Computing Systems*, 10, 99–127. 3411
- Vitko, I., Chen, Y. C., Arias, J. M., Shen, Y., Wu, X. R., & Perez- 3412  
Reyes, E. (2005). Functional characterization and neuronal 3413  
modeling of the effects of childhood absence epilepsy vari- 3414  
ants of CACNA1H, a T-type calcium channel. *Journal of* 3415  
*Neuroscience*, 25, 4844–4855. 3416
- Vogels, T. P., & Abbott, L. F. (2005). Signal propagation and 3417  
logic gating in networks of integrate-and-fire neurons. *Jour-* 3418  
*nal of Neuroscience*, 25, 10786–10795. 3419
- Waikul, K. K., Jiang, L. J., Wilson, E. C., Harris, F. C. Jr, & 3420  
Goodman, P. H. (2002). Design and implementation of a 3421  
web portal for a NeoCortical Simulator. In *Proceedings of* 3422  
*the 17th International Conference on Computers and their* 3423  
*Applications (CATA 2002)* (pp. 349–353). 3424
- Wang, Y., Markram, H., Goodman, P. H., Berger, T. K., Ma, J., 3425  
& Goldman-Rakic, P.S. (2006). Heterogeneity in the pyra- 3426  
midal network of the medial prefrontal cortex. *Nature Neu-* 3427  
*roscience*, 9, 534–542. 3428
- Watts, L. (1994). Event-driven simulation of networks of spiking 3429  
neurons. *Advances in neural information processing systems* 3430  
(pp. 927–934). 3431
- Wiebers, J. L., Goodman, P. H., & Markram, H. (2000). Block- 3432  
ade of A-type potassium channels recovers memory impair- 3433  
ment caused by synaptic loss: Implications for Alzheimer's 3434  
dementia (abstract). *Journal of Investigative Medicine*, 48,  
283S. 3435  
3436
- Wills, H. R., Kellogg, M. M., & Goodman, P. H. (1999). A bi- 3437  
ologically realistic computer model of neocortical associative 3438  
learning for the study of aging and dementia (abstract). *Jour-* 3439  
*nal of Investigative Medicine*, 47, 11S. 3440
- Wilson, M. A., & Bower, J. M. (1989). The simulation of large- 3441  
scale neural networks. In C. Koch & I. Segev (Eds.), *Methods* 3442  
*in neuronal modeling: From synapses to networks* (pp. 291– 3443  
333). Cambridge: MIT Press. 3444
- Wohrer, A., Kornprobst, P., & Vieville, T. (2006). From light 3445  
to spikes: A large-scale retina simulator. In *Proceedings of* 3446  
*the IJCNN 2006* (pp. 8995–9003). Vancouver, ISBN: 0-7803- 3447  
9490-9. 3448
- Wolf, J. A., Moyer, J. T., Lazarewicz, M. T., Contreras, D., 3449  
Benoit-Marand, M., O'Donnell, P., et al. (2005). NMDA/ 3450  
AMPA ratio impacts state transitions and entrainment to 3451  
oscillations. *Journal of Neuroscience*, 25, 9080–9095. 3452
- Zeigler, B., Praehofer, H., & Kim, T. (2000). *Theory of modeling* 3453  
*and simulation, second edn. Integrating discrete event and* 3454  
*continuous complex dynamic systems*. New York: Academic 3455  
Press. 3456
- Zeigler, B. P., & Vahie, S. (1993). DEVS formalism and method- 3457  
ology: Unity of conception/diversity of application. In 3458  
*Proceedings of the 1993 Winter Simulation Conference* 3459  
(pp. 573–579). Los Angeles, December 12–15. 3460

## AUTHOR QUERIES

### **AUTHOR PLEASE ANSWER ALL QUERIES**

- Q1. A list of keywords was provided. Please check if they are appropriate.
- Q2. Grill et al. (2005) was cited in text but was not listed in the reference list. Please provide the data for this reference item or, alternatively, delete the citation from the text.
- Q3. Wiebers et al. 2003 and Maass et al. 2002 were cited in text but was not listed in the reference list. Please provide the data for this reference item or, alternatively, delete the citation from the text.
- Q4. The citation to Markram et al. 1997 was modified to cite Markram et al. 1997a and b. Please check if this was appropriate.
- Q5. Citations to Figs. 14 and 15 were inserted in the text. Please check if this location is appropriate
- Q6. Ermentrout 2004 was cited in text but was not listed in the reference list. Please provide the data for this reference item or, alternatively, delete the citation from the text.
- Q7. Frye 2005 was cited in text but was not listed in the reference list. Please provide the data for this reference item or, alternatively, delete the citation from the text.
- Q8. A citation to Fig. 16 was inserted in the text. Please check if this location is appropriate.
- Q10. Please check if Table 1 was presented correctly.
- Q9. Rochel and Cohen 2005 was cited in text but was not listed in the reference list. Please provide the data for this reference item or, alternatively, delete the citation from the text.
- Q11. Please check if the publication data of Brette 2007 need to be updated.
- Q12. Please check if the publication data of Laing 2007 need to be updated.
- Q13. Please check if the publication data of Lundqvist et al. 2007 need to be updated.
- Q14. Please check if the publication data of Morrison et al. 2007 need to be updated.
- Q15. Please check if the publication data of Rochel and Cohen 2007 need to be updated.
- Q16. Please check if the publication data of Rudolph and Destexhe 2007 need to be updated.
- Q17. Please check if the publication data of Sandstrom et al. 2007 need to be updated.
- Q18. Please provide better quality figure.
- Q19. Kozlov et al. 2006 and Tonnelier et al. 2006 were understood to be a currently unpublished manuscript. As such, the reference items were deleted and the corresponding citation in the text was modified accordingly.